NASA/CR—1998–208859

A Compendium of Wind Statistics and Models for the NASA Space Shuttle and Other Aerospace Vehicle Programs

O.E. Smith and S.I. Adelfang
Computer Sciences Corporation, Huntsville, Alabama

Prepared for Marshall Space Flight Center
under Contract NAS8–60000

October 1998

The NASA STI Program Office...in Profile

Since its founding, NASA has been dedicated to the advancement of aeronautics and space science. The NASA Scientific and Technical Information (STI) Program Office plays a key part in helping NASA maintain this important role.

The NASA STI Program Office is operated by Langley Research Center, the lead center for NASA's scientific and technical information. The NASA STI Program Office provides access to the NASA STI Database, the largest collection of aeronautical and space science STI in the world. The Program Office is also NASA's institutional mechanism for disseminating the results of its research and development activities. These results are published by NASA in the NASA STI Report Series, which includes the following report types:

- TECHNICAL PUBLICATION. Reports of completed research or a major significant phase of research that present the results of NASA programs and include extensive data or theoretical analysis. Includes compilations of significant scientific and technical data and information deemed to be of continuing reference value. NASA's counterpart of peer-reviewed formal professional papers but has less stringent limitations on manuscript length and extent of graphic presentations.

- TECHNICAL MEMORANDUM. Scientific and technical findings that are preliminary or of specialized interest, e.g., quick release reports, working papers, and bibliographies that contain minimal annotation. Does not contain extensive analysis.

- CONTRACTOR REPORT. Scientific and technical findings by NASA-sponsored contractors and grantees.

- CONFERENCE PUBLICATION. Collected papers from scientific and technical conferences, symposia, seminars, or other meetings sponsored or cosponsored by NASA.

- SPECIAL PUBLICATION. Scientific, technical, or historical information from NASA programs, projects, and mission, often concerned with subjects having substantial public interest.

- TECHNICAL TRANSLATION. English-language translations of foreign scientific and technical material pertinent to NASA's mission.

Specialized services that complement the STI Program Office's diverse offerings include creating custom thesauri, building customized databases, organizing and publishing research results...even providing videos.

For more information about the NASA STI Program Office, see the following:

- Access the NASA STI Program Home Page at ***http://www.sti.nasa.gov***

- E-mail your question via the Internet to help@sti.nasa.gov

- Fax your question to the NASA Access Help Desk at (301) 621-0134

- Telephone the NASA Access Help Desk at (301) 621-0390

- Write to:
  NASA Access Help Desk
  NASA Center for AeroSpace Information
  800 Elkridge Landing Road
  Linthicum Heights, MD 21090-2934

NASA/CR—1998–208859

A Compendium of Wind Statistics and Models for the NASA Space Shuttle and Other Aerospace Vehicle Programs

O.E. Smith and S.I. Adelfang
Computer Sciences Corporation, Huntsville, Alabama

Prepared for Marshall Space Flight Center
under Contract NAS8–60000

National Aeronautics and
Space Administration

Marshall Space Flight Center • MSFC, Alabama 35812

October 1998

Acknowledgments

Gratitude is extended to Mr. Steven D. Pearson, Chief, Electromagnetics and Aerospace Environments Branch (EL23), Systems Analysis and Integration Laboratory (EL01) and Mr. Alexander A. McCool, Manager, Space Shuttle Projects Office (SA01) who sponsored this report. It was perceived that documentation of wind statistics and wind models development from past to present aerospace programs would benefit not only for the continued life of Space Shuttle but also future NASA space vehicle programs. With this technical challenge, Dr. C.G. Justus, Computer Sciences Corporation (CSC PrISMS Contract NAS8–60000) team leader for natural environment support, assigned this task to the authors who, in turn, appreciate his interest and encouragement in the preparation of this report. Thanks are extended to our colleague, Dr. R.E. Smith (CSC), for his critical discussions that helped clarify the presentation of this work. Also, thanks to Ms. Belinda Hardin, Member of Technical Staff (Associate) (CSC), for preparing the manuscript and to Ms. Margaret Alexander (EL23) for editing the draft.

The authors wish to acknowledge the close association and participation over the years with the various NASA Space Shuttle working groups. This includes all past and current chairpersons and team members of the following:

(1) Ascent Flight Systems Integration Group (AFSIG)
(2) Performance Panel
(3) Loads Panel
(4) Launch Support Evaluation and Advisory Team (LSEAT).

The MSFC Meteorological Coordinator for the Space Shuttle program, Mr. Dale Johnson/EL23, is recognized for his review comments.

Available from:

NASA Center for AeroSpace Information
800 Elkridge Landing Road
Linthicum Heights, MD 21090–2934
(301) 621–0390

National Technical Information Service
5285 Port Royal Road
Springfield, VA 22161
(703) 487–4650

FOREWORD

This report presents work performed under Contract NAS8-60000, Program Information Systems Mission Services (PrISMS), Computer Sciences Corporation. This work was sponsored by the Electromagnetics and Aerospace Environments Branch, Systems Engineering Division, Systems Analysis and Integration Laboratory of the NASA Marshall Space Flight Center.

Mr. Steven Pearson, Chief of the Electromagnetics and Aerospace Environments Branch, reviewed with the authors the scope of work and encouraged the preparation of this technical report.

Questions or comments on this report should be direct to the authors:

O. E. Smith
Phone: (256) 544-9500
Fax: (256) 544-8807
E-mail: o.e.smith@msfc.nasa.gov

S. I. Adelfang
Phone: (256) 544-9142
Fax: (256) 544-8807
E-mail: stan.adelfang@msfc.nasa.gov

A Compendium of Wind Statistics and Models for the NASA Space Shuttle and Other Aerospace Vehicle Programs

TABLE OF CONTENTS

TABLE OF CONTENTS (continued)

LIST OF ILLUSTRATIONS

LIST OF ILLUSTRATIONS (continued)

LIST OF ILLUSTRATIONS

LIST OF TABLES

LIST OF TABLES (continued)

LIST OF TABLES (continued)

ACRONYMS

AMPS	Automated Meteorological Profiling System
DRWP	Doppler Radar Wind Profiler
ETR	Eastern Test Range
HRFE	High Resolution Flight Element for the AMPS
KSC	Kennedy Space Center
LP	Low Pass
LMM	Load Minimum Margin
LRFE	Low Resolution Flight Element for the AMPS
MSFC	Marshall Space Flight Center
MSS	Meteorological Sounding System
NASA	National Aeronautics and Space Administration
RWLPI	Revised Wind Load Persistence Increment
WL	Wavelength
WLPI	Wind Load Persistence Increment
VAFB	Vandenburg Air Force Base

1.0 INTRODUCTION

After a review of over 40 years work on the subject of wind models for aerospace vehicle programs covering the period from 1957 to 1998 it was realized that the preparation of a comprehensive report on this subject would not be an easy task. This realization lead to the concept reflected by the title of this report. By definition a compendium is "a brief compilation or composition, containing general principles or substance of a larger work or system". The purpose of this report is to document the ascent wind profile models that have been used for aerospace vehicle programs with special emphasis on the Space Shuttle and X-33 programs. This report will review the lessons and misconceptions of the past with the aim of preventing reinvention and false starts in the future.

This report consists of eight sections including the introduction (Section 1). The remaining sections are summarized below.

Section 2. Statistical Analysis

This section presents discussions on sample size, wind persistence, tests for bivariate normality and properties of multivariate normal distributions as applied to wind data samples.

Section 3. Ascent Wind Models (0 to 27 km)

The primary application of wind profile modeling is for establishing dispersions of launch vehicle aerodynamic load indicators. In the past, program managers were reluctant to establish ascent wind loads alleviation techniques during the initial design phase of an aerospace vehicle. Hence, the scalar wind profile model was used (wind loads alleviation is not feasible for a scalar wind profile.) With the technological advancements in computational speed, communications, and guidance and control systems, wind loads alleviation techniques based on vector wind profiles are readily incorporated into the design and operations phases of aerospace vehicle systems. The wind dispersions produced by wind profile models may not be highly correlated with the dispersions of the aerodynamic load indicators estimated with a trajectory model for a specific vehicle. This is because the wind model dispersions are for a particular reference period (annual, monthly...) whereas the vehicle aerodynamic load indicators dispersions are relative to the wind profile used for first stage vehicle guidance. For the early pre-Saturn and Saturn NASA launch vehicles, adjustment of first stage guidance in the pitch plane relative to the monthly mean pitch-plane wind was used for wind loads alleviation. These launch vehicles were constructed to withstand the monthly wind loads dispersions with penalties to payload capability. Beginning with Saturn/Skylab and continuing with the remaining Saturn/Apollo launches, adjustment of the first stage guidance in the pitch and yaw planes relative to the monthly mean pitch and yaw plane wind components was used to achieve additional wind loads relief. Further modifications of Space Shuttle first stage guidance have contributed to recent improvements in Space Shuttle operability because

of reductions in wind loads dispersions. This was achieved first by selecting launch guidance from the one of four trajectory runs that produced the minimum loads using a day-of-launch wind profile and four pre-established seasonal alternate ascent guidance profiles. More recently, Space Shuttle first stage guidance is derived based on an analysis of a trajectory simulation using a Jimsphere wind profile at T-4 (launch time minus 4) hours. This produces the smallest ascent loads dispersions achieved to date. This latest derivation of ascent guidance has been called "day-of-launch ILOAD update" or DOLILU by the Space Shuttle program, where ILOAD represents ascent guidance. When DOLILU is used, it is the wind profile perturbations of relatively small scale (say < 6000 meters wavelength) that force control system responses to maintain the guidance path. Heretofore, even the largest wavelengths in a wind profile could contribute to load indicator dispersions because these large wavelengths could deviate from the monthly mean component (vector) wind profile previously used to establish ascent guidance.

This section describes the evolution of wind models developed at MSFC for aerospace vehicle programs. Statistical concepts and advantages and disadvantages of five ascent wind models are presented. The five models are:

(1) The scalar wind profile model, used in the 1960's for the Saturn program and was initially tried for the Space Shuttle program.

(2) A wind component profile model developed for Saturn/Skylab, the first major launch system that was wind biased (guidance programmed) in both pitch and yaw planes for ascent structural wind loads alleviation.

(3) The monthly vector wind profile model used by the Space Shuttle program. This monthly vector wind model was established for the two initial Space Shuttle launch sites, Vandenberg AFB and Cape Kennedy(*). The vector wind profile models for December at Vandenberg AFB and February at Cape Kennedy were used as design criteria because the wind statistics for these two months effectively envelope the wind statistics for all months at these two sites.

(4) The monthly enveloping scalar wind profile model (MESWP) was developed for the National Launch System (NLS). This model was not implemented because it was quickly superseded by an enveloping version of the improved monthly vector wind profile model (IVWP).

(5) An improved monthly vector wind profile model (IVWP) was developed in 1992 (Ref. 3.7). This model is more complete, has no simplifying assumptions, and is proposed for all future launch vehicle development programs. The enveloping version uses the same approach in model (4) to define the given wind vectors on the monthly enveloping probability ellipse at a reference altitude.

(*) name changes have been made for the location of upper air wind measurements from Cape Canaveral, Florida to Cape Kennedy, Florida and now back to Cape Canaveral, Florida. The location for all Rawinsonde and Jimsphere winds is 28 deg 29 min N latitude and 80 deg 35 min W longitude

Section 4. Ascent Structural Loads Analysis

This section describes the development of the time conditional wind loads persistence increment used for protection of the Space Shuttle commit to launch decision. This development is based on applications of Gumbel extreme value probability functions. The theory of extreme value statistics was first proposed for Space Shuttle ascent loads analysis in 1976, but it was not until 1986, after the Challenger accident, that the extreme value statistical concepts were implemented for ascent wind loads analysis.

Section 5. Wind Loads Uncertainty Attributable to Wind Profile Smoothing and Temporal Variability.

Examples are presented on the effects of wind profile smoothing on Space Shuttle ascent loads statistics and launch probabilities. The justification is presented for using relatively low resolution wind profile measurement systems for pre-launch assessment of wind loads, provided that adequate additional loads protection is developed which accounts for the additional wind loads uncertainty attributable to wind profile smoothing.

Section 6. Gust Models for Launch Vehicle Ascent

The origin of the widely used NASA 9 m/s discrete gust model and the development of a new discrete gust model based on the MIL- Standard "1-cosine" model are described. This improved model is used for Space Shuttle tail assembly flexible body loads analysis.

Section 7. Wind Profile Measurement Systems

Technology development for wind profile measurement systems is described. This includes the Jimsphere, the NASA 50 MHz Doppler Radar Wind Profiler and the Automated Meteorological Profiler System (AMPS), which is under development. Studies are also outlined for improvements in wind analysis to enhance operations of the Space Shuttle and future aerospace vehicles.

2.0 STATISTICAL ANALYSIS

This section presents three topics on the statistical analysis for winds aloft developed specifically for this report. They are (1) wind sample size, (2) wind persistence and a discussion on random samples, and (3) bivariate normality tests for wind samples and a discussion on the properties of multivariate probability distribution functions.

2.1 Wind Data Sample Size

Ask a statistician: what is the sample size desired for a statistical analysis? A quick response might be: 'as large as possible'. However, the thoughtful statistician will ask for more information. What is the nature of the variable? What is the purpose of the analysis? What are the consequences of decisions based on the analysis? Some guidance on the determination of appropriate sample size is quoted from S.S. Wilkes in connection with the establishment of tolerance limits for quality control of manufactured products (Ref. 2.1) :"If the largest and smallest values of X in samples are used as tolerance limits and if we wish to state that the probability is 0.99 that such tolerance limits will include at least 99 percent of the universe (population), the sample size required is 660. If the probability is lowered to 0.95 of including at least 99 percent of the universe, with such tolerance limits, the size of sample required is 130." Wilkes continues: "The degree of stability expected of the tolerance limits for samples of size range 500 to 1000 appears to be of about the order of that demanded by the engineering statistician."

The probability density function that is the basis for the derivation of tolerance limits for the largest and smallest observed values of X as a function of sample size, n, is from Lindgren (Ref. 2.2):

$$f(Z) = n(n-1)(1-Z)Z^{n-2}, \quad 0 < Z < 1, \tag{2.1}$$

This function is independent of the universe (population) distribution function F(x). That is, no assumption is made as to the form of the probability distribution function of the variable. The probability that the observed limits in a sample will include the fraction P_u of the universe is obtained by:

$$P_u = n(n-1)\int_{P_s}^{1}(1-Z)\,Z^{n-2}\,dZ, \tag{2.2}$$

which is:

$$P_u = 1 + (n-1)P_s^{\,n} - nP_s^{\,n-1}. \tag{2.3}$$

where, P_s is the sample probability.

Eq. 2.3 can also be written

$$P_u = 1 + [(n-1) - \frac{n}{P_s}] P_s^n \ . \qquad (2.4)$$

Values of P_u calculated from Eq. 2.4 for $P_s = 0.95$ and 0.99 for commonly used wind data sample sizes n, are listed in Table 2.1 The sample sizes in Table 2.1 can be used to establish sample size requirements for empirical percentile values. For example: a sample size ≥ 130 is required to be 99 percent sure that the sample contains the 95^{th} percentile and a sample size $\geq$ 660 is required to be 99 percent sure that the sample contains the 99^{th} percentile value.

Table 2.1 Sample Size n Required for Probability P_s that the Sample is Within the P_u Percentile Value.

Sample size, n	Probability P_s	Percent of Universe P_u
130	0.95	99
660	0.99	99
114	0.95	98.0
114	0.99	31.6
150	0.95	99.6
150	0.99	44.3
228	0.95	99.99
228	0.99	66.6
473	0.99	95.0

If the procedure described above shows that the sample size is not large enough to justify using an empirical percentile for a particular engineering application, the analysis must advance to development of a theoretical probability function that can be demonstrated to be an adequate fit to the empirical distribution of the sample variable; this theoretical distribution would be used to obtain estimates of the percentile values.

2.2 Wind Persistence

An underlying principle for a normally distributed variate is that the data sample be a random variable from a homogeneous population. Wind data are grouped by monthly reference periods in an attempt to obtain homogeneous samples. To group wind samples for January with July or pooling wind samples for all months for the period of record

would certainly yield a heterogeneous sample. Some groupings would produce a mixture of several probability distributions. A series of twice daily Rawinsonde wind measurements for Cape Kennedy, Florida exhibited persistence. That is, there is a time dependence from wind at one time interval to the next. For a continuous variable, such as wind, a measure for persistence is the autocorrelation coefficient, which is sometimes referred to as the serial correlation coefficient. The following discussion is taken from Refs. 2.3 and 2.4 .

From an 8-year period of twice daily, 00Z (1900 EST) and 12Z (0700 EST), Rawinsonde wind database, the maximum wind speed in the 10 to 15-km altitude region for each 12-hour interval was computed. The autocorrelation coefficient (r_k) was computed for the 62 values of maximum wind speed for each January of the 8-year period (Fig. 2.1) using the equation from Kendall and Stuart (Ref. 2.5):

$$r_k = \frac{\frac{1}{n-k}\sum_{i=1}^{n-k}\left(x_i - \frac{1}{n-k}\sum_{i=1}^{n-k}x_i\right)\left(x_{i+k} - \frac{1}{n-k}\sum_{i=1}^{n-k}x_{i+k}\right)}{\left[\frac{1}{n-k}\sum_{i=1}^{n-k}\left\{x_i - \frac{1}{n-k}\sum_{i=1}^{n-k}x_i\right\}^2 \frac{1}{n-k}\sum_{i=1}^{n-k}\left\{x_{i+k} - \frac{1}{n-k}\sum_{i=1}^{n-k}x_{i+k}\right\}^2\right]^{\frac{1}{2}}} \qquad (2.5)$$

This equation accounts for the change in the variance and covariance for each lag, k. This function is preferred for a short time series. There is a large variation in the autocorrelation coefficients (Fig. 2.1.) for the eight January months, thus indicating greater time dependence (persistence) in some years than others. The thick line in Fig. 2.1 is the mean of the eight January autocorrelation coefficients. This mean autocorrelation coefficient is computed by using the Fisher's Z-transformed values for the autocorrelation coefficients for the eight years for like values of k:

$$Z = \frac{1}{2}\ln\left(\frac{1+r}{1-r}\right), \qquad (2.6)$$

The average Z for all like lags k, $\bar{Z}_k$, is converted to $\bar{r}_k$ by:

$$\bar{r}_k = \tanh^{-1}\bar{Z}_k , \qquad (2.7)$$

As a historical note: The maximum wind speed in the 10 to 15-km altitude region was an important launch commit criteria for the Saturn programs at MSFC.

The autocorrelation coefficients are used to compute the appropriate statistical time units (ASTU) (Ref. 2.6) required to obtain a statistically independent variable.

$$\text{ASTU} = \left(n + 2\sum(n-k)\,r_k\right)/n , \qquad (2.8)$$

where, the summation is terminated when r_k is not significantly different from zero. This is determined from the standard error of correlation coefficient, r_{σ_ε} ,

$$r_{\sigma_\varepsilon} = \left[\frac{1}{n-k}\right]^{1/2} \qquad (2.9)$$

Closely related to ASTU is the effective number of random ordinates (variables) ENRO given by:

$$\text{ENRO} = \frac{n^2}{n + 2\sum(n - k)\, r_k} \qquad (2.10)$$

Table 2.2 presents examples for the mean time interval between uncorrelated scalar, zonal, and meridional wind components.

Table 2.2 Mean Time Interval (in days) Between Uncorrelated Winds at 12 km for January and July, Cape Kennedy, Florida

					January					
Years	1956	1957	1958	1959	1960	1961	1962	1963	$\bar{\tau}_0$	$\tilde{\tau}_0$
Scalar	3.45	4.39	2.10	1.88	7.45	2.28	8.89	1.92	4.04	3.54
Zonal	3.59	4.38	2.08	2.01	6.70	2.54	8.95	2.34	4.07	3.43
Meridional	3.78	2.41	1.66	1.28	1.71	1.52	4.12	1.35	2.23	1.86
					July					
Scalar	2.26	1.61	1.73	2.43	1.28	1.29	3.00	1.74	1.92	1.70
Zonal	2.87	2.13	4.68	4.26	3.06	2.39	1.60	2.86	2.98	2.72
Meridional	2.97	2.06	2.97	1.05	1.83	1.67	2.05	1.86	2.05	1.94

The monthly average, $\bar{\tau}_0$,computed from the eight year-months, and from the monthly average autocorrelation coefficients, $\tilde{\tau}_0$, are also presented. This table indicates that the wind is more persistent in some years than others. From the variation of the autocorrelations from year to year, it is concluded that the stochastic properties of the wind are significantly different from year to year. The monthly average autocorrelation coefficients for the wind speed plotted and analyzed for altitude versus lag times for January and July are presented in Figs. 2.2 and 2.3 respectively. The wind speeds are most highly correlated at 12 km, the height of maximum wind over Cape Kennedy. Near 21 km and below 1.5 km altitude the diurnal variability of wind speed in all the summer months is evidenced in Fig. 2.3 by the periodicity of the autocorrelation functions variability.

2.3 Tests for Bivariate Normality in Wind Data Samples

It is important to test wind data samples for bivariate normality in order to take advantage of the many statistical properties that can be derived from bivariate normal variables. A

major interest in the application of the bivariate normal probability function began in the late 1950's for aerospace vehicle applications. An early publication (1960) by Vaughan (Ref. 2.7) gives the necessary bivariate normal statistical parameters for wind. Crutcher and Baer (1962) describe bivariate normal probability ellipses for wind (Ref. 2.8). It was not until Henry (1963) that the multivariate normal distribution was used to model the wind profile (Ref.2.9).

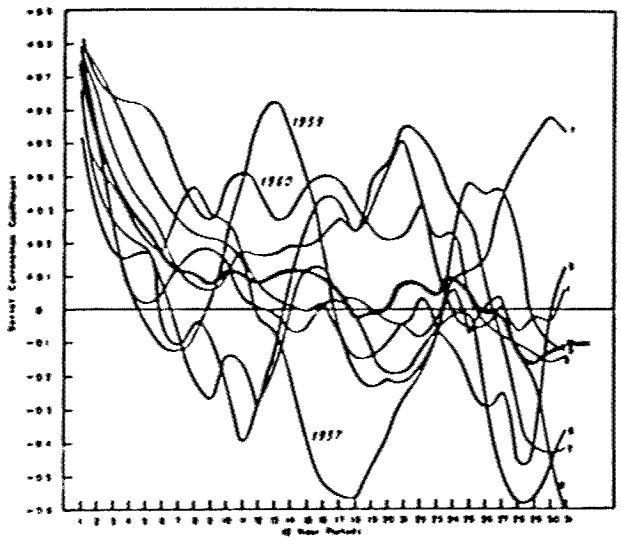

Figure 2.1 Autocorrelation Coefficients for Maximum Wind Speed, 10 to 15-km layer, Cape Kennedy, FL, January 1956-63

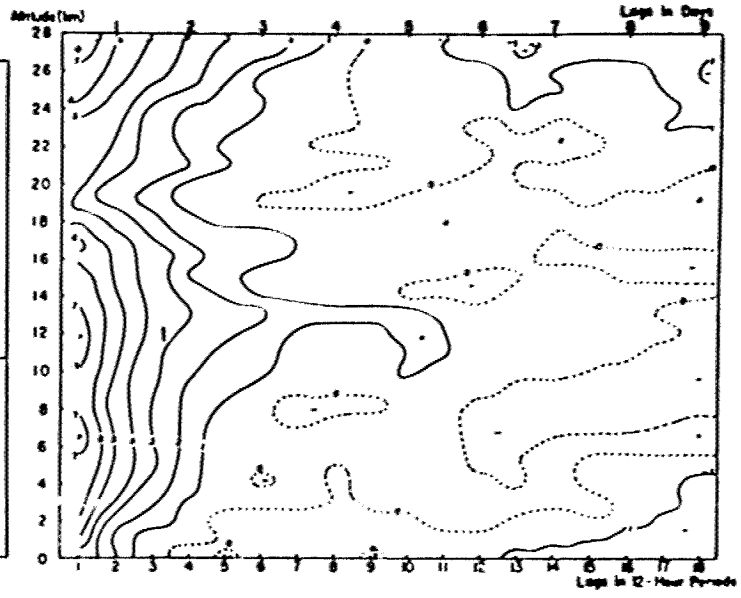

Figure 2.2 Average January Autocorrelation Coefficients for Wind Speed, Cape Kennedy, FL, 1956-1963

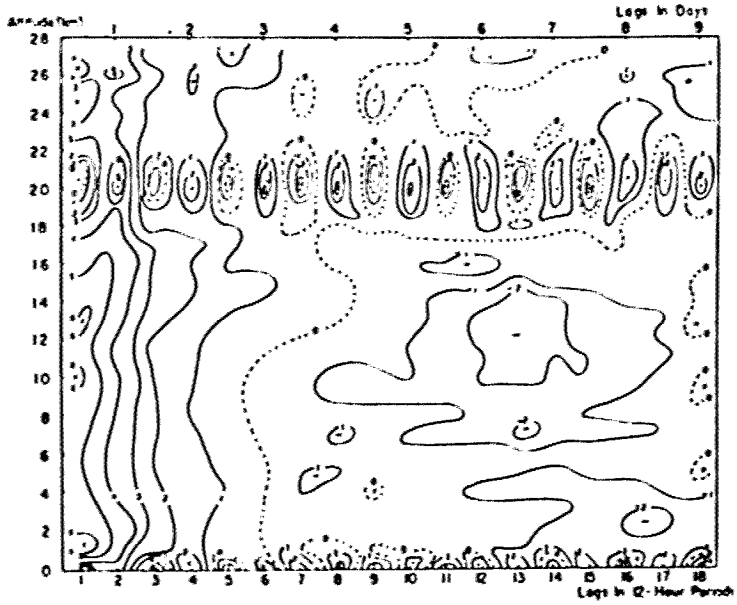

Figure 2.3 Average July Autocorrelation Coefficients for Wind Speed, Cape Kennedy, FL, 1956-1963

The usual procedure is to test the wind components for univariate normality using the Chi-square test or the Kolmogorov-Smirov (K-S) test, and if accepted assume that the wind sample is bivariate normally distributed. It is a necessary but not sufficient condition that the components be normally distributed for the joint distribution to be bivariate normally distributed.

Two tests for bivariate normality are applied to wind data samples for Cape Canaveral, Florida. The first test follows that by Crutcher and Falls (Ref. 2.10). This test is based on a comparison of the theoretical and sample numbers of wind vectors that lie outside bivariate normal probability ellipses. The 96 percent confidence bands are derived by simulating a bivariate normal distribution with a sample size of 10,000. A modification of the methodology used in Ref. 2.10 for the two dimensional case with some changes in notation is presented herein.

The bivariate normal probability density function is:

$$f(x,y) = \frac{1}{2\sigma_x\sigma_y\sqrt{1-\rho^2}}\exp\left[-\left\{\left(\frac{x-\bar{x}}{\sigma_x}\right)^2 - \frac{2\rho(x-\bar{x})(y-\bar{y})}{\sigma_x\sigma_y} + \left(\frac{y-\bar{y}}{\sigma_y}\right)^2\right\}\right] \quad (2.11)$$

This function is completely defined by the five parameters: the mean values, $\bar{x}$, $\bar{y}$, the standard deviations σ_x, σ_y; and the correlation coefficient, ρ, which is a measure of the association between the two variables, x and y. When the exponent of Eq. 2.11 is set equal to a constant, λ^2,

$$\left(\frac{x-\bar{x}}{\sigma_x}\right)^2 - 2\rho\frac{(x-\bar{x})(y-\bar{y})}{\sigma_x\sigma_y} + \left(\frac{y-\bar{y}}{\sigma_y}\right)^2 = \lambda^2 \quad (2.12)$$

Eq. 2.12 forms a family of ellipses of equal probability density centered on the centroid $(\bar{x}, \bar{y})$. The double integration of f(x,y) over the region bounded by the contours of equal probability density yields the probability that the variables (x and y) will lie within the probability ellipses, $P(\lambda)$. This is expressed by:

$$P(\lambda) = \iint_{R(\lambda)} f(x,y)\,dxdy \quad (2.13)$$

which yields,

$$P(\lambda) = 1 - \exp\left[-\frac{\lambda^2}{2(1-\rho^2)}\right] \quad (2.14)$$

Solving 2.14 for λ^2:

$$\lambda^2 = -2(1-\rho^2)\ln[1-P(\lambda)] \tag{2.15}$$

The correlation coefficient in Eq. 2.15 can be set equal to zero by rotation of the coordinate system by an angle ψ defined by:

$$\Psi = \frac{1}{2}\tan^{-1}\left[\frac{2\rho\sigma_x\sigma_y}{\left|\sigma_x^2 - \sigma_y^2\right|}\right] \tag{2.16}$$

Thus,
$$\lambda^2 = -2\ln[1-P(\lambda)] \tag{2.17}$$

For common logarithms (log) Eq. 2.17 becomes:

$$\lambda^2 = -4.605218\log[1-P(\lambda)] \tag{2.18}$$

Table 2.3 presents the selected values for the probability ellipses used to test the Kennedy Space Center (KSC) wind vector data samples for bivariate normality. A method for calculating probability ellipses is given in the Appendix.

Table 2.3 Selected values for probability ellipses and λ^2

$P(\lambda)$	$[1 - P(\lambda)]$	λ^2	$\log_{10}[1 - P(\lambda)]$
0	1.00	0.0000	0.000000
.10	.90	0.2010	-0.04576
.20	.80	0.4463	-0.09691
.30	.70	0.7133	-0.15490
.40	.60	1.02165	-0.22185
.50	.50	1.3863	-0.30103
.60	.40	1.8326	-0.39794
.70	.30	2.4079	-0.52288
.80	.20	3.21888	-0.69897
.85	.15	3.7942	-0.82391
.90	.10	4.6052	-1.00000
.9250	.0750	5.1053	-1.12494
.9500	.0500	5.9915	-1.301030
.9750	.0250	7.3778	-1.60206
.9900	.0100	9.2103	-2.00000
.9985	.0015	13.0045	-2.82391
.9990	.0010	13.8155	-3.00000

For this application there is no loss in the generalization by setting $\bar{x} = \bar{y} = 0$ in Eq. 2.12.

Rather than performing a simulation of the bivariate normal distribution to compute the confidence bands on Eq. 2.18 as was done in Ref. 2.10, a distribution free confidence

bound is used for this purpose. If all data points lie within the confidence bounds, the wind data sample is considered to be bivariate normally distributed. The equation for the lower and upper 95 percent confidence band, CL, is:

$$CL = \frac{n}{n+t^2}\left[P+\frac{t^2}{2n} \pm t\left\{P\frac{(1-P)}{n}+\left(\frac{t}{2n}\right)^2\right\}^{\frac{1}{2}}\right], \qquad (2.19)$$

where, t = 1.96 for the 95 percent confidence band.

The second test is called the quadrant test in which the probability of the sample wind vectors in each quadrant is compared with the theoretical bivariate normal probability value of 0.25 for each quadrant. Each wind vector in the data sample is converted to the zonal (u) and meridional (v) components from which the mean components ($\bar{u}$, $\bar{v}$) are subtracted and then the coordinate axes rotated by an angle (ψ) to eliminate the correlation coefficient using Eq. 2.16. This operation establishes the four quadrants, each containing a probability 0.25 for the theoretical bivariate normal variables. The number of observed wind vectors that lie in each quadrant is then computed. If the sample counts for the wind vectors in each quadrant are one-fourth of the total sample, then there would be perfect agreement with the symmetry of the bivariate normal distribution. This is a necessary but not a sufficient condition for a sample to be bivariate normally distributed. The schematic in Fig. 2.4 will aid in understanding these operations.

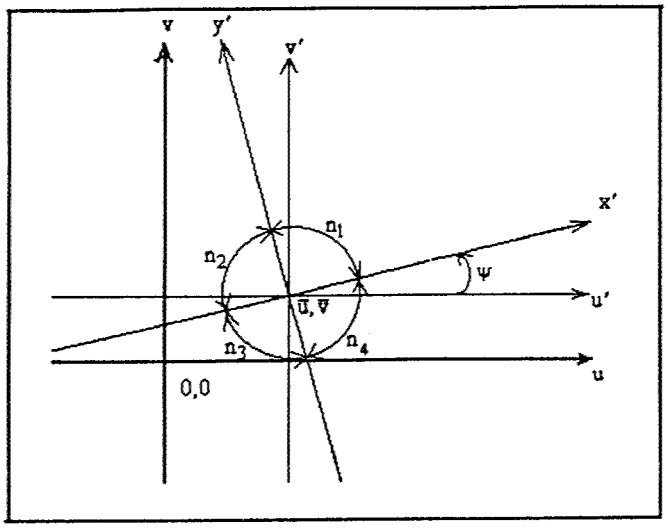

Figure 2.4 Schematic for bivariate normal test

The sample counts for the quadrants, n_1, n_2, n_3, and n_4, may deviate from being exactly 1/4 the sample size n. The chi-square test is then used to accept or reject the sample as being bivariate normally distributed. The chi-square, χ^2, value is computed by:

$$\chi^2 = \frac{\left[\left(n_1 - \frac{n}{4}\right)^2 + \left(n_2 - \frac{n}{4}\right)^2 + \left(n_3 - \frac{n}{4}\right)^2 + \left(n_4 - \frac{n}{4}\right)^2\right]}{n/4} \qquad (2.20)$$

If the value for χ^2 is ≤ 3.84 (for one degree of freedom) then the sample is accepted as bivariate normally distributed at the five percent level of significance.

2.4 Bivariate Normal Tests Applied to Wind Samples

The wind data samples selected to illustrate the bivariate normal test are for Cape Canaveral (February) using the 19-years twice daily complete sample (n = 1074) and every fifth sample (n=215). The probability ellipses from the complete data sample, n = 1074, are shown in Fig. 2.5 for the 8-km altitude winds and Fig. 2.6 for the 12-km altitude winds merely for the purpose of illustrating the wind data sample.

As shown Sec. 2.2 these wind vectors (Figs. 2.5 and 2.6) are not from a random sample because of the autocorrelation, i.e., persistence. The sample does not meet the criteria for randomness. Hence, the sample may not be bivariate normally distributed. The two tests previously described for bivariate normality are applied to the complete wind sample. Next, only every fifth wind is selected from the complete sample which gives a sample size of 215. This arbitrary selection is based in part on a knowledge of the mean time between independent observation in an attempt to obtain a random wind sample. This reduced wind sample is also tested for bivariate normality. The ellipse test for bivariate normality for the 8-km altitude for the complete sample (Figure 2.7a) rejects the sample because one or more data points fall outside the 95 percent confidence bands and accepts the sample for the 12-km winds. For the reduced wind samples all points fall within the 95 percent confidence bands (Figure 2.7b); therefore, the samples are accepted as being bivariate normally distributed at both 8-km and 12-km altitude.

The quadrant test for bivariate normality is applied to the complete wind sample and the reduced wind sample at both the 8-km and 12-km altitude. The complete wind sample is rejected as being bivariate normally distributed using the quadrant test but accepted for the reduced sample. These results are summarized in Table 2.4 for all altitudes for the complete and reduced wind data samples. Heterogeneous wind data samples occur as mixed distributions at KSC in the boundary layer due to the land and sea breeze. The wind samples for 12Z and 00Z are at 0700 hours EST and 1900 hours EST. This analysis illustrates that large wind data samples which are not random may not be bivariate normally distributed. As seen in Table 2.4 a random sample of wind data in the 3 to 17-km altitude layer passes the test for normality. This is the altitude region in which aerospace vehicles are most sensitive to the wind profile during ascent. Further study is indicated to make a more careful selection for randomness in the wind data samples and to isolate the systematic diurnal variation.

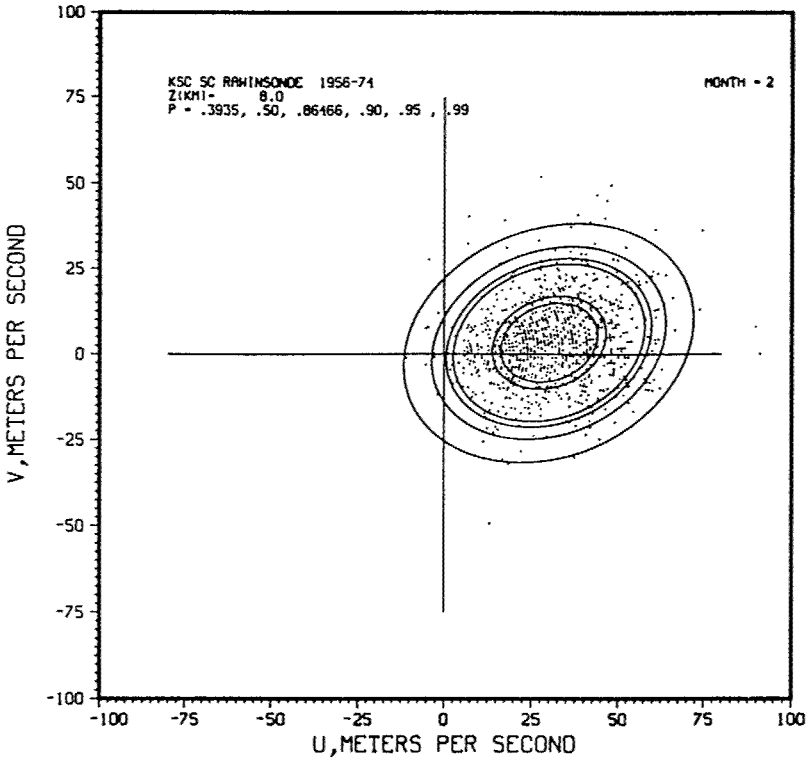

Figure 2.5 Probability ellipses for February wind sample (n = 1074) at 8-km altitude, Cape Canaveral, FL

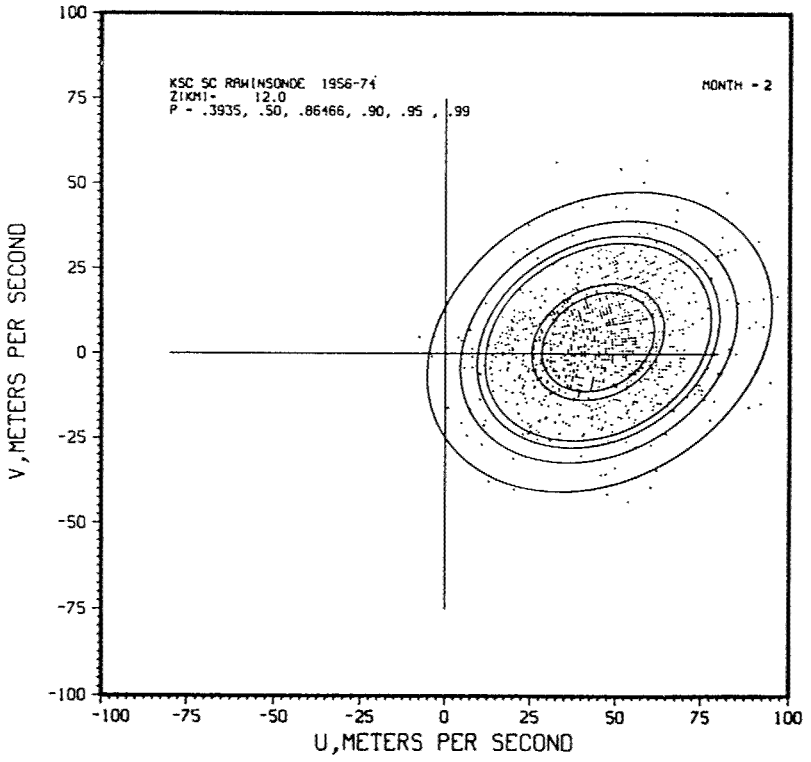

Figure 2.6 Probability ellipses for February wind sample (n = 1074) at 12-km altitude, Cape Canaveral, FL

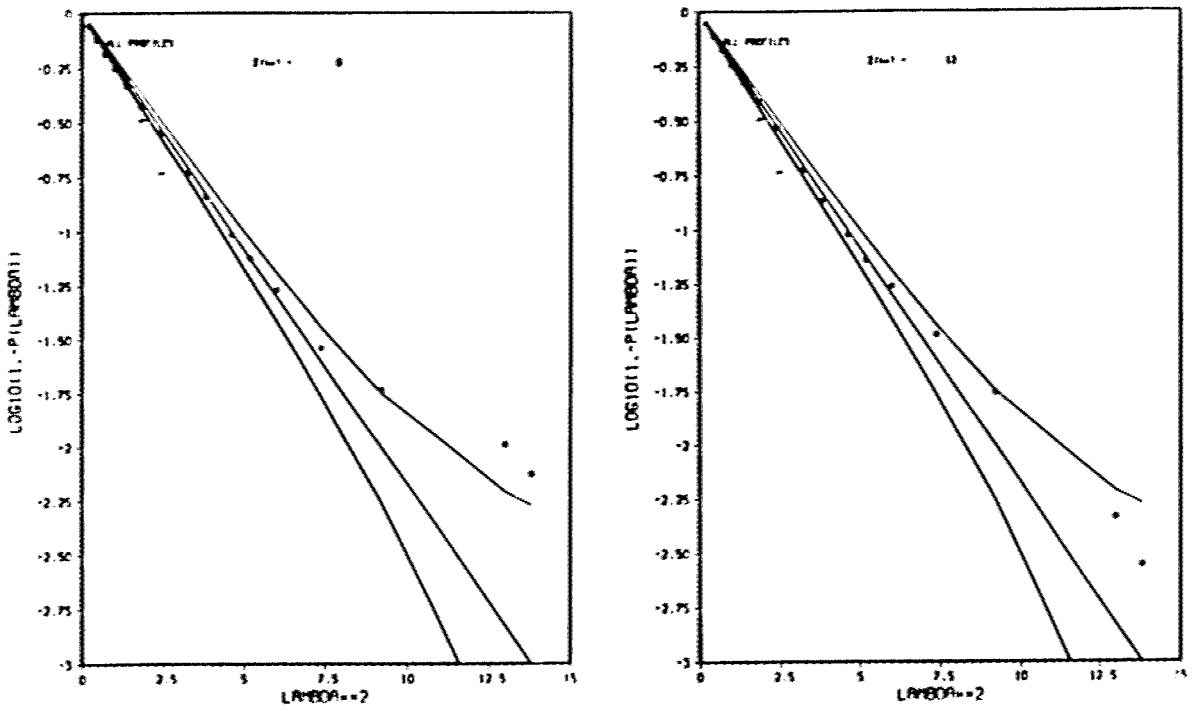

Figure 2.7a Bivariate normal probability wind ellipses test with 95 percent confidence interval for 8-km and 12-km altitude for sample size n = 1074, February, KSC

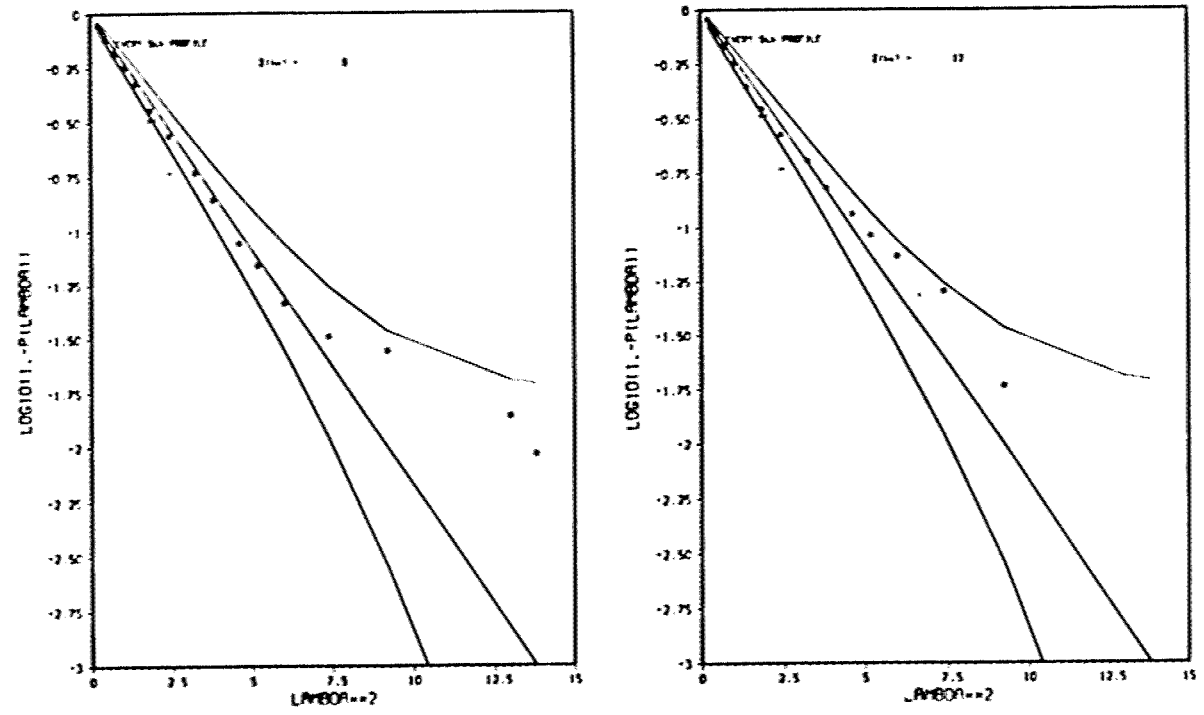

Figure 2.7b Bivariate normal probability wind ellipses test with 95 percent confidence interval for 8-km and 12-km altitude for sample size n = 215, February, KSC

Table 2.4 Tests for KSC February Winds for Bivariate Normality for Complete Sample twice daily for 19 years, n=1074 and for Reduced Sample every 5th data point, n=215

Altitude km	Complete Sample		Reduced Sample	
	Ellipse test	Quadrant test	Ellipse test	Quadrant test
0	R	R	A	R
1				R
2				A
3				
4				
5		R		
6		A		
7		A		
8		R		
9	R	A		
10	A	R		
11	A	R		
12	A	R		
13	A	A		
14	A	A		
15	R	A		
16		A		
17		A		A
18		R		R
19				R
20			A	A
21			R	R
22				A
23		R		
24		A		
25		R		
26		R		A
27	R	R	R	R

(1) R = Rejection A = Acceptance for 95% confidence interval

(2) Quadrant test Chi-square test with one degree of freedom 95% critical value is 3.84, Rejection if $\geq$3.84, Acceptance if <3.84.

It was stated in the beginning of this section that there is an advantage in using the bivariate normal probability distribution for winds because many other probability functions can be derived from the five parameters that define the bivariate normal distribution. For wind data samples the five parameters are the zonal and meridional components means $(\bar{u}$ and $\bar{v})$, the standard deviation (s_u and s_v) and the correlation coefficient between the u and v wind components, r(u, v). Ref. 2.11 gives the general probability functions and some special cases for wind statistics that can be derived from the properties of the bivariate normal distribution. These functions include:

1. The joint probability between the zonal and meridional wind components, i.e., bivariate normal probability ellipses.
2. The marginal distributions for u and v wind components are univariate normally distributed.
3. The wind speed is derived as a generalized Rayleigh distribution.
4. The frequency distribution for wind direction is derived.
5. The mean values for $\bar{u}$ and $\bar{v}$ and the interpercentile range rotated through 360 degrees are derived
6. The conditional distribution for wind speed, given a wind direction, is derived. This distribution is called a wind rose when empirical methods are used.
7. The sum and differences of two normally distributed variables are univariate normally distributed.
8. The conditional distribution for one wind component, given the other, is univariate normally distributed.

Practical equations are presented (Ref. 2.11) to compute these wind models given the wind parameters at discrete altitudes at one-km intervals. The above listed probability functions are used to model the winds at discrete altitude levels for the 17 published Range Reference Atmospheres (Ref. 2.12). These Range Reference Atmospheres also contain statistical parameters, means, standard deviations, and skewness coefficients, for pressure, temperature and density, and for water vapor pressure, virtual temperature, and dewpoint temperature. All statistical parameters are tabulated in a standard manner by monthly and annual reference periods for the Range Reference Atmospheres.

Assuming that the wind vectors at any altitude are bivariate normally distributed and the wind vectors at two altitudes are quadravariate normally distributed, then the differences in the wind vectors (wind shears) between two altitudes are bivariate normally distributed and the conditional wind shears between two altitudes, given a wind vector at one altitude are bivariate normally distributed. The conditional wind shears were used in the wind profile model used for the Space Shuttle design for ascent structural loads and performance (Ref. 2.10). Further details on the model are presented in Section 3.2.3. Later, an improvement was made (Section 3.3) to the original Space Shuttle wind profile model which eliminated the simplifying assumptions used in the earlier model and derived the wind profiles directly from conditional wind vectors rather than

Table 2.5 Interlevel and intralevel coefficients of linear correlation between like wind components

STATION	ELEVATION MSL (meters)	LOCATION LATITUDE	LOCATION LONGITUDE	PERIOD OF DATA
PATRICK AFB, FLORIDA	7	28° 14' N	80° 36' W	JAN. 1, 1956 to NOV. 17, 1956
CAPE KENNEDY, FLORIDA	5	28° 29' N	80° 33' W	NOV. 18, 1956 to DEC. 31, 1963

NOTES: ZONAL MEAN VALUES - POSITIVE FOR WIND COMPONENTS FROM WEST, UNIT ms^{-1}
MERIDIONAL MEAN VALUES - POSITIVE FOR WIND COMPONENTS FROM SOUTH, UNIT ms^{-1}
SD - STANDARD DEVIATION, UNIT ms^{-1}

INTRALEVEL CORRELATION COEFFICIENTS
BETWEEN ZONAL AND MERIDIONAL WIND COMPONENTS ARE THE VALUES BETWEEN THE DIAGONAL LINES.

INTERLEVEL CORRELATION COEFFICIENTS
FOR MERIDIONAL WIND COMPONENTS USE VALUES ABOVE AND TO THE RIGHT OF THE DIAGONAL LINES.
FOR ZONAL WIND COMPONENTS USE VALUES BELOW AND TO THE LEFT OF THE DIAGONAL LINES.

FEBRUARY

ZONAL AND MERIDIONAL WIND COMPONENT CORRELATIONS

CAPE KENNEDY, FLORIDA

PREPARED FROM EIGHT YEARS, TWICE DAILY, SERIALLY COMPLETE RECORDS BY:
TERRESTRIAL ENVIRONMENT BRANCH, AEROSPACE ENVIRONMENT DIVISION
AERO-ASTRODYNAMICS LABORATORY
GEORGE C. MARSHALL SPACE FLIGHT CENTER, HUNTSVILLE, ALABAMA

NUMBER OF OBSERVATIONS FOR EACH ALTITUDE LEVEL: 452

ALTITUDE (MSL) km	ZONAL MEAN	SD	ALTITUDE (MSL) km / MERIDIONAL MEAN	SFC	1	2	3	4	5	6	7	8	9	10	11	12	13	14	15	16	17	18	19	20	21	22	23	24	25	26	27
			SD	-0.04	2.41	1.83	1.96	2.23	2.44	3.03	3.52	3.81	4.04	3.93	4.06	4.20	4.02	3.67	2.75	2.37	1.44	0.92	0.83	0.72	-0.23	-0.68	-0.26	-0.62	-0.53	-0.42	-0.14
				3.92	6.46	6.42	7.03	7.77	8.72	9.28	10.14	11.22	12.31	13.84	15.01	14.91	12.51	11.29	9.62	8.45	7.18	6.02	4.88	4.19	5.01	6.46	6.76	7.97	7.69	6.62	3.96
SFC	0.54	3.82	-.281	.679	.520	.425	.393	.266	.193	.132	.103	.051	.011	-.014	-.036	-.080	-.027	-.010	-.039	.004	-.020	.000	-.040	.021	.005	.003	.022	.111	.140	.159
1	3.74	7.08	.645	-.078	.824	.679	.608	.497	.385	.272	.209	.160	.142	.087	.065	-.024	.021	.074	.051	.089	.078	.075	-.028	.074	-.012	.011	-.022	.103	.130	.137
2	7.71	7.49	.602	.836	-.053	.851	.757	.671	.589	.478	.435	.337	.348	.280	.259	.170	.192	.235	.218	.270	.254	.208	.104	.091	-.002	.002	-.021	.126	.124	.139
3	11.15	8.31	.593	.721	.685	-.052	.857	.811	.731	.638	.593	.539	.497	.426	.399	.315	.338	.356	.359	.392	.340	.268	.168	.110	.007	.020	.029	.167	.170	.186
4	14.21	9.37	.576	.656	.812	.922	-.078	.918	.830	.741	.681	.622	.564	.499	.470	.375	.410	.410	.405	.441	.378	.321	.234	.110	-.004	.039	.071	.193	.204	.230
5	17.63	10.57	.544	.594	.763	.860	.535	-.098	.910	.816	.746	.680	.628	.554	.526	.438	.454	.494	.454	.489	.425	.357	.240	.119	-.001	.037	.061	.175	.205	.241
6	21.36	11.74	.543	.553	.714	.818	.901	.950	.079	.912	.840	.778	.709	.639	.606	.552	.557	.565	.537	.547	.502	.419	.284	.117	.006	.038	.059	.134	.168	.199
7	24.82	13.27	.501	.514	.679	.783	.866	.912	.951	.155	.918	.848	.778	.713	.677	.634	.630	.620	.592	.580	.537	.429	.302	.131	.001	.057	.072	.119	.141	.161
8	28.15	14.98	.467	.483	.642	.752	.826	.881	.917	.956	.212	.928	.850	.781	.727	.706	.687	.629	.607	.588	.546	.430	.304	.104	.003	.051	.069	.109	.127	.160
9	31.98	16.90	.422	.437	.567	.710	.783	.832	.869	.859	.952	.275	.925	.858	.759	.749	.728	.650	.620	.594	.534	.447	.314	.092	.000	.052	.046	.090	.090	.141
10	35.43	18.21	.382	.387	.548	.668	.724	.773	.811	.835	.892	.946	.291	.933	.873	.780	.750	.686	.648	.634	.562	.485	.301	.117	.010	.063	.076	.100	.094	.162
11	38.89	19.37	.369	.357	.516	.644	.697	.729	.768	.794	.845	.908	.954	.342	.529	.824	.775	.705	.666	.638	.567	.499	.324	.119	.037	.085	.066	.094	.072	.152
12	41.59	18.66	.364	.363	.529	.642	.686	.715	.750	.772	.818	.867	.904	.938	.350	.874	.813	.734	.717	.684	.616	.537	.357	.093	.031	.106	.081	.071	.090	.158
13	41.56	16.97	.357	.340	.506	.613	.659	.689	.731	.755	.795	.826	.854	.873	.859	.438	.881	.789	.755	.715	.660	.559	.368	.051	-.020	.090	.107	.012	.015	.098
14	38.88	14.39	.330	.251	.413	.535	.561	.635	.679	.706	.744	.773	.806	.823	.834	.865	.414	.868	.796	.755	.705	.591	.391	.098	-.021	.078	.105	.045	.052	.096
15	34.17	12.47	.311	.257	.409	.521	.569	.615	.655	.670	.691	.716	.761	.766	.805	.846	.878	.275	.877	.792	.754	.668	.410	.158	.070	.124	.132	.061	.081	.168
16	29.41	10.85	.291	.214	.374	.486	.532	.564	.608	.619	.636	.655	.696	.712	.763	.771	.786	.849	.207	.837	.772	.675	.446	.230	.127	.140	.165	.059	.122	.165
17	23.80	9.64	.243	.171	.313	.423	.497	.525	.560	.578	.606	.619	.631	.652	.691	.701	.719	.731	.824	.157	.812	.703	.497	.271	.192	.185	.196	.178	.115	.137
18	17.56	8.56	.232	.160	.294	.386	.466	.485	.505	.526	.542	.541	.535	.551	.578	.591	.587	.562	.559	.751	.248	.749	.485	.334	.212	.207	.223	.157	.141	.164
19	11.58	7.86	.243	.173	.290	.372	.429	.447	.472	.485	.488	.497	.485	.498	.508	.521	.512	.507	.575	.588	.612	.263	.521	.349	.314	.263	.256	.214	.150	.095
20	6.55	7.73	.148	.092	.205	.290	.292	.320	.327	.328	.346	.351	.370	.359	.347	.377	.410	.408	.469	.466	.384	.516	.278	.454	.317	.318	.235	.214	.194	.099
21	3.47	7.16	-.024	-.067	.030	.069	.108	.094	.097	.103	.119	.149	.166	.178	.154	.162	.249	.170	.244	.272	.343	.334	.442	.159	.595	.363	.250	.284	.175	.060
22	1.68	7.46	-.031	-.080	-.033	-.005	.053	.048	.078	.058	.066	.096	.135	.150	.148	.135	.386	.145	.209	.252	.289	.366	.353	.595	.122	.522	.371	.369	.225	.096
23	0.64	7.26	-.098	-.092	-.041	-.045	-.012	-.024	-.000	.004	.011	.013	.052	.076	.039	.047	.100	.097	.147	.189	.225	.267	.422	.468	.611	.148	.490	.332	.215	.115
24	0.45	7.28	-.137	-.111	-.077	-.053	-.003	.002	.033	.028	.059	.080	.114	.123	.100	.095	.156	.144	.138	.198	.233	.231	.225	.507	.528	.540	.107	.384	.155	.122
25	0.35	7.79	-.085	-.097	-.071	-.033	.010	.018	.051	.048	.028	.036	.074	.092	.059	.065	.115	.143	.156	.157	.212	.219	.156	.212	.495	.456	.569	.159	.023	.248
26	0.71	8.29	-.083	-.060	-.057	-.022	.006	.001	.032	.014	.021	.026	.055	.054	.031	.042	.102	.110	.133	.148	.184	.206	.191	.241	.330	.444	.618	.695	.595	.377
27	0.86	9.08	-.112	-.065	-.040	-.017	.001	.012	.030	.006	.014	.021	.057	.056	.044	.028	.098	.110	.108	.131	.187	.195	.130	.214	.340	.330	.615	.664	.515	.278

Table 2.6 Interlevel and intralevel coefficients of linear correlations between unlike wind components

STATION	ELEVATION MSL (meters)	LATITUDE	LONGITUDE	PERIOD OF DATA
PATRICK AFB, FLORIDA	7	28°14' N	80°36' W	JAN 1, 1956 to NOV 17, 1958
CAPE KENNEDY, FLORIDA	5	28°29' N	80°33' W	NOV 18, 1958 to DEC 31, 1963

INTRALEVEL CORRELATION COEFFICIENTS
BETWEEN ZONAL AND MERIDIONAL WIND COMPONENTS AT THE SAME ALTITUDES ARE VALUES BETWEEN THE DIAGONAL LINES

CROSSLEVEL CORRELATION COEFFICIENTS
FOR MERIDIONAL WIND, USE ALTITUDE VALUES ACROSS THE TOP OF THE TABLE WITH ZONAL WIND, GIVEN BY ALTITUDE IN THE VERTICAL COLUMN AT THE LEFT

FEBRUARY

ZONAL AND MERIDIONAL WIND COMPONENT CORRELATIONS

CAPE KENNEDY, FLORIDA

NOTES: ZONAL MEAN VALUES - POSITIVE FOR WIND COMPONENTS FROM WEST, UNIT $m s^{-1}$
MERIDIONAL MEAN VALUES - POSITIVE FOR WIND COMPONENTS FROM SOUTH, UNIT $m s^{-1}$
SD - STANDARD DEVIATION, UNIT $m s^{-1}$

PREPARED FROM EIGHT YEARS, TWICE DAILY, SERIALLY COMPLETE RECORDS BY:
TERRESTRIAL ENVIRONMENT BRANCH, AEROSPACE ENVIRONMENT DIVISION
AERO-ASTRODYNAMICS LABORATORY
GEORGE C. MARSHALL SPACE FLIGHT CENTER, HUNTSVILLE, ALABAMA

NUMBER OF OBSERVATIONS FOR EACH ALTITUDE LEVEL: 452

ALTITUDE (MSL) km	ZONAL MEAN	SD	SFC	1	2	3	4	5	6	7	8	9	10	11	12	13	14	15	16	17	18	19	20	21	22	23	24	25	26	27
		MERIDIONAL MEAN	[illegible]	[illegible]	[illegible]	[illegible]	[illegible]	[illegible]	[illegible]	[illegible]	[illegible]	[illegible]	[illegible]	[illegible]	[illegible]	[illegible]	[illegible]	[illegible]	[illegible]	[illegible]	[illegible]	[illegible]	[illegible]	[illegible]	[illegible]	[illegible]	[illegible]	[illegible]	[illegible]	[illegible]
		SD	[illegible]	[illegible]	[illegible]	[illegible]	[illegible]	[illegible]	[illegible]	[illegible]	[illegible]	[illegible]	[illegible]	[illegible]	[illegible]	[illegible]	[illegible]	[illegible]	[illegible]	[illegible]	[illegible]	[illegible]	[illegible]	[illegible]	[illegible]	[illegible]	[illegible]	[illegible]	[illegible]	[illegible]
SFC	[illegible]	[illegible]	[illegible]	[illegible]	[illegible]	[illegible]	[illegible]	[illegible]	[illegible]	[illegible]	[illegible]	[illegible]	[illegible]	[illegible]	[illegible]	[illegible]	[illegible]	[illegible]	[illegible]	[illegible]	[illegible]	[illegible]	[illegible]	[illegible]	[illegible]	[illegible]	[illegible]	[illegible]	[illegible]	[illegible]
1	[illegible]	[illegible]	[illegible]	[illegible]	[illegible]	[illegible]	[illegible]	[illegible]	[illegible]	[illegible]	[illegible]	[illegible]	[illegible]	[illegible]	[illegible]	[illegible]	[illegible]	[illegible]	[illegible]	[illegible]	[illegible]	[illegible]	[illegible]	[illegible]	[illegible]	[illegible]	[illegible]	[illegible]	[illegible]	[illegible]
2	[illegible]	[illegible]	[illegible]	[illegible]	[illegible]	[illegible]	[illegible]	[illegible]	[illegible]	[illegible]	[illegible]	[illegible]	[illegible]	[illegible]	[illegible]	[illegible]	[illegible]	[illegible]	[illegible]	[illegible]	[illegible]	[illegible]	[illegible]	[illegible]	[illegible]	[illegible]	[illegible]	[illegible]	[illegible]	[illegible]
3	[illegible]	[illegible]	[illegible]	[illegible]	[illegible]	[illegible]	[illegible]	[illegible]	[illegible]	[illegible]	[illegible]	[illegible]	[illegible]	[illegible]	[illegible]	[illegible]	[illegible]	[illegible]	[illegible]	[illegible]	[illegible]	[illegible]	[illegible]	[illegible]	[illegible]	[illegible]	[illegible]	[illegible]	[illegible]	[illegible]
4	[illegible]	[illegible]	[illegible]	[illegible]	[illegible]	[illegible]	[illegible]	[illegible]	[illegible]	[illegible]	[illegible]	[illegible]	[illegible]	[illegible]	[illegible]	[illegible]	[illegible]	[illegible]	[illegible]	[illegible]	[illegible]	[illegible]	[illegible]	[illegible]	[illegible]	[illegible]	[illegible]	[illegible]	[illegible]	[illegible]
5	[illegible]	[illegible]	[illegible]	[illegible]	[illegible]	[illegible]	[illegible]	[illegible]	[illegible]	[illegible]	[illegible]	[illegible]	[illegible]	[illegible]	[illegible]	[illegible]	[illegible]	[illegible]	[illegible]	[illegible]	[illegible]	[illegible]	[illegible]	[illegible]	[illegible]	[illegible]	[illegible]	[illegible]	[illegible]	[illegible]
6	[illegible]	[illegible]	[illegible]	[illegible]	[illegible]	[illegible]	[illegible]	[illegible]	[illegible]	[illegible]	[illegible]	[illegible]	[illegible]	[illegible]	[illegible]	[illegible]	[illegible]	[illegible]	[illegible]	[illegible]	[illegible]	[illegible]	[illegible]	[illegible]	[illegible]	[illegible]	[illegible]	[illegible]	[illegible]	[illegible]
7	[illegible]	[illegible]	[illegible]	[illegible]	[illegible]	[illegible]	[illegible]	[illegible]	[illegible]	[illegible]	[illegible]	[illegible]	[illegible]	[illegible]	[illegible]	[illegible]	[illegible]	[illegible]	[illegible]	[illegible]	[illegible]	[illegible]	[illegible]	[illegible]	[illegible]	[illegible]	[illegible]	[illegible]	[illegible]	[illegible]
8	[illegible]	[illegible]	[illegible]	[illegible]	[illegible]	[illegible]	[illegible]	[illegible]	[illegible]	[illegible]	[illegible]	[illegible]	[illegible]	[illegible]	[illegible]	[illegible]	[illegible]	[illegible]	[illegible]	[illegible]	[illegible]	[illegible]	[illegible]	[illegible]	[illegible]	[illegible]	[illegible]	[illegible]	[illegible]	[illegible]
9	[illegible]	[illegible]	[illegible]	[illegible]	[illegible]	[illegible]	[illegible]	[illegible]	[illegible]	[illegible]	[illegible]	[illegible]	[illegible]	[illegible]	[illegible]	[illegible]	[illegible]	[illegible]	[illegible]	[illegible]	[illegible]	[illegible]	[illegible]	[illegible]	[illegible]	[illegible]	[illegible]	[illegible]	[illegible]	[illegible]
10	[illegible]	[illegible]	[illegible]	[illegible]	[illegible]	[illegible]	[illegible]	[illegible]	[illegible]	[illegible]	[illegible]	[illegible]	[illegible]	[illegible]	[illegible]	[illegible]	[illegible]	[illegible]	[illegible]	[illegible]	[illegible]	[illegible]	[illegible]	[illegible]	[illegible]	[illegible]	[illegible]	[illegible]	[illegible]	[illegible]
11	[illegible]	[illegible]	[illegible]	[illegible]	[illegible]	[illegible]	[illegible]	[illegible]	[illegible]	[illegible]	[illegible]	[illegible]	[illegible]	[illegible]	[illegible]	[illegible]	[illegible]	[illegible]	[illegible]	[illegible]	[illegible]	[illegible]	[illegible]	[illegible]	[illegible]	[illegible]	[illegible]	[illegible]	[illegible]	[illegible]
12	[illegible]	[illegible]	[illegible]	[illegible]	[illegible]	[illegible]	[illegible]	[illegible]	[illegible]	[illegible]	[illegible]	[illegible]	[illegible]	[illegible]	[illegible]	[illegible]	[illegible]	[illegible]	[illegible]	[illegible]	[illegible]	[illegible]	[illegible]	[illegible]	[illegible]	[illegible]	[illegible]	[illegible]	[illegible]	[illegible]
13	[illegible]	[illegible]	[illegible]	[illegible]	[illegible]	[illegible]	[illegible]	[illegible]	[illegible]	[illegible]	[illegible]	[illegible]	[illegible]	[illegible]	[illegible]	[illegible]	[illegible]	[illegible]	[illegible]	[illegible]	[illegible]	[illegible]	[illegible]	[illegible]	[illegible]	[illegible]	[illegible]	[illegible]	[illegible]	[illegible]
14	[illegible]	[illegible]	[illegible]	[illegible]	[illegible]	[illegible]	[illegible]	[illegible]	[illegible]	[illegible]	[illegible]	[illegible]	[illegible]	[illegible]	[illegible]	[illegible]	[illegible]	[illegible]	[illegible]	[illegible]	[illegible]	[illegible]	[illegible]	[illegible]	[illegible]	[illegible]	[illegible]	[illegible]	[illegible]	[illegible]
15	[illegible]	[illegible]	[illegible]	[illegible]	[illegible]	[illegible]	[illegible]	[illegible]	[illegible]	[illegible]	[illegible]	[illegible]	[illegible]	[illegible]	[illegible]	[illegible]	[illegible]	[illegible]	[illegible]	[illegible]	[illegible]	[illegible]	[illegible]	[illegible]	[illegible]	[illegible]	[illegible]	[illegible]	[illegible]	[illegible]
16	[illegible]	[illegible]	[illegible]	[illegible]	[illegible]	[illegible]	[illegible]	[illegible]	[illegible]	[illegible]	[illegible]	[illegible]	[illegible]	[illegible]	[illegible]	[illegible]	[illegible]	[illegible]	[illegible]	[illegible]	[illegible]	[illegible]	[illegible]	[illegible]	[illegible]	[illegible]	[illegible]	[illegible]	[illegible]	[illegible]
17	[illegible]	[illegible]	[illegible]	[illegible]	[illegible]	[illegible]	[illegible]	[illegible]	[illegible]	[illegible]	[illegible]	[illegible]	[illegible]	[illegible]	[illegible]	[illegible]	[illegible]	[illegible]	[illegible]	[illegible]	[illegible]	[illegible]	[illegible]	[illegible]	[illegible]	[illegible]	[illegible]	[illegible]	[illegible]	[illegible]
18	[illegible]	[illegible]	[illegible]	[illegible]	[illegible]	[illegible]	[illegible]	[illegible]	[illegible]	[illegible]	[illegible]	[illegible]	[illegible]	[illegible]	[illegible]	[illegible]	[illegible]	[illegible]	[illegible]	[illegible]	[illegible]	[illegible]	[illegible]	[illegible]	[illegible]	[illegible]	[illegible]	[illegible]	[illegible]	[illegible]
19	[illegible]	[illegible]	[illegible]	[illegible]	[illegible]	[illegible]	[illegible]	[illegible]	[illegible]	[illegible]	[illegible]	[illegible]	[illegible]	[illegible]	[illegible]	[illegible]	[illegible]	[illegible]	[illegible]	[illegible]	[illegible]	[illegible]	[illegible]	[illegible]	[illegible]	[illegible]	[illegible]	[illegible]	[illegible]	[illegible]
20	[illegible]	[illegible]	[illegible]	[illegible]	[illegible]	[illegible]	[illegible]	[illegible]	[illegible]	[illegible]	[illegible]	[illegible]	[illegible]	[illegible]	[illegible]	[illegible]	[illegible]	[illegible]	[illegible]	[illegible]	[illegible]	[illegible]	[illegible]	[illegible]	[illegible]	[illegible]	[illegible]	[illegible]	[illegible]	[illegible]
21	[illegible]	[illegible]	[illegible]	[illegible]	[illegible]	[illegible]	[illegible]	[illegible]	[illegible]	[illegible]	[illegible]	[illegible]	[illegible]	[illegible]	[illegible]	[illegible]	[illegible]	[illegible]	[illegible]	[illegible]	[illegible]	[illegible]	[illegible]	[illegible]	[illegible]	[illegible]	[illegible]	[illegible]	[illegible]	[illegible]
22	[illegible]	[illegible]	[illegible]	[illegible]	[illegible]	[illegible]	[illegible]	[illegible]	[illegible]	[illegible]	[illegible]	[illegible]	[illegible]	[illegible]	[illegible]	[illegible]	[illegible]	[illegible]	[illegible]	[illegible]	[illegible]	[illegible]	[illegible]	[illegible]	[illegible]	[illegible]	[illegible]	[illegible]	[illegible]	[illegible]
23	[illegible]	[illegible]	[illegible]	[illegible]	[illegible]	[illegible]	[illegible]	[illegible]	[illegible]	[illegible]	[illegible]	[illegible]	[illegible]	[illegible]	[illegible]	[illegible]	[illegible]	[illegible]	[illegible]	[illegible]	[illegible]	[illegible]	[illegible]	[illegible]	[illegible]	[illegible]	[illegible]	[illegible]	[illegible]	[illegible]
24	[illegible]	[illegible]	[illegible]	[illegible]	[illegible]	[illegible]	[illegible]	[illegible]	[illegible]	[illegible]	[illegible]	[illegible]	[illegible]	[illegible]	[illegible]	[illegible]	[illegible]	[illegible]	[illegible]	[illegible]	[illegible]	[illegible]	[illegible]	[illegible]	[illegible]	[illegible]	[illegible]	[illegible]	[illegible]	[illegible]
25	[illegible]	[illegible]	[illegible]	[illegible]	[illegible]	[illegible]	[illegible]	[illegible]	[illegible]	[illegible]	[illegible]	[illegible]	[illegible]	[illegible]	[illegible]	[illegible]	[illegible]	[illegible]	[illegible]	[illegible]	[illegible]	[illegible]	[illegible]	[illegible]	[illegible]	[illegible]	[illegible]	[illegible]	[illegible]	[illegible]
26	[illegible]	[illegible]	[illegible]	[illegible]	[illegible]	[illegible]	[illegible]	[illegible]	[illegible]	[illegible]	[illegible]	[illegible]	[illegible]	[illegible]	[illegible]	[illegible]	[illegible]	[illegible]	[illegible]	[illegible]	[illegible]	[illegible]	[illegible]	[illegible]	[illegible]	[illegible]	[illegible]	[illegible]	[illegible]	[illegible]
27	[illegible]	[illegible]	[illegible]	[illegible]	[illegible]	[illegible]	[illegible]	[illegible]	[illegible]	[illegible]	[illegible]	[illegible]	[illegible]	[illegible]	[illegible]	[illegible]	[illegible]	[illegible]	[illegible]	[illegible]	[illegible]	[illegible]	[illegible]	[illegible]	[illegible]	[illegible]	[illegible]	[illegible]	[illegible]	[illegible]

from conditional wind shears. The improved wind profile model is based on the concept that: given a wind vector at any altitude, the conditional distribution of wind vectors at any other altitude is bivariate normal. The required statistical parameters to model the vector wind profile include all of the interlevel and intralevel correlation coefficients between the like and unlike wind components at any two selected altitudes and the means and standard deviations of the wind components at each altitude. These statistical parameters are required for the complete variance-covariance matrices. Examples of these statistical parameters for February at Cape Kennedy, FL. from Ref. 2.13 are illustrated in Table 2.5 for the interlevel and intralevel correlation coefficients for like wind components and in Table 2.6 for unlike wind components (note that the term "crosslevel" used in Table 2.6 denotes the interlevel correlation coefficients between unlike wind components). These parameters were derived from wind profile data sets as early as 1960 (Ref. 2.7) and 1968 (Ref. 2.13), but it was not until 1994 (see Section 3.3) that a direct application was made in a vector wind profile model.

The Global Reference Atmosphere Models (GRAM)

The original GRAM model, published in 1964 containing the atmospheric parameters (pressure, temperature, density) and wind components (Ref. 2.14 and 2.15) at latitude, longitude grid points versus altitude, was used to design the Shuttle Orbiter flight control system, aerodynamic heating, and reactor control system (RCS) requirements for the re-entry flight path from 121-km altitude half-way around the world to the landing site. The density and density perturbations from 80 to 35-km altitude are the most important atmospheric parameters for the Orbiter systems re-entry design. As more data and theoretical developments became available, updates for the GRAM were made in 1980, 1988, 1991 (Ref. 2.16, 2.17, 2.18) to the most improved model GRAM 1995 (Ref. 2.19). The GRAM-95 with modifications to merge with the site-specific RRA is being used for the X-33 design studies. The most valuable feature of the GRAM-95 is the computer code to simulate individual atmosphere and wind profiles along a vehicle trajectory in the altitude and space domain for which no other data are available.

2.5 References

2.1 Wilkes, S. S., "Determination of Sample Sizes for Setting Tolerance Limits". Annals of Mathematical Statistics, vol.12, pp. 91-96, 1941.

2.2 Lindgren, B. W., Statistical Theory, The Macmillian Company, New York, London, 1966, 1961 and 1962: First printing Library of Congress catalog card number: 61-8161.

2.3. Smith, Orvel E.: "The Application of Upper-Air Statistics for Space Vehicle Programs." Paper presented at the Second Conference on Climatology, Program of the 209th National Meeting of the American Meteorological Society, Asheville, North Carolina, October 22-25, 1962.

2.4. Smith, Orvel E., Falls, Lee W. and Brown, S. Clark: "Atmospheric Statistics for Aerospace Vehicle Design, Mission Planning and Operations." Paper in the Proceedings of the Third National Conference on Aerospace Meteorology, American Meteorological Society, New Orleans, LA, May 6-9, 1968.

2.5. Kendal, M. G. and Stuart, A., The Advanced Theory of Statistics, Volume II. 3rd edition, Hafter Publishing Company, 1951.

2.6. Brooks, C. E. P and Carruthers N.: Handbook of Statistical Methods in Meteorology. Her Majesty's Stationary Office, London, 1953.

2.7 Vaughan, W. W.: "Interlevel and Intralevel Correlations of Wind Components for Six Geographical Locations." NASA TN P-561, December 1960.

2.8 Crutcher, H. L. and Baer, L.: "Computations from Elliptical Wind Distribution Statistics." *Journal of Applied Meteorology*, American Meteorological Society, Vol. 1, December 1962, pp. 522-530.

2.9 Henry, R. M.: "A Statistical Model for Synthetic Wind Profiles for Aerospace Vehicle Design and Launching Criteria." NASA TN D-1813, 1963.

2.10 Crutcher, H. L. and Falls, L. W.: "Multivariate Normality." NASA TN D-8226, May 1976.

2.11 Smith, O.E.: "Vector Wind and Vector Wind Shear Models 0 to 27km Altitude for Cape Kennedy, Florida and at Vandenberg AFB, California." NASA TMX-73319, July 1976.

2.12 The Range Reference Atmosphere Documents are published by Secretariat, Range Commander's Council, White Sands Missile Range, New Mexico. The following reference atmospheres have been published:

Kwajalein Missile Range, Kwajalein, Marshall Islands, Range Reference Atmosphere, 0- to 70-km Altitude, Document 360-82, December 1982. (AD-A123424)

Cape Canaveral, Florida, Range Reference Atmosphere, 0- to 70-km Altitude, Document 361-83, February 1983. (AD-A125553)

Vandenberg AFB, California, Range Reference Atmosphere, 0- to 70-km Altitude, Document 362-83, April 1983. (AD-A128125)

Dugway, Utah, Range Reference Atmosphere, 0- to 70-km Altitude, Document 363-83, June 1983. (AD-A131110)

Wallops Island Test Range, Virginia, Range Reference Atmosphere, 0- to 70-km Altitude, Document 364-83, July 1983. (AD-A131327)

White Sands Missile Range, New Mexico, Range Reference Atmosphere, 0- to 70-km Altitude, Document 365-83, August 1983. (AD-A132471)

Edwards AFB, California, Range Reference Atmosphere, 0- to 70-km Altitude, Document 366-83, August 1983. (AD-A132487)

Eglin AFB, Florida, Range Reference Atmosphere, 0- to 70-km Altitude, Document 367-83, September 1983. (AD-A133506)

Taquac, Guam Island, Range Reference Atmosphere, 0- to 70-km Altitude, Document 368-83, September 1983. (AD-A133618)

Point Magu, California, Range Reference Atmosphere, 0- to 70-km Altitude, Document 369-83, September 1983. (AD-A134186)

Barking Sands, Hawaii, Range Reference Atmosphere, 0- to 70-km Altitude, Document 370-83, December 1983. (AD-A137406)

Ascension Island, Range Reference Atmosphere, 0- to 70-km Altitude, Document 371-84, January 1984. (AD-A138470)

Wake Island, North Pacific, Range Reference Atmosphere, 0- to 30-km Altitude, Document 376-91, August 1991.

Nellis Air Force Base, Nevada, Range Reference Atmosphere, 0- to 30-km Altitude, Document 377-91, August 1991.

Shemya, Alaska, Range Reference Atmosphere, 0- to 50- to 70-km Altitude, Document 380-91, August 1991.

Thule, Greenland, Range Reference Atmosphere, 0- to 70-km Altitude, Document 379-91, August 1991.

Fairbanks, Alaska, Range Reference Atmosphere, 0- to 30-km Altitude, Document 378-91, August 1991.

2.13 Daniels, G. E. and Smith, O.E.: "Scalar and Component Wind Correlations Between Altitude Levels for Cape Kennedy, Florida and Santa Monica, California." NASA TN D-3815, April 1968.

2.14 Justus, C. G., Woodrum, A., Roper, R. G., and Smith, O. E.: "A Global Scale Engineering Atmospheric Model for Surface to orbital Altitudes, 1: Technical Description." NASA TMX-64871, 1974.

2.15 Justus, C. G., Roper, R. G., Woodrum, A., and Smith, O. E.: "Global Reference Atmosphere Model for Aerospace Applications." *J. Spacecraft and Rockets*, 12(8), pp. 449-450, 1975.

2.16 Justus, C. G., Fletcher, G. R., Gramling, F. E., and pace, W. B.: "The NASA/MSFC Global Reference Atmospheric Model—MOD 3 (With Spherical Harmonic Wind Model)." NASA CR-3256, Contract NAS8-32897, 1980.

2.17 Justus, C. G., Alyea, F. N., Cunnold., D. M., Blocker, R. A., and Johnson, D. L.: "GRAM-88 Improvements in the Perturbation Simulations of the Global Reference Atmospheric Model." NASA Special Report ES44-11-9-88, 1988.

2.18 Justus, C. G., Alyea, F. N., Dunnold, D. M., Jeffries, W. R. III, and Johnson, D. L.: "The NASA/MSFC Global Reference Atmsopheric Model—1990 Version (GRAM-990); Part I: Technical/Users Manual." NASA TM-4268, NASA Marshall Space Flight Center, Huntsville, Alabama, April 1991.

2.19 Justus, C. G., Jeffries, W. R. III, Yung, S. P., and Johnson, D. L.: "The NASA/MSFC Global Reference Atmospheric Model - 1995 Version (GRAM-95)." NASA TM-4715, August 1995.

3.0 ASCENT WIND MODELS (0 to 27 km)

The development of ascent wind profile models for aerospace vehicle design has been continuous throughout the lifetime of the U.S. Space Program. The five ascent wind models for launch vehicle design described herein are:

(1) The classical scalar wind profile model (SWP), which was developed in the early 1960's. The current version is contained in NASA TM-4511 (Ref. 3.1).

(2) The wind component wind profile model developed for the SaturnV/Skylab launch (Ref. 3.2).

(3) The original monthly vector wind profile (VWP) model, which is described in NASA TMX 73319 (Ref. 3.3). This model was used for the design of the National Space Transportation System (NSTS) as described in Refs. 3.4 and 3.5.

(4) The monthly enveloping scalar wind profile model (MESWP) was developed for the National Launch System (NLS). This model was not implemented because it was quickly superseded by an enveloping version of model (5).

(5) An improved monthly vector wind profile model (IVWP) was developed in 1992 (Ref. 3.7). The enveloping version uses the same approach used in model (4) to define the given wind vectors on the monthly enveloping probability ellipse at a reference altitude.

The enveloping version of the IVWP for Kennedy Space Center, Florida (KSC) and Edwards Air Force Base, California (EAFB) has been used in design studies for the NLS and X-33 respectively. An ascent wind profile model will be needed for development of future launch vehicles such as the Space Shuttle liquid fueled fly-back booster and the full scale X-33 follow-on. The recommended model for a particular vehicle program must be tailored to meet specific program requirements and vehicle mission objectives. Therefore, it is not possible to use the general characteristics of an ascent wind profile model presented in this report as design criteria.

3.1 Applications

The engineering design application for a wind profile model is the establishment of preliminary design ranges for angle-of-attack, α, angle of sideslip, β, aerodynamic pressure, Q, and two aerodynamic load indicators, $Q\alpha$ and $Q\beta$. These and other important flight parameters are derived from ascent flight six degree-of-freedom trajectory simulations using the wind profiles constructed with the model. This and other trajectory parameters are used to compute structural load indicator values for suspected wind sensitive points or members over the vehicle. A load indicator is an algorithm that relates external loads, such as axial force, shear, bending moment, and dynamic pressure to stress

(Refs. 3.4, 3.5). For the NSTS the load indicators are for rigid body loads. For some structural members the algorithms are linear functions of Q, α, and β; however, most are not. Elastic body loads, which are highly sensitive to wind gust, must be determined by other means such as finite element matrix analysis and flutter and vibration analysis. To size the fuel requirements, wind profile models are used in the estimation of flight performance reserves (FPR); that is, the propellant required to protect for in-flight dispersions to reach orbital insertion (Refs. 3.4, 3.5).

Following the preliminary vehicle design activities using a wind profile model, trade studies can be made to determine if there is a requirement to bias the ascent trajectory to reduce wind loads. If the wind profile model is for a monthly reference period, it is appropriate to establish steering commands based on the profiles of monthly mean winds in both pitch and yaw planes to guide the vehicle through first stage. The current NSTS wind biasing is with respect to the wind profile measurement at T-3.5 hours (Refs. 3.8, 3.9). Following the establishment of the wind biasing methodology, structural loads and performance assessments are made using a sample of Jimsphere high resolution wind profile measurements. Currently for KSC this data sample is 150 Jimsphere wind profiles per month.

3.2 Models Based on Conditional Wind Shear

These wind profile models require given values for either wind speed or wind vectors at some probability level at assigned reference altitudes. For the scalar models (Ref. 3.1) calculated conditional percentile values for wind speed shear versus shear interval, given a wind speed at the reference altitude, are subtracted from the reference altitude wind speed to obtain a model wind profile. For the original vector wind model, values for conditional vector shear, given a wind vector at a reference altitude are calculated for all altitudes above and below the reference altitude. A model profile is constructed by subtraction of the conditional vector shears from the given vector at the reference altitude. The computational methods for determination of wind percentiles at reference altitudes and for determination of conditional shears given the wind at the reference altitude are described below. These statistics are derived from Rawinsonde and Jimsphere wind profile data bases for KSC.

3.2.1 Scalar Wind Profile Model (SWP)

The SWP model for KSC taken from Ref. 3.1 is summarized herein to facilitate comparisons with related models. Table 3.1 gives various percentile values for steady state wind speed at assigned altitudes and Figure 3.1 illustrates the tabulated values. "Steady state" is a term to denote that these percentile values are based on the historical Rawinsonde wind profile data base in contrast with higher resolution Jimsphere wind profile measurements. The term "envelopes" used below signifies that these statistics are percentile bounds at discrete altitudes. These envelopes should not be misinterpreted; for example, 95 percent of the wind speed profiles are not contained within the 95th percentile envelope at all altitudes. This is because the interlevel correlation coefficients for wind

speed are less than unity (Ref. 3.6). From a theoretical analysis of multivariate normal distributions (Ref. 3.13) and from empirical observation of the percentage of wind

Table 3.1 Wind Speed (m/s) Profile Envelopes, KSC

Altitude	Percentile				
(km)	50	75	90	95	99
1	8	13	16	19	24
6	23	31	39	44	52
11	43	55	66	73	88
12	45	57	68	75	92
13	43	56	67	74	86
20	7	12	17	20	25
23	7	12	17	20	25
40	43	57	70	78	88
50	75	83	91	95	104
58	85	96	106	112	123
60	85	96	106	112	123
75	15	22	28	30	37
80	15	22	28	30	37

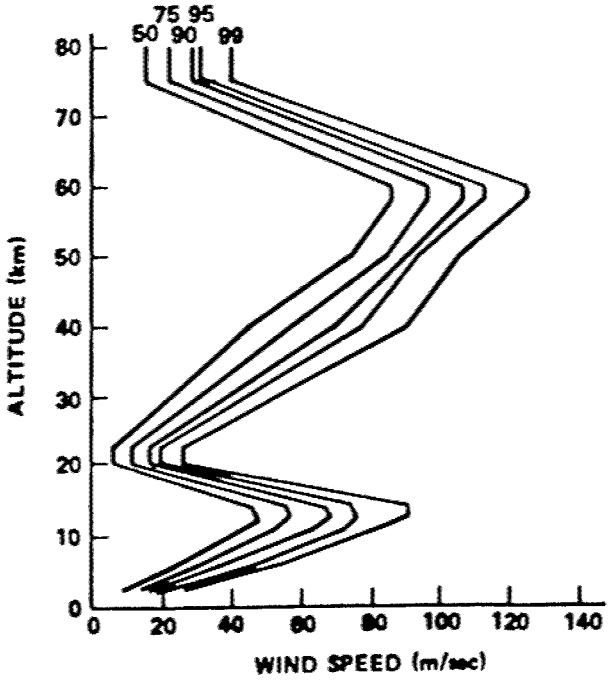

Figure 3.1 Wind Speed Profile Envelopes, KSC

profiles that lie within a probability ellipse for wind vectors at discrete altitudes for an assigned probability, it has been estimated that there are only approximately five independent wind altitude levels for winds over a 12-km layer for wind samples taken at 1-km intervals. Thus, only 77 percent (i.e. $.95^5$ x 100) of the wind vectors over all altitudes for a 12-km layer will lie within the 95 percent wind vector ellipses taken at discrete altitudes at 1-km intervals. Furthermore, this implies that the 99 percent wind speeds at discrete altitudes are required to contain 95 percent of the wind speed profiles at all altitudes over a 12-km layer; where $(0.95)^{1/5} = 0.99$. This significant conclusion is often overlooked in engineering applications of wind profile models. For clarity let us repeat this conclusion: A wind speed profile envelope derived at discrete altitudes for a specified percentile does not contain the same percentage of wind profiles within that envelope. An aerospace vehicle should be designed to have the capability to fly through a certain percentage of wind profiles for monthly reference periods. The percentage of profiles that are within the envelope at all altitudes is always smaller than the percentage for the envelope derived at discrete altitudes.

Tables 3.2 and 3.3 from Ref. 3.1 contain the 99th conditional percentile values for wind speed shear (versus shear interval) for various given wind speeds. The term build-up is for wind speed increasing with altitude (positive shear) and back-off is for wind speed decreasing with altitude (negative shear). Each conditional wind speed shear in Tables 3.2 and 3.3 is conditional with respect to a given wind speed at the top of the altitude increment associated with the shear; the caption "wind speed change" is the difference in wind speed between two altitudes separated by the scales of distance (altitude interval). The caption reference to envelopes in Tables 3.2 and 3.3 refers to the 99th conditional wind speed shears for the entire data sample (all months). In the construction of the SWP model, the given value for wind speeds at reference altitudes are linearly interpolated from Table 3.1. This wind speed is entered into Table 3.2 to find the 99th percentile conditional wind speed shear versus shear interval and subtracted from the given wind speed at reference altitudes for altitudes below the reference altitude; thus, the caption reference to "build-up" in Table 3.2 is for altitudes below the reference altitude. Similarly, the wind speed is entered into Table 3.3 to find the 99th percentile conditional wind speed shear versus shear interval and subtracted from the given wind speed at reference altitudes for altitudes above the reference altitude; thus, the caption reference to "back-off".

The methodology used to establish the percentile values for wind speed (Table 3.1) and the 99th conditional wind speed shear versus altitude interval for a given wind speed (Tables 3.2 and 3.3) is empirical. The percentiles in Tables 3.1 to 3.3 for altitude intervals $\geq$ 1000 m are derived from Rawinsonde data; for altitude intervals less than 1000 m the following empirical formula is used.

$$\Delta W = (\Delta W)_{1000} \, (\Delta H/1000)^{0.7} \tag{3.1}$$

where, the shear, ΔW, is in m/s and the altitude interval, ΔH, is in m. The classical 9 m/s wind gust (Fig. 3.2) is reduced to 0.85 of its value when applied as an extension to the

Table 3.2 Build-up Design Envelopes of 99 Percentile Wind Speed Change, 1 to 80-km Altitude Region, KSC

Wind Speed at Reference Altitude (m/sec)	Scales of Distance (m)									
	5000	4000	3000	2000	1000	800	600	400	200	100
≥ 90	65.6	59.5	52.3	43.5	34.0	29.0	23.8	17.9	11.2	6.8
= 80	60.4	55.5	49.7	42.0	32.7	27.7	22.7	17.0	10.6	6.5
= 70	56.0	51.7	47.0	40.4	31.2	26.6	21.8	16.4	10.1	6.2
= 60	51.3	48.5	44.5	38.6	30.0	25.6	21.1	15.8	9.8	6.0
= 50	46.5	45.0	41.2	36.5	28.5	24.4	20.0	15.0	9.2	5.7
= 40	36.5	37.7	36.8	34.9	26.5	22.6	18.5	13.8	8.6	5.3
= 30	28.0	27.5	26.5	24.5	20.8	17.8	14.5	10.8	6.7	4.1
= 20	17.6	17.3	16.6	15.8	14.6	12.5	10.2	7.2	4.7	2.9

Table 3.3 Back-Off Design Envelopes of 99 Percentile Wind Speed Change, 1 to 80-km Altitude Region, KSC

Wind Speed at Reference Altitude (m/sec)	Scales of Distance (m)									
	5000	4000	3000	2000	1000	800	600	400	200	100
≥ 90	77.5	74.4	68.0	59.3	42.6	36.4	29.7	22.4	13.8	8.5
= 80	71.0	68.0	63.8	56.0	40.5	34.7	28.5	21.4	13.2	8.1
= 70	63.5	61.0	57.9	52.0	38.8	33.1	27.0	20.3	12.5	7.7
= 60	56.0	54.7	52.3	47.4	36.0	31.0	25.3	18.9	11.7	7.2
= 50	47.5	47.0	46.2	43.8	33.0	28.3	23.2	17.5	10.7	6.6
= 40	39.0	38.0	37.0	35.3	29.5	25.3	20.6	15.5	9.6	5.9
= 30	30.0	30.0	29.4	26.9	22.6	19.4	15.8	11.9	7.3	4.5
= 20	18.0	17.5	16.7	15.7	14.2	12.2	9.9	7.5	4.6	2.8

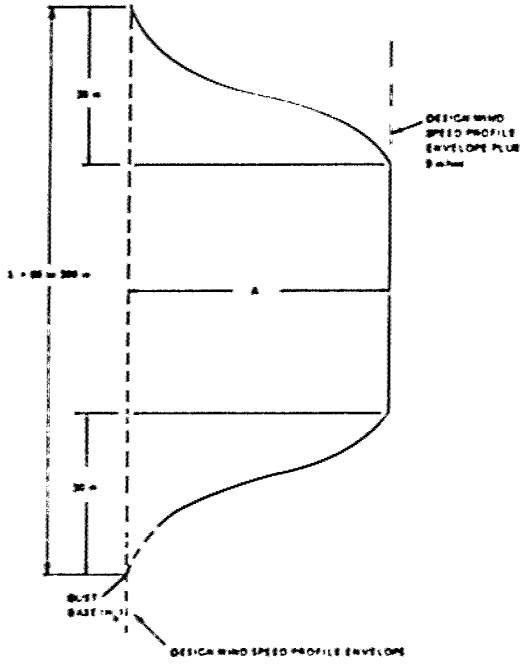

Figure 3.2 NASA Classical 9 m/s Discrete Gust Model

wind speed at the reference altitude. For further details see Ref. 3.1 . An example of the SWP with gust is shown in Fig. 3.3.

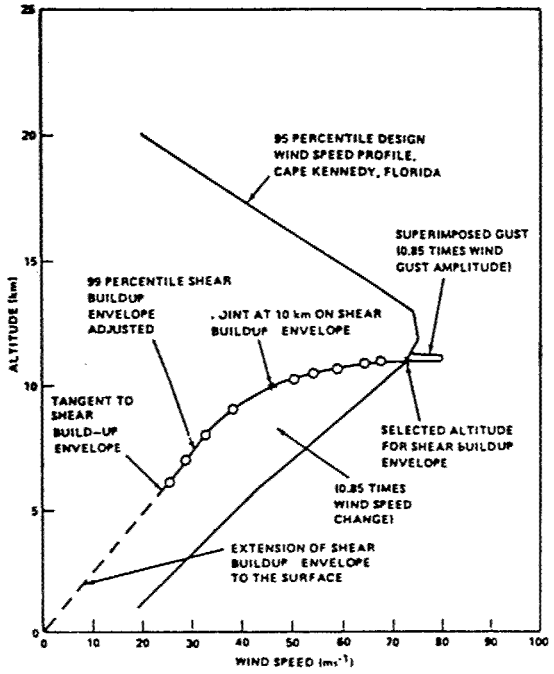

Figure 3.3 Example of Scalar Wind Profile Model Construction With Addition of Gust

Critique of the SWP model:

Advantages

None

Disadvantages

1. It is a scalar wind model. Wind is a vector quantity.

2. The given value for the wind speed is to be applied in all directions. This is not realistic. For example, a wind speed ≥ 75 m/s at 12-km altitude from the east has never been observed over KSC.

3. Wind trajectory biasing techniques for ascent structural loads alleviation are not applicable.

4. Subjective analysis was used to derive the wind speeds and wind shears that envelope all the reference months.

3.2.2 Wind Component Wind Profile Model

For the Saturn V Skylab mission, the ascent wind trajectory was biased for both in-plane and out-of-plane wind components to reduce ascent loads. This was necessary because the mission required a revision of the flight azimuth from east to northeast, which created concern for the effect of out-of-plane winds on the 100-ton payload. The wind component profile model (Ref.3.2) uses properties of the bivariate normal probability function to compute the conditional wind component shears given the 95th percentile values for the wind component at various reference altitudes. These conditional shears are subtracted from the given wind components. The in-plane and out-of-plane wind components are treated independently for this model. Hence, there is no association between components. The Skylab mission was launched successfully on May 14, 1973.

3.2.3 Monthly Vector Wind Profile (VWP) Model, Original Version for the Space Shuttle

The scalar wind profile model was found to be inadequate for the Space Shuttle System. A program decision was made during the summer of 1976, to wind bias the ascent trajectory to the profiles of monthly mean wind components (vector mean wind) in both pitch and yaw planes to reduce ascent structural wind loads. This was required because some subsystems of the Space Shuttle vehicle (SSV) are more sensitive to ascent wind loads in the yaw plane than in the pitch plane. This led to the development of the vector wind profile (VWP) model as documented with several options by Smith (Ref. 3.3). A synopsis of this model and a description of applications in studies of SSV aerodynamic load indicators and flight performance is given in Refs. 3.4 and 3.5 . The VWP model uses the properties of the quadravariate normal probability distribution function. The 14 statistical parameters for this probability function are estimated for monthly reference periods from a long period of Rawinsonde wind records for Cape Canaveral, FL and Vandenberg AFB, CA. The wind vectors at discrete altitudes, at 1-km intervals from 0 to 27 km, are modeled as bivariate normal probability ellipses. The wind vectors at two altitudes are quadravariate normally distributed. The components of vector wind shear are bivariate normally distributed for each altitude increment. The conditional distribution for wind shear given a wind vector at the reference altitudes is bivariate normally distributed. In general functional notation, the conditional distribution is

$$f(x_3, x_4 | x_1, x_2) = \frac{f(x_1, x_2, x_3, x_4)}{f(x_1, x_2)} \tag{3.2}$$

where x_1, x_2, x_3, and x_4 are quadravariate normally distributed variables. Here x_1 and x_2 are the components of the given wind vector at the reference altitude, and x_3 and x_4 are the components of the wind shear between the reference and any other selected altitude below and above the reference altitude. To obtain the VWP, the first step is to compute the wind vector to an assigned probability ellipse at a reference altitude as illustrated in Fig. 3.4. For this 'given wind vector' the conditional bivariate normal distributions for wind shear at 1-

km intervals are computed versus altitudes below and above the reference altitude. These bivariate conditional ellipses are made circular to simplify the modeling (see Fig. 3.5). In Fig. 3.5 the dashed curve is the conditional mean wind vectors versus altitude given the wind vector at the reference altitude. The locus of the conditional shear (heavy line), that is in-plane with the given wind vector, gives the largest conditional wind shear.

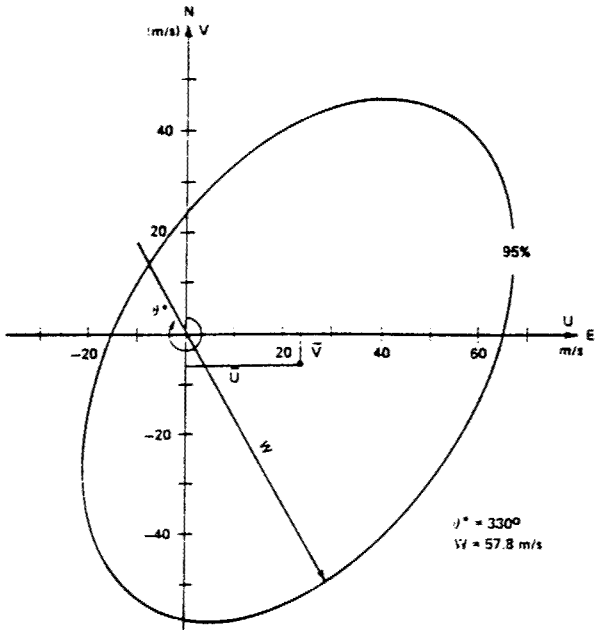

Figure 3.4 The 95 Percent Vector Wind Ellipse, VAFB,10 km, December

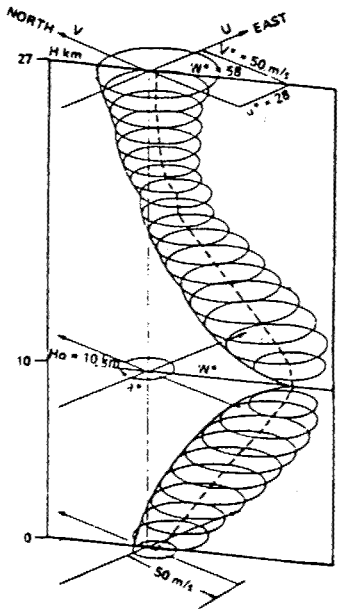

Figure 3.5 Conditional 99 Percent Bivariate Normal Vector Wind Shear Circles, Given the Wind Vector at 10 km, VAFB, December

The cross section of Fig. 3.5 in-plane with the given wind vector is shown in Fig. 3.6.

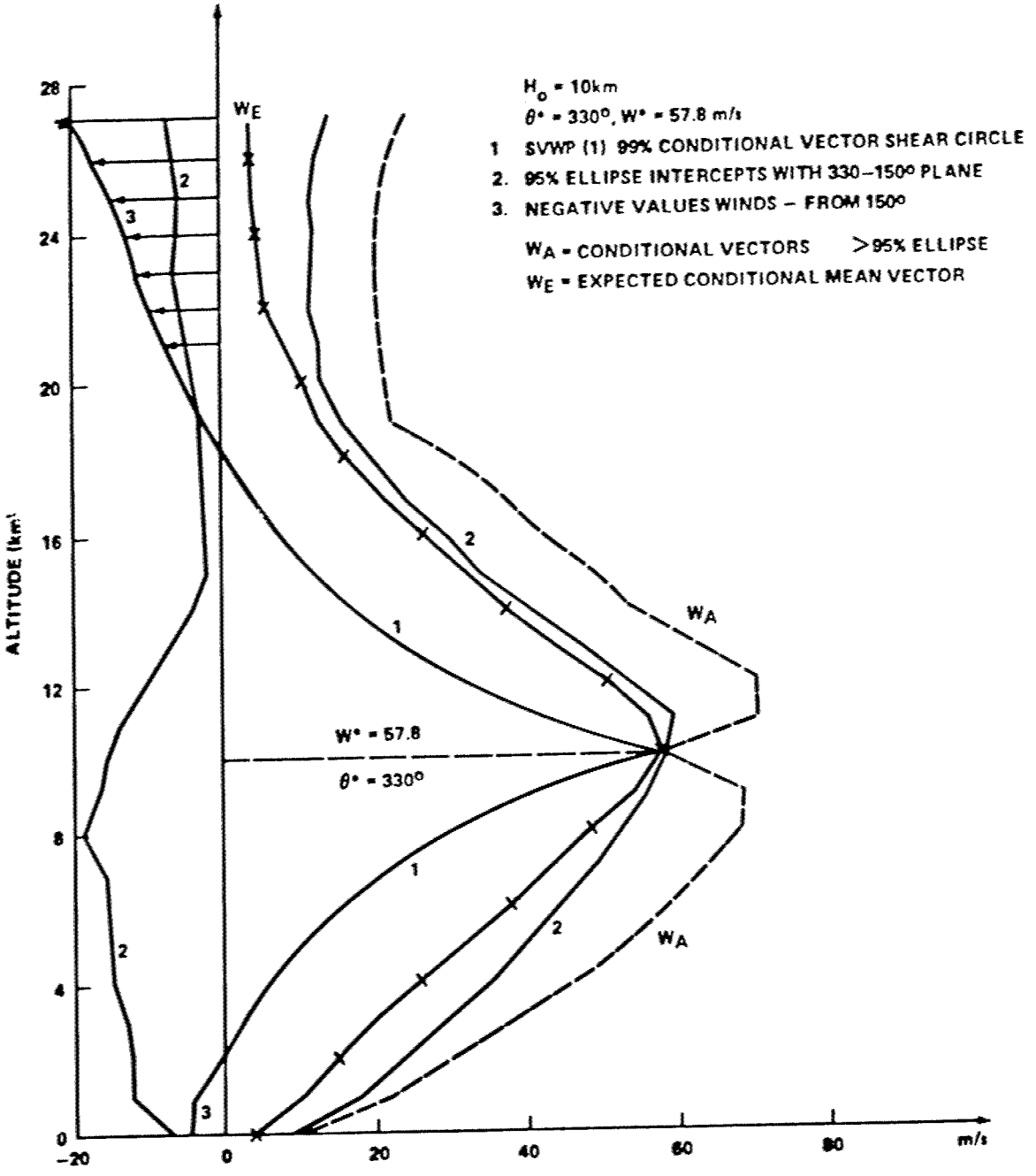

Figure 3.6 Synthetic Vector Wind Profile, (1) in-plane with given wind vector, December VAFB

The selection of eight given wind vectors at an assigned reference altitude is usually sufficient to describe the engineering systems design parameters. The VWP is formed as the distribution of wind shears which varies with (1) the given wind vector at the reference altitude, (2) altitude, (3) shear interval, (4) month, and (5) launch site. Because this model is based on the properties of the multivariate normal distribution, it can be made completely general for any probability level. By convention, the 99 percent conditional

shears are used for the VWP and the 95 percent wind vector ellipse is used for the selection of the given wind vectors. For wind shear at less than 1000 m-shear intervals Eq. 3.1 is used. The classical 9 m/s square wave gust model is reduced to 0.85 of its value when it is used with the VWP model.

The performance of the VWP model for two important engineering design parameters is illustrated in Figs. 3.7 and 3.8 for the SSV, (Refs. 3.4, 3.5).

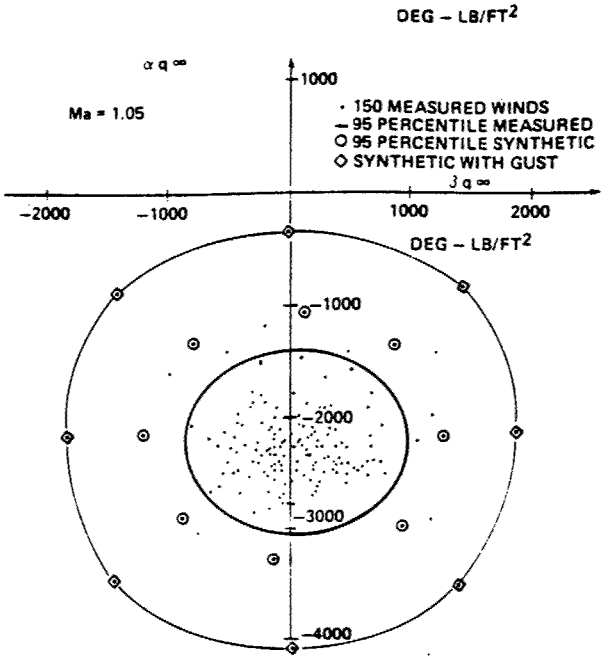

Figure 3.7 STS-1 Pitch and Yaw Load Indicators, Mach = 1.05, April, KSC

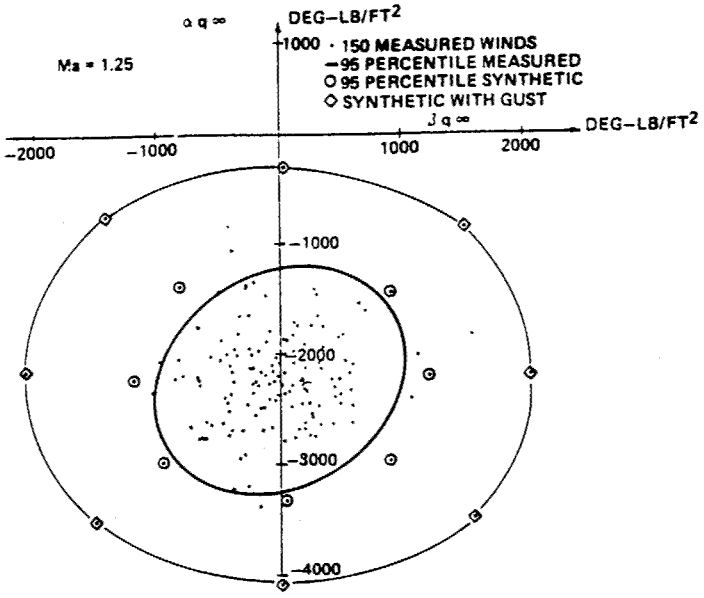

Figure 3.8 STS-1 Pitch and Yaw Load Indicators, Mach 1.25, April KSC

The VWP model yields excellent agreement between the Qα, Qβ dispersions from only eight trajectory simulations compared with the dispersions from simulations using 150 April Jimsphere wind profile measurements. These ascent trajectory simulation results for Qα and Qβ are from a trajectory biased to the April monthly vector mean wind in both pitch and yaw planes. Here, Qα is the product of dynamic pressure, Q, and angle-of-attack α; and Qβ is the product of Q and the angle of sideslip β. Note the larger range for these parameters derived from the VWP when the design gust is applied at the reference altitude corresponding to the respective Mach number (Ma). These results are for specific discrete altitudes. In retrospect, it may be fortunate that this gust was applied as the design procedure in view of the fact that the 95 percent envelopes of wind vectors taken at discrete altitudes do not contain 95 percent of the wind vector profiles. Hence, it is suggested that the 99 percent given winds for the VWP without gust may give comparable results.

The usual vehicle design objective is to have the capability to fly through 95 percent of the wind profiles in all months, not just a certain percent of winds at discrete altitudes or Mach numbers. The determination of the sample size required to achieve this objective was discussed in Section 2 .

Critique of the Original Monthly VWP Model

Advantages

1. This model has been proven for derivation of aerospace engineering design parameters for launch vehicles.

2. It is based on objective statistical techniques.

3. Trajectory biasing techniques for ascent wind loads relief can be used.

4. Vehicle assessments can be evaluated for monthly reference periods.

Disadvantages

1. It is a complex model.

2. The complete quadravariate normal model has not been implemented; i.e. the inter-level and intra-level cross-component correlations are assumed to be negligible, and the conditional ellipse for shears is made circular by taking the root summed square of the conditional standard deviations.

3.2.4 Monthly Enveloping Scalar Wind Profile (MESWP) Model

This was the first 'enveloping' wind profile model that takes advantage of desirable attributes of the SWP and the original VWP models. The MESWP is less complex than the VWP because it is for the most part a scalar model. The only "vector" attribute of the MESWP is the derivation of the given wind speed at the reference altitude, which is the magnitude of a selected wind vector to the monthly enveloping probability ellipse. Unlike the SWP model which is based on subjective empirical statistical techniques, the MESWP is based on analytical probability functions.

The justification for 'enveloping' is given in Fig 3.9, which illustrates (for KSC) the ellipse that envelopes the 95 percent wind vector probability ellipses for all months at 12 km altitude, and the 95 percent scalar wind speed (from Table 3.1), represented by a circle with 75 m/s radius. For the monthly enveloping ellipse illustrated in Fig. 3.9, there is a large range of wind directions for which the wind speed is less than 75 m/s; thus, a scalar wind model could unduly overestimate the wind magnitude.

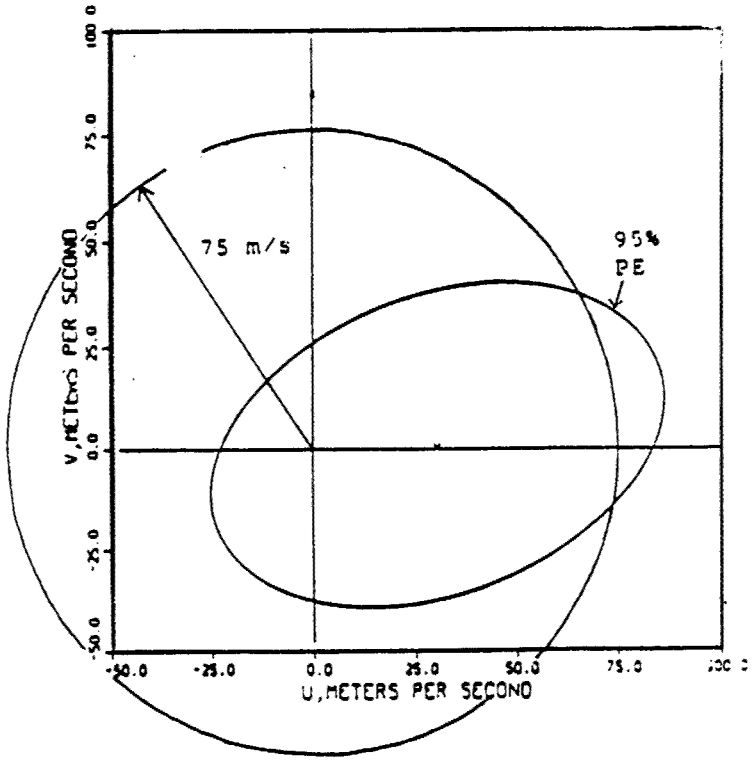

Figure 3.9 Comparison of 95 Percent Scalar Wind (circle) with the Ellipse that Envelopes the 95 Percent Monthly Ellipses

Construction of a MESWP model wind speed profile for each reference altitude requires the following derivations:

1. The monthly enveloping probability ellipse.

2. The conditional wind speed shear for all altitude increments above and below the reference altitude.

The derivations are described below.

3.2.4.1 Monthly Enveloping Ellipses

The monthly enveloping ellipse is defined by five proxy bivariate normal parameters; the means and standard deviations of the wind components are estimated from statistics derived from the monthly ellipses and the correlation coefficient between the wind components which is the value calculated from the entire data sample (all months).

The means for the enveloping ellipse are computed by:

$$\bar{u}_A = \frac{u_{L_E} - u_{s_E}}{2} \tag{3.3}$$

$$\bar{v}_A = \frac{v_{L_E} - v_{s_E}}{2} \tag{3.4}$$

where, u_{L_E}, v_{L_E} and u_{s_E}, v_{s_E} are the largest and smallest values of the monthly largest and smallest zonal (u) and meridional (v) wind components to the monthly 95 percent probability ellipses at each altitude for each month, u_{LS} and v_{LS}, calculated from

$$u_{LS} = \bar{u} \pm \lambda_c s_u \tag{3.5}$$

$$v_{LS} = \bar{v} \pm \lambda_c s_v \tag{3.6}$$

where, $\bar{u}$ and $\bar{v}$ are the monthly mean wind components, s_u and s_v are the standard deviations with respect to the monthly means, $\lambda_c = \sqrt{-2\ln(1-p)}$ and p is probability.

The standard deviations for the enveloping ellipse are:

$$s_{Au} = (u_{L_E} - \bar{u}_A)/\lambda_c \tag{3.7}$$

$$s_{Av} = (v_{L_E} - \bar{v}_A)/\lambda_c \tag{3.8}$$

The fifth parameter required to establish the enveloping ellipse is the correlation coefficient. The monthly correlation coefficients between the u and v wind components are not greatly different from the annual correlation coefficients. Therefore, the annual correlation coefficients were adopted. These five parameters are given in Table 3.4.

A comparison of the monthly enveloping 95 percent ellipse with the annual 95 and 99 percent vector wind ellipses is shown in Fig. 3.10. It is not recommended that the annual vector wind probability ellipse be used because the annual wind distribution is a mixture of the several monthly distributions which have different means and standard deviations. It is further suggested that the means (centroids) of the monthly enveloping wind ellipses, $\bar{u}_A$ and $\bar{v}_A$, contained in Table 3.4, could be used if a single wind biased trajectory representing all months is to be used for ascent structural wind loads alleviation. It is understood that such an application may not be realistic because launch vehicle designers would rather reap the benefits of loads alleviation and performance enhancements gained by biasing to a wind profile that is a better approximation of the wind profile on the day of launch. The adjusted means $\bar{U}_A$ and $\bar{V}_A$, the adjusted standard deviations S_{AU} and S_{AV} and the correlation coefficient are defined in Section 3.2.4.1.

Table 3.4 Adjusted Bivariate Normal Statistical Parameters for the Probability Ellipse at each Altitude that Envelopes the Monthly Ellipses, KSC

ALT (km)	$\bar{U}_A$ m/s	S_{AU} m/s	R(U,V) m/s	$\bar{V}_A$ m/s	S_{AV} m/s
0	-0.191	3.713	-0.141	-0.089	3.745
1	2.271	7.823	0.108	1.751	6.790
2	5.648	8.788	0.150	1.634	6.766
3	8.781	9.649	0.143	1.778	7.538
4	11.887	10.651	0.152	2.225	8.204
5	14.895	11.956	0.187	2.776	9.038
6	18.002	13.273	0.227	2.969	9.772
7	21.174	14.823	0.255	3.505	10.781
8	24.567	16.459	0.270	3.433	12.006
9	28.465	18.234	0.278	3.106	13.252
10	30.155	19.948	0.286	2.079	14.526
11	31.309	21.713	0.277	1.274	15.855
12	30.338	22.672	0.292	0.509	16.237
13	27.493	22.465	0.325	0.349	15.313
14	24.420	20.208	0.353	-0.556	13.201
15	22.182	17.438	0.359	0.377	11.275
16	19.874	14.990	0.340	0.775	9.520
17	16.342	12.970	0.305	0.967	8.167
18	12.012	11.302	0.282	0.957	6.526
19	6.818	10.236	0.208	0.629	5.162
20	1.833	9.606	0.230	0.028	4.409
21	-0.137	9.658	0.150	0.008	4.588
22	-0.561	9.837	0.104	-0.312	4.158
23	-0.573	10.431	0.126	0.435	4.277
24	0.961	11.561	0.154	0.526	4.201
25	2.213	12.750	0.184	1.181	4.307
26	3.292	13.983	0.196	1.425	4.776
27	4.205	14.899	0.213	2.083	5.443

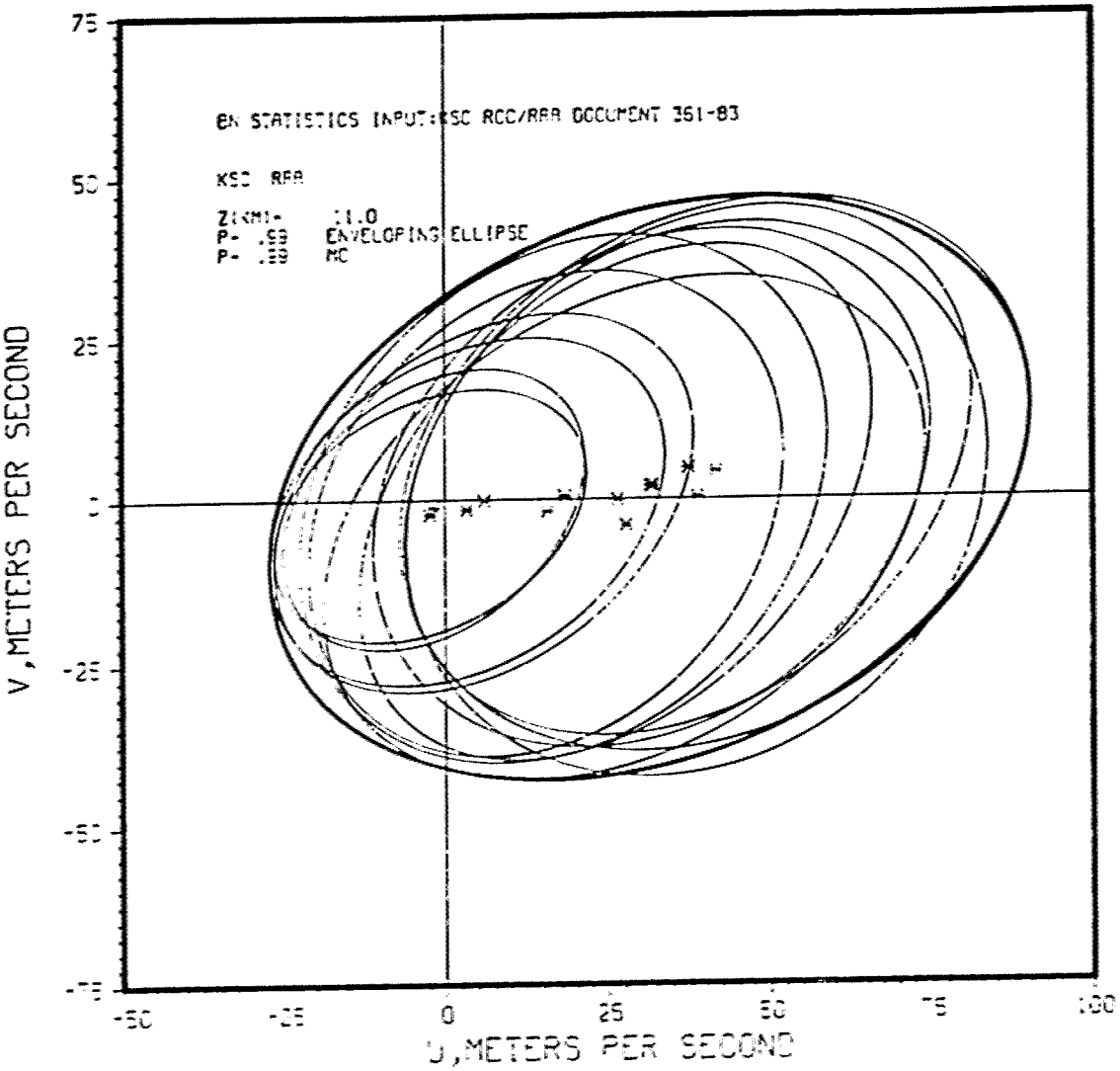

Figure 3.10 The 99 Percent Wind Ellipses for Each Month and the Enveloping 99 Percent Wind Ellipse, KSC, 11 km

3.2.4.2 Conditional Extreme Value Wind Speed Shear, Given the Wind Speed

A bivariate extreme value probability distribution function (Refs. 3.10, 3.11, 3.12) is used to model the conditional distribution for extreme largest wind speed shear versus shear layer altitude interval for given values for wind speed. The statistics for this wind speed shear model are derived from the KSC Jimsphere 150 wind profile per month data base. For each Jimsphere wind profile between 3 to 16-km altitude, the largest wind speed shear for selected shear layer intervals and the associated wind speed at the top of the interval were computed. In general, the extreme largest wind speed shear in the profile is associated with the largest wind speed. This is especially true for the larger altitude intervals. Because the Jimsphere data usually terminates at 16-km altitude and the largest wind speed usually occurs in the 10 to 15-km layer, the negative wind speed shears (decreasing wind speed with respect to altitude) are truncated or censored. Hence this wind

speed shear model is based only on the positive wind shear. If negative ("back-off") shears as listed in Table 3.3 are required, it is suggested that the positive shear statistics be used. Note from the analysis of wind speed shears calculated from Rawinsonde wind profiles the empirical "back-off" shears listed in Table 3.3 are only slightly larger than those for "build-up" listed in Table 3.2. The univariate extreme value probability distribution (Ref. 3.10) is an excellent fit to the observed wind shears and to a lesser degree for the associated wind speed. The values for the extreme largest wind speed shear given in Table 2-60 of Ref. 3.1 are based on the assumption that the extreme wind speed shear is conditional extreme value distributed given the wind speed at the top of the shear layer. These shear statistics are presented for February because this month typifies the range of conditional extreme largest wind speed shears given the wind speed for the other months. An illustration for the 99 percent conditional extreme wind shear versus shear layer interval for a given wind speed is shown in Figure 3.11.

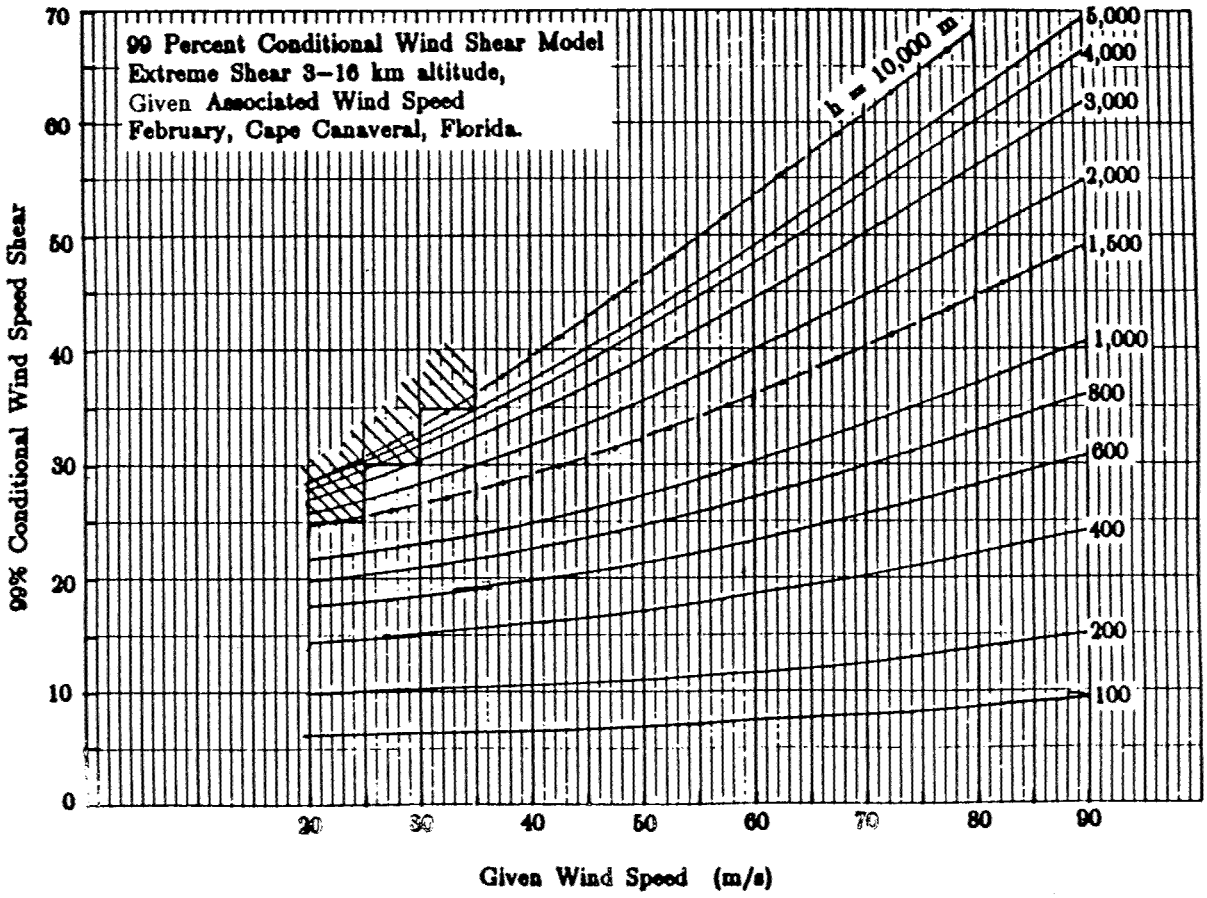

Figure 3.11 The 99 Percent Conditional Extreme Wind Speed Shear, 3 to 16-km altitude, Given the Wind Speed, February, KSC

3.3 An Improved Vector Wind Profile Model (IVWP) Based on Conditional Wind Vectors

3.3.1 Theoretical Concepts

A quadravariate normal distribution for wind vectors, $\{U_1, V_1\}$, at an altitude, Z_1, and wind vectors, $\{U_2, V_2\}$, at an altitude, Z_2, has the property that the conditional wind vectors at an altitude, Z_2, are bivariate normally distributed given specific values for the wind vector, $\{U_1^*, V_1^*\}$, at altitude, Z_1.

Symbolically, this is expressed as:

$$f\left(U_2, V_2 \,\middle|\, U_1^*, V_1^*\right) = \frac{f\left(U_1, V_1, U_2, V_2\right)}{f\left(U_1^*, V_1^*\right)} \tag{3.9}$$

The 14 statistical parameters for the quadravariate normal distribution for the zonal, U, and meridional, V, wind components are the mean values, $\overline{U}_1$, $\overline{V}_1$, $\overline{U}_2$, and $\overline{V}_2$; the four standard deviations, SDU_1, SDV_1, SDU_2, and SDV_2; and the six correlation coefficients, which are for like and unlike variables between altitudes Z_1 and Z_2: $R(U_1,U_2)$ and $R(V_1,V_2)$ and $R(U_1,V_2)$ and $R(V_1,U_2)$, respectively, and unlike variables at the same altitude Z_1 or Z_2: $R(U_1,V_1)$ and $R(U_2,V_2)$.

3.3.2 Wind Profile Construction

The procedure is, (1) define 12 specific wind vectors to the 99 percent probability ellipse at a fixed reference altitude, (2) compute the five parameters for the conditional bivariate normal probability distributions for all altitude levels above and below the reference altitude and (3) find the intercept to the conditional probability ellipse toward the mean values at the reference altitude. This conditional wind vector closely approximates the largest vector wind shear between the reference altitude and each of the other altitudes.

For engineering applications, the conditional wind vectors are expressed in polar coordinates as wind speed and wind direction in the standard meteorological coordinate system. Thus, the vector wind profile model is defined by the 12 equally spaced (30°) increments from the centroid of the 99 percent probability ellipses at each reference altitude which are the given values for the 99 percent conditional wind vectors that yield the largest shear at all other altitudes above and below the reference altitude.

For the N altitudes for the available data base there are 12 x N vector wind profiles from the surface (station elevation) to the maximum altitude. These vector wind profiles as a function of altitude above mean sea level are expressed as wind speed and wind direction in the standard meteorological coordinate system.

The vector wind profiles are derived from the vector wind profile model for a selected month, called the design reference month, that is representative of the high wind months.

This coordinate system is chosen because a vehicle could have a flight azimuth that may differ from either axis associated with the wind components. Furthermore, for operations, the wind data will be provided in the meteorological coordinate system.

The wind coordinate system used in the Space Shuttle program as a function of flight azimuth, (FA), is:

$$W_x(FA) = W \cos(\theta - FA) \text{ [in-plane wind component]} \quad (3.10)$$

where, a headwind is a positive in plane wind component and a tailwind is negative.

$$W_y(FA) = W \sin(\theta - FA) \text{ [out-of-plane wind component]} \quad (3.11)$$

where, a right-to-left out-of-plane wind component is a positive crosswind and left-to-right is a negative crosswind. The wind direction, θ, measured in degrees clockwise from true north, is the direction from which the wind is blowing. W is wind speed and FA is flight azimuth measured in degrees clockwise from true north.

3.3.3 Equations

This section presents the specific equations from Ref. 3.6 to compute (1) the given wind vectors at the reference altitude, Z_1; and (2) the five conditional bivariate normal parameters at Z_2, which are the conditional component means, the conditional component standard deviations, and the conditional correlation coefficients. The five conditional statistical parameters are used to compute the conditional bivariate normal 99 percent probability ellipse from which the conditional wind vector that approximates the largest shear between the reference altitude, Z_1, and all other altitudes Z_2 above and below the reference altitude. The following notation for the statistical parameters is used:

Means	**Variances**	**Standard Deviations**	**Correlation Coefficients**	**Covariances**
(m/s)	**(m^2/s^2)**	**(m/s)**	**(unitless)**	**($m^2/s^{2)}$**
MU_1	SU_1	SDU_1	RU_1V_1	SU_1V_1
MV_1	SV_1	SDV_1	RU_1V_2	SU_1V_2
MU_2	SU_2	SDU_2	RV_1U_2	SV_1U_2
MV_2	SV_2	SDV_2	RU_2V_2	SU_2V_2
			RU_1U_2	SU_1U_2
			RV_1V_2	SV_1V_2

The general expression for the covariance is $SU_iV_j = RU_iV_j(SDU_i)(SDV_j)$.

The first step is to define the 12 given wind vectors to the 99% probability ellipse at the reference altitude. These given wind vectors from the centroid of the probability ellipse are defined at 30° increments of clocking angle, CA, measured in the standard mathematical convention (counterclockwise).

$$U_I^* = MU_1 + RS \cos(CA) \tag{3.12}$$

$$V_I^* = MV_1 + RS \sin(CA) \tag{3.13}$$

where, $$RS = \frac{1}{A\sqrt{-2 \ln (1 - P)}}$$

where, P is probability = 0.99 , and

$$A^2 = \frac{1}{1-(RU_1V_1)^2} \left[\left(\frac{\cos(CA)}{SDU_1} \right)^2 - \frac{2RU_1V_1 \cos(CA) \sin(CA)}{SDU_1\, SDV_1} + \left(\frac{\sin(CA)}{SDV_1} \right)^2 \right] \tag{3.14}$$

The conditional mean vectors, $\{CMU_2, CMV_2\}$, at altitude, Z_2, given specific wind vectors, $\{U_I^*, V_I^*\}$, at the reference altitude are:

$$CMU_2 = MU_2 + (T_1 + T_2) / [1 - RU_1V_1 * RU_1V_1)] \tag{3.15}$$

where,

$$T_1 = [RU_1U_2 - RU_1V_2 * RU_1V_1] * (U_I^* - MU_1) (SDU_2 / SDU_1)$$

and

$$T_2 = [RU_1V_2 - RU_1U_2 * RU_1V_1] * (V_I^* - MV_1) (SDU_2 / SDV_1)$$

$$CMV_2 = MV_2 + (T_3 + T_4) / [1 - RU_1V_1 * RU_1V_1] \tag{3.16}$$

where,

$$T_3 = [RV_1U_2 - RV_1V_2 * RU_1V_1] (U_I^* - MU_1) (SDV_2 / SDU_1)$$

and

$$T_4 = [RV_1V_2 - RV_1U_2 * RU_1V_1] (V_I^* - MV_1) (SDV_2 / SDV_1)$$

The conditional standard deviations are:

$$CSDU_2 = [\text{sigma}(1,1)]^{1/2} \tag{3.17}$$

and

$$CSDV_2 = [\text{sigma}\ (2,2)]^{1/2} \tag{3.18}$$

The conditional correlation coefficient is:

$$CRU_2V_2 = \text{sigma}\ (1,2) / (CSDU_2)(CSDV_2) \tag{3.19}$$

where,

$$\text{sigma}\ (1,1) = SU_2 - SU_1U_2[SU_1U_2 * SV_1 - SU_2V_1 * SU_1V_1] / D$$
$$- SV_1U_2[- SU_1U_2 * SU_1V_1 + SU_2V_1 * SU_1] / D$$

$$\text{sigma}\ (2,2) = SV_2 - SU_1V_2[SU_1V_2 * SV_1 - SV_1V_2 * SU_1V_1] / D$$
$$- SV_1V_2[- SU_1V_2 * SV_1U_2 + SV_1V_2 * SU_1] / D$$

$$\text{sigma}\ (1,2) = SU_2V_2 - SU_1V_2[SU_1U_2 * SV_1 - SU_2V_1 * SU_1V_1] / D$$
$$- SV_1V_2[SU_1U_2 * SU_1V_1 + SU_2V_1 * SU_1](1/D)$$

and, $$D = (SU_1)(SV_1) - (SU_1V_1)(SU_1V_1).$$

Note that the given wind values U_1^* and V_1^* are required for the conditional mean component and not for the conditional standard deviations.

The intercept of the conditional 99 percent probability ellipse (PE) toward the centroid of the 99 percent PE at the reference altitude is computed for each altitude above and below the reference altitude. This is the vector wind profile model. The computations are:

$$UC_2 = CMU_2 + RSC\ \cos(CC) \tag{3.20}$$

and

$$VC_2 = CMV_2 + RSC\ \sin(CC) \tag{3.21}$$

Where CC = CA + 180, i.e., the clocking angle to the given vector plus 180 degrees.

$$RSC = \frac{1}{A_c\sqrt{-2\ \ln\ (1-P)}}$$

where, P is probability = 0.99, and,

$$A_c^2 = \frac{1}{1-(CRU_2V_2)^2}\left[\left(\frac{\cos(CC)}{CSDU_2}\right)^2 - \frac{2CRU_2V_2\cos(CC)\sin(CC)}{CSDU_2 * CSDV_2} + \left(\frac{\sin(CC)}{CSDV_2}\right)^2\right] \tag{3.22}$$

A schematic (Fig. 3.12) taken from Ref. 3.6 shows the construction of a given wind vector at 12-km altitude for a clocking angle of 30° and the conditional wind vector at 10-km, which is 210°, (30 + 180), on the 99 percent conditional probability ellipses.

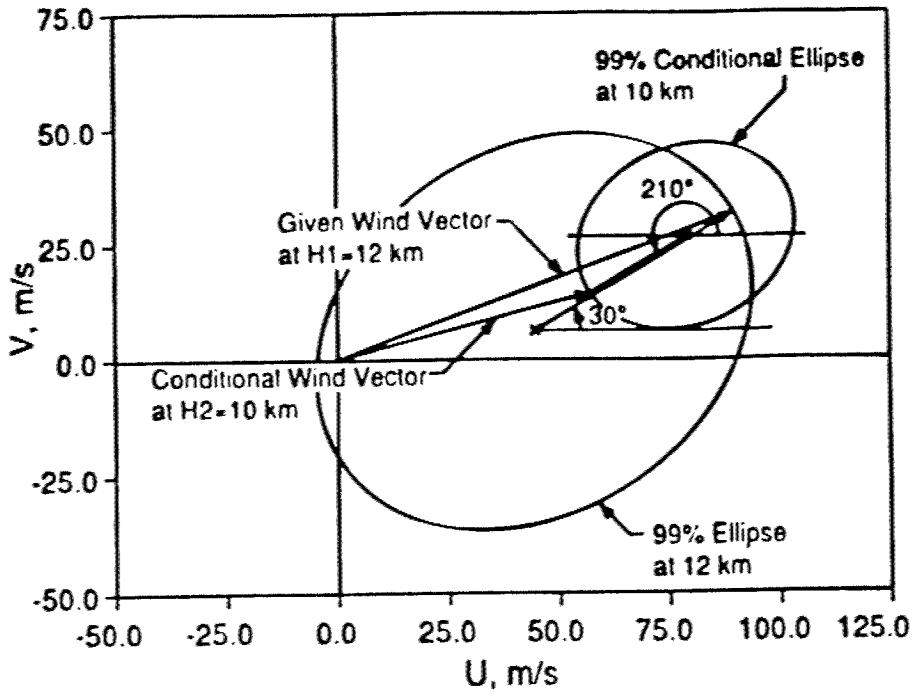

Figure 3.12 Schematic of Profile Construction Between a Reference Altitude of 12-km and an Altitude of 10 km. Clocking Angle 30°

An example of the 12 vector wind profiles for KSC, February for the 12-km reference altitude is presented in Fig.3.13 for the zonal (U) and Fig.3.14 for the meridional (V) wind components.

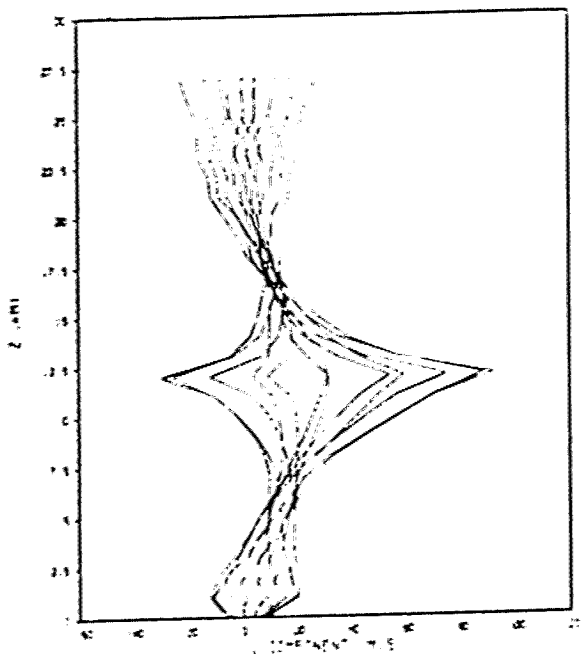

Figure 3.13 Vector Wind Model, U-Component KSC, February, Z_n = 12 km

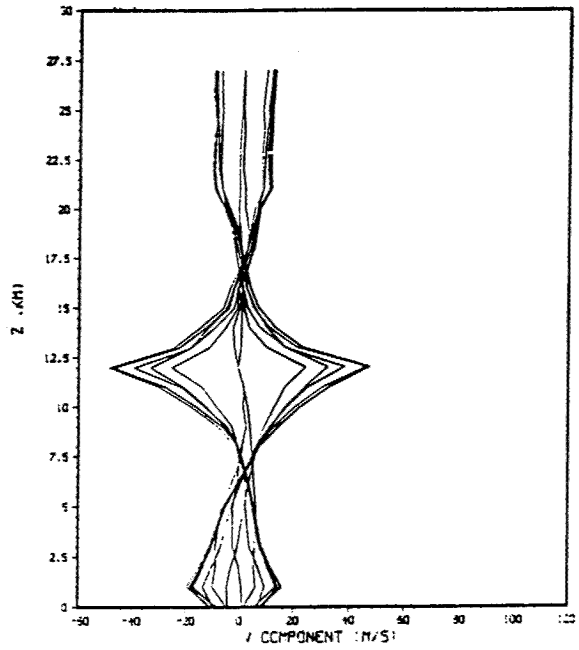

Figure 3.14 Vector Wind Model, V-Component ,KSC, February Z_0 = 12 km

3.3.4 Application of the Vector Wind Profile Model

The vector wind profile model described herein is appropriate for monthly reference periods. It is intended to be used in conjunction with the ascent guidance and control system (auto-pilot) steering commands programmed to fly the profile of monthly mean winds. Various vehicle programs have used different terms for the programmed steering commands (e.g., the early Saturn program called the commands the chi-tilt program, later they were called the wind-biased trajectory, and the Space Shuttle program calls the steering commands the I-Load). The launch vehicle designer may choose a few months to find the monthly VWP model that produces the largest monthly dispersions of ascent vehicle aerodynamic load indicators $Q\alpha$, $Q\beta$. The largest monthly dispersions for wind occur during the winter high-wind months so that it is appropriate to use the worst month from the winter season for the design reference $Q\alpha$, $Q\beta$ dispersions.

3.4 Conclusion

This chapter has presented a description of five wind profile models for aerospace vehicle ascent design. The improved monthly vector wind profile model is the most general and is recommended for future launch vehicle design studies.

The development of wind profile models for aerospace vehicle design applications has been an evolutionary process. There will continue to be requirements for wind models for future aerospace vehicle design applications. As aerospace engineering science advancements are made, there will be requirements for more advanced wind models. The recommended model for a particular vehicle program must be tailored to meet specific program requirements and vehicle mission objectives. Therefore, it is not possible to use

the specific characteristics of any ascent wind profile model presented in this report as design criteria.

3.5 References

3.1 Johnson, D.L. (Editor), "Terrestrial Environment (Climatic Criteria Guidelines for Use in Aerospace Vehicle Development)", 1993 Revision, NASA TM 4511, August, 1993.

3.2 Smith, O.E., "An Application of Distributions Derived from the Bivariate Normal Density Function", American Meteorological Society International Symposium on Probability and Statistics in the Atmospheric Sciences, University of Hawaii, June 1-4, 1971.

3.3 Smith, O. E., "Vector Wind and Vector Wind Shear Models 0-27 km Altitude for Cape Kennedy, Florida, and Vandenberg AFB, California." NASA TMX-73319, July 1976

3.4 Smith, O. E. and Austin L. D. Jr., "Sensitivity Analysis of the Space Shuttle to Ascent Wind Profiles", NASA TP 1988, March 1982.

3.5 Smith, O. E. and Austin L. D. Jr.: "Space Shuttle Response to Ascent Wind Profiles", Journal of Guidance Control and Dynamics, AIAA, Vol. 6, No. 5, Sept-Oct. (pp. 355-360), 1983.

3.6 Daniels, Glenn E. and Orvel E. Smith, "Scalar and Component Wind Correlations Between Altitude Levels for Cape Kennedy, Florida and Santa Monica, California", NASA TN D-3815, April 1968.

3.7 Adelfang, S.I., Smith, O.E., and Batts, G.W., "Ascent Wind Model for Launch Vehicle Design", J. Spacecraft and Rockets, Vol.9, No.3, pp.502-508, May-June 1994.

3.8 Norbraten, L., "Day-of-Launch I-Load Updates for the Space Shuttle", Paper 92-1274, AIAA Space Programs and Technologies Conference, March 24-27, 1992, Huntsville, AL.

3.9 Smith, O.E., and Adelfang, S.I., "STS Ascent Structural Loads Statistics", Paper 92-0720, AIAA 30th Aerospace Sciences Meeting and Exhibit, January 6-9, 1992, Reno, NV.

3.10 Gumbel, E. J. and Mustafi, C. K., "Some Analytical Properties of the Bivariate Extremal Distribution", American Statistical Association Journal, pp. 569-588, June 1967.

3.11 Gumbel, E. J., Mustafi, C. K. and Smith O. E., "Tables of the Probability and Density Functions for the Bivariate Extremal Distributions", Dept. of Industrial Engineering, Columbia University Press, New York, NY, April 1968.

3.12 Smith, O. E., Adelfang, S. I. and Brown R. P., "Ascent Structural Wind Loads for the National Space Transportation System (NSTS)", AIAA paper number 88- 0293, Proceedings of the AIAA 26th Aerospace Sciences meeting, January 10-14, 1988 at Reno, Nevada.

3.13 Wood, Joy L., "The Use of Multivariate Statistics in Evaluating Wind Profile Envelopes Over Cape Kennedy", Lockheed Missiles and Space Company, LMSC-HREC D225040, prepared for NASA/MSFC under Contract NAS8-20082, April 1971.

4.0 ASCENT STRUCTURAL LOADS ANALYSIS

4.1 Introduction

In 1988 the authors introduced (Ref. 4.1) the use of extreme value (Gumbel) statistics (Refs. 4.2 and 4.3) as a methodology for analysis of aerospace vehicle ascent structural loads and establishment of wind load increments for protection of the commit-to-launch decision for the Space Transportation System (STS). This section describes further application of extreme value analysis to a larger wind loads data base and development of methods for analysis of Go and No-Go joint and conditional probabilities for the STS for various day-of-launch (DOL) wind biasing scenarios (Ref. 4.4).

The STS commit to launch decision is based on trajectory and loads simulations using a wind profile measurement 3.5 hours prior to launch. Load increments, that protect for 99 percent of the load change during the 3.5-hour period, are calculated for all wind profile sensitive load indicators. Trajectories that are biased to a DOL wind profile produce smaller protection increments than trajectories that are biased to the profile of monthly mean wind. Smaller wind load protection increments are desirable because of the inverse correlation with the probability of 'Go' for launch. The probability of launch 'Go' or 'No-Go' is examined for individual, joint, and conditional combinations, with or without the protection increment, for 41 load variables that are calculated for each wind profile of the 114 KSC winter 3.5-hour Jimsphere pairs data base.

The concepts and the statistical analytical methodology presented herein have general applicability for future launch systems that use a trajectory and loads assessment based on a DOL wind profile for the commit to launch decision.

4.2 Procedures and Definitions

A sample of 114 winter 3.5-hour Jimsphere wind pairs for Kennedy Space Center (KSC) is used in an STS ascent flight trajectory simulation program; trajectory parameters are used in algorithms for the computation of load variables as a function of Mach number. The trajectory parameters of primary importance are the dynamic pressure, Q, the angle of attack, α, and the angle of sideslip, β. The load indicator algorithms relate external loads such as axial force, shear, bending moment, and dynamic pressure, to stress at critical locations over the Space Shuttle structure. The load indicator values are for rigid body loads due to the combined effects of the trajectory and the wind profile. Some load indicators have either positive or negative sign conventions. Some load indicators have both positive and negative sign conventions. Hence, there are more load variables than load indicators. The trajectory and loads simulations were performed for each of the 3.5-hour wind pairs. A selection of 41 of the most wind sensitive load variables was made for statistical analysis.

4.3 Wind Biased Trajectories

For this analysis of simulated STS winter launches , three techniques called I-Loads are used to bias the ascent trajectory in the pitch and yaw planes to alleviate wind loads. An I-Load is the steering commands that guide the vehicle through the first stage. These I-Loads are:

1. Baseline - The profile of the KSC February vector mean wind is used to establish the Baseline I-Load.

2. DIBS - Day-of-Launch I-Load Biasing System. The DIBS I-Load is derived from low-pass filtered (smoothed) $Q\alpha$ and $Q\beta$ trajectory profiles for a Jimsphere wind profile 3.5 hours prior to launch, which is simulated by using the 1st of the wind pairs from a sample of 114 KSC Jimsphere winter pairs.

3. FIBS (or modified DIBS). The FIBS I-Load is derived from $Q\alpha$ and $Q\beta$ trajectory profiles for a 6000-m low-pass filtered Jimsphere wind profile 3.5 hours prior to launch, which is simulated by using the filtered 1st of the wind pairs from a sample of 114 KSC Jimsphere winter pairs.

The DIBS technique appeals to the engineering community. The FIBS technique appeals to meteorologists because the wind profile used for the biased trajectory is defined.

Rigid body ascent loads simulations were performed for each of the 114 wind pairs for each of the three I-Loads. This work was performed by the Rockwell Space Operations Company (RSOC) Houston, Texas.

4.4 Loads Data Definitions

The structural load parameters of interest for the launch decision are expressed as Load Minimum Margin (LMM). The definitions for these variables, LMM and peak load (PL) are given below ; the relationship between the variables is illustrated in Figure 4.1.

1. The load limit is the ultimate structural load.
2. The Redline is the load limit reduced by the 1.4 safety factor for manned vehicles.
3. The Load Allowable (LA) is defined as:

$$LA = \text{Redline} - \sqrt{L^2_S + L^2_g} \tag{4.1}$$

where, L_S and L_g are the contributions to the load by systems uncertainties and the flexible body response to the design gust, respectively.

4. The LMM is defined as: If the simulated rigid body load exceeds the LA, the load margin is negative, which is a 'No-Go' for launch. If a negative margin occurs at any time over the Mach range of interest (0.6 to 2.2), the LMM is negative and is equal to the largest negative value of the load margin. If the simulated load is less than the LA for the entire Mach range of interest, the load margin is positive, which is a 'Go' for launch; in this case the LMM is a positive and is equal to the smallest value of the load margin over the Mach range of interest.

5. The wind load persistence increment accounts for the contribution to loads variability by the variability of the wind profile with respect to time. This is the principal topic of this paper.

6. The Peak Load (PL) is the largest load for positive load indicators (smallest for negative load indicators) from the rigid body load simulation for a wind profile.

For some load indicators the LA is highly variable over the Mach range of interest (0.6 to 2.2). This is primarily due to the aerodynamic uncertainties contribution to loads near Mach one. For such indicators the LMM could yield a load exceedance and the PL could yield a non-exceedance (See Figure 4.1). For some load indicators, the LA is approximately constant over the Mach range. For these load indicators, the LMM and the peak load occur at the same Mach number.

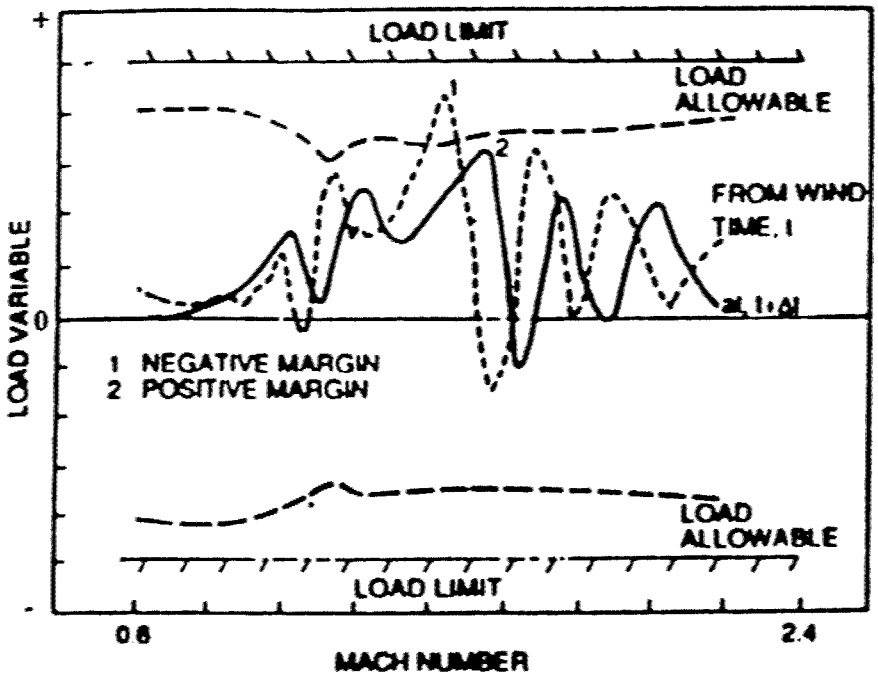

Figure 4.1 Schematic for Load Minimum Margin (LMM) and Peak Load (PL) from a wind profile loads simulation

The loads data are derived from rigid body loads simulations for each of the 114 winter 3.5-hour KSC Jimsphere wind pairs for each of the three I-Load(s) (i.e., Baseline, DIBS, and FIBS) giving for each load indicator the LMM and the Mach number at which the LMM occurred, the PL, the Mach number at which the PL occurred, and the LA versus Mach number. The original load data set contained approximately 300 load variables, which were reduced to 63 variables for a general analysis, and then further reduced to the 41 most wind sensitive load variables for statistical analysis.

4.5 Extreme Value Probability Functions

This section presents, in general notation, the extreme value probability functions used in the analyses of the STS ascent structural loads described in the previous section.

4.5.1 Univariate Distribution

The first asymptotic extreme value distribution developed by Gumbel (Ref. 4.2), that now often bears his name, has the probability density function, $\varphi(Y)$, given by:

$$\varphi(Y) = 1/\alpha_y \exp [-Y - e^{-Y}] \tag{4.2}$$

The Gumbel cumulative probability function (CPF) is:

$$\Phi(Y) = \exp [- e^{-Y}] \tag{4.3-1}$$

where, the reduced variate, Y ($-\infty \leq Y \leq \infty$) is:

$$Y = (y - \mu_y)/\alpha_y \tag{4.3-2}$$

where, y is the extremal random variate, μ_y is the location parameter (the mode), and α_y is the dispersion parameter. Gumbel's modified moment method is used to estimate μ_y and α_y.

$$\alpha_y = s_y / \sigma_n \tag{4.4}$$

$$\mu_y = \bar{y} - \alpha_y \bar{y}_n, \tag{4.5}$$

where, s_y and $\bar{y}$ are the sample standard deviation and mean values, respectively; σ_n and $\bar{y}_n$, the standard deviation and mean values for the reduced variate, are a function of sample size, n. For n = 114, σ_n = 1.2118, $\bar{y}_n$ = 0.5613. As $n \rightarrow \infty$, $\bar{y}_n$ approaches Euler's constant (0.57722), and σ_n approaches $\pi / \sqrt{6}$ (1.2855). The inverse solution of Eq. 4.3-1 (i.e. the reduced variate as function of probability, p) is:

$$Y_p = - \ln [- \ln(p)] \tag{4.6}$$

The variate y_p is calculated from Y_p,

$$y_p = \mu_y + \alpha_y \; Y_p \tag{4.7}$$

4.5.2 Bivariate Distribution

For the Gumbel bivariate extreme value distribution, there are two forms (Ref. 4.3). They are designated as the a-case and the m-case. The two forms are identical only when the variates are independent. The m-case is more general and is the one selected for subsequent analysis. The probability density function for the m-case is:

$$\varphi(X,Y,m) = \Phi(X,Y,m)\left[\left(e^{-mX} + e^{-mY}\right)^{1/m-2} e^{-mX-mY}\left\{\left(e^{-mX-mY}\right)^{1/m} + m - 1\right\}\right] \tag{4.8}$$

where $\Phi(X,Y,m)$, the bivariate extreme value probability distribution function (PDF) for the m-case is:

$$\Phi(X,Y,m) = \exp\left[-(e^{-mX} + e^{-mY})^{1/m}\right] \tag{4.9}$$

where, $\Phi(X,Y,m)$ is the probability p that X and Y are contained in a rectangle, expressed as $P = Pr\{-\infty \le X \le X^*, -\infty \le Y \le Y^*; m\}$. Y is the reduced variate as defined previously (Eq. 4.3-2) and X is the reduced variate, similarly defined as:

$$X = (x - \mu_X)/\alpha_X. \tag{4.10}$$

The parameter, m, is a measure of association between the two extreme value variates given by:

$$m = [1 - \rho]^{-1/2}, \text{ where } m \ge 1 \tag{4.11}$$

and ρ is the correlation coefficient between either the original random variates or the reduced variates. From Eq. 4.11, ρ must be ≥ 0.

In summary, the required Gumbel parameters for Eq. 4.8 μ_X, μ_y, α_X, α_y, and m are estimated from the sample parameters $\bar{x}, \bar{y}$, s_X, s_y, and r(x, y). In the loads analysis described in later paragraphs, the load indicator values for the 1st and 2nd of the wind pairs are designated as Y and X respectively.

4.5.2.1 Probability Within Contours

Contours of equal probability for the bivariate extreme value distribution are calculated by a double numerical integration of Eq.4.8 that takes advantage of the symmetry of the contours with respect to a coordinate system that is rotated by 45 degrees counter-

clockwise relative to the original coordinate system. Figs. 4.2 through 4.4 illustrate the contours for variables that are independent (m=1), moderately correlated (m=1.414) and highly correlated (m=2), respectively; the probability density values and the probabilities for the numbered contours are listed in Table 4.1; the values for positive X′ at the intersection of each contour with the rotated X axis are also listed in Table 4.1. The solution of the bivariate extreme distribution in this form has valuable theoretical and practical applications in the analysis of the joint relations between extremals.

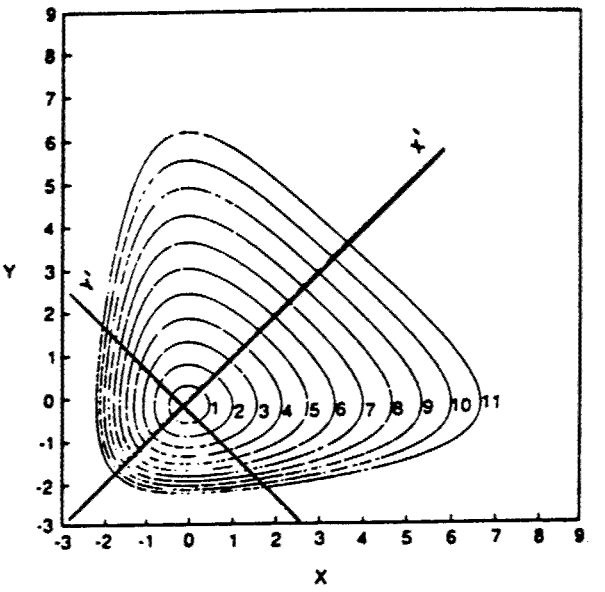

Figure 4.2 Bivariate Extreme Value Density Contours (m=1.00)

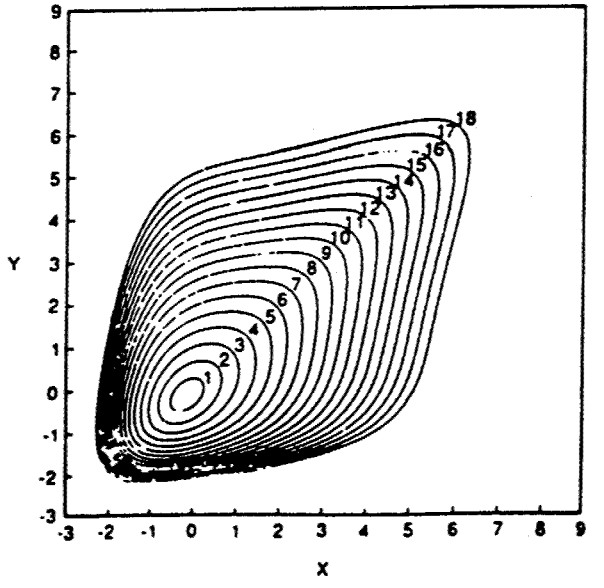

Figure 4.3 Bivariate Extreme Value Density Contours (m=1.414)

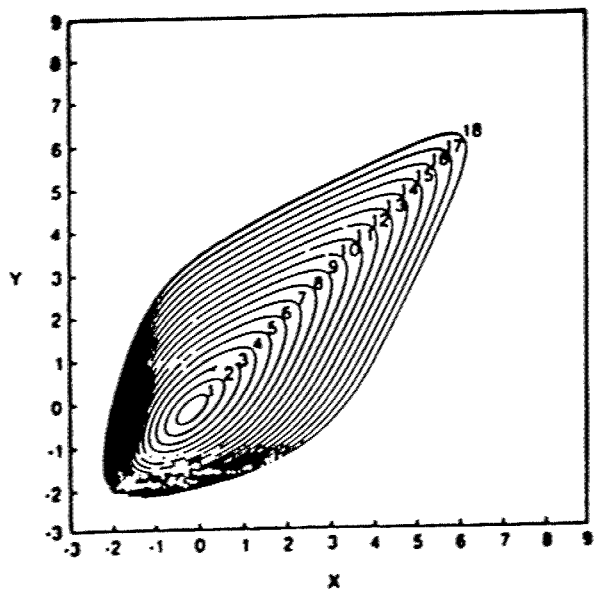

Figure 4.4 Bivariate Extreme Value Density Contours (m=2.00)

Table 4.1 Probability Contained within Contours (Figs. 4.2 through 4.4) of Equal probability Density for the Gumbel Bivariate Extreme Value Probability Function, m-case

	M = 1.000, ρ = 0.0000 X′ mode = 0.000 Modal Density = 0.13534			M = 1.414, ρ = 0.500 X′ mode = -0.14916 Modal Density = 0.16471			M = 2.000, ρ = 0.7500 X′ mode = -0.19041 Modal Density = 0.20999		
Contour Number	X′	Density Contour	Prob.	X′	Density Contour	Prob.	X′	Density Contour	Prob.
1	.50	.12106	.0905	.35	.15039	.0704	.31	.19480	.0578
2	1.00	.09069	.2892	.85	.11964	.2265	.81	.16147	.1888
3	1.50	.05998	.5016	1.35	.08733	.4000	1.31	.12479	.3403
4	2.00	.03635	.6769	1.85	.06067	.5535	1.81	.09246	.4824
5	2.50	.02071	.8022	1.35	.04112	.6750	2.31	.06686	.6028
6	3.00	.01131	.8841	2.85	.02763	.7656	2.81	.04769	.6994
7	3.50	.00599	.9341	3.35	.01858	.8314	3.31	.03376	.7746
8	4.00	.00310	.9634	3.85	.01255	.8785	3.81	.02381	.8320
9	4.50	.00159	.9801	4.35	.00855	.9122	4.31	.01675	.8753
10	5.00	.00080	.9892	4.85	.00586	.9364	4.81	.01178	.9078
11	5.50	.00040	.9942	5.35	.00404	.9538	5.31	.00827	.9320
12	6.00	.00020	.9970	5.85	.00280	.9664	5.81	.00581	.9500
13				6.35	.00194	.9755	6.31	.00408	.9633
14				6.85	.00135	.9822	6.81	.00287	.9731
15				7.35	.00095	.9870	7.31	.00201	.9803
16				7.85	.00066	.9906	7.81	.00141	.9856
17				8.35	.00048	.9931	8.31	.00099	.9895
18				8.85	.00033	.9950	8.81	.00070	.9924

4.5.3 Logistic Distribution

The differences between the reduced variates, X and Y for the m-case bivariate extreme value distribution function is a form of the logistic distribution. Let

$$(X - Y) = t \tag{4.12}$$

The logistic PDF is:

$$F(t) = [1 + e^{-mt}]^{-1} \tag{4.13}$$

where, the mean t = 0, and the theoretical standard deviation, σ_t, is:

$$\sigma_t = \frac{\pi}{\sqrt{3}m} \tag{4.14}$$

Eq. 4.13 is a symmetrical function about zero. An important application of the logistic PDF is as a hypothesis test for establishing the m-case for bivariate extremals i.e. the logistic distribution for the differences of extremals X and Y is a necessary and sufficient condition for the m-case bivariate extreme value distribution of X and Y.

An alternate method for estimating the m-parameter is to solve Eq. 4.14 for m using the sample standard deviation of the differences between two variables (s_t) for σ_t .

4.5.4 Conditional Distribution

An important application of the conditional extreme value probability function is made to obtain the wind loads persistence increment using the data bases described in Section 4.4. The conditional extreme value probability distribution function for the m-case is:

$$\Phi \{X \leq X^* \mid Y = Y_1\} = Z^{1/m-1} \exp [-Z^{1/m} - (m - 1)\, Y + e^{-Y_1}] \tag{4.15}$$

where, $Z = (e^{-mX} + e^{-mY})$, and X and Y are the reduced variates. Eq. 4.15 has the following meaning: It is the probability that X will be less than or equal to an assigned value X* given that Y is equal to Y_1 .

It is the inverse solution of Eq. 4.15 that is desired to obtain the time conditional percentile value for the wind loads persistence increment; namely, for a conditional probability of 0.99, and a known value of X, what is the value of Y ? This solution cannot be obtained in closed form. It is obtained by an application of Newton's numerical method of successive approximations. In applications for the LMM data set, the conditional reduced variate is converted to the original variate having physical units. The conditional 99th percentile value for LMM is called the 99% wind loads persistence increment.

From the functional relationships between Eqs. 4.3-1 and 4.9, the conditional probability function for an interval is derived as:

$$\Phi\left\{X \le X^* | Y_1 \le Y \le Y_2; m\right\} = \frac{\Phi\left\{X^*, Y_2; m\right\} - \Phi\left\{X^*, Y_1; m\right\}}{\Phi\left\{Y_2\right\} - \Phi\left\{Y_1\right\}} \qquad (4.16)$$

where, $Y_2 > Y_1$. By setting $Y_2 = Y_1 + \varepsilon$, where ε is a small increment, this function will approximate Eq. 4.15.

4.6 Statistical Analysis

To illustrate the specific analyses techniques, four Space Shuttle orbiter load variables are selected, they are:

(1) WINGRA14(-), this is the right (R) wing spar cap.
(2) WING LA 14(-), this is the left (L) wing spar cap.

The sign convention for the load variables is in parenthesis.

(3) VTL 11(+), this is the left (L) vertical tail root rib beaded panel web (positive side).
(4) VTL 11(-), this is the left (L) vertical tail root rib beaded panel web (negative side).

Detailed statistical analysis for these load variables for the three I-Loads are presented. Summary statistics are presented for the 41 most wind sensitive load variables. The physical units for all load indicators have been purposely omitted.

4.6.1 Load Minimum Margin (LMM)

The five bivariate Gumbel extreme value statistical parameters for LMM for the four orbiter load variables listed in Table 4.2 were computed using Eqs. 4.3-1 and 4.7. The first step in the analysis is to establish that the sample marginal distributions are univariate Gumbel distributed. The next step is to justify application of the m-case bivariate Gumbel distribution by establishing that the differences between the paired reduced variates fit the logistic distribution.

Figure 4.5 compares the LMM Baseline I-Load sample probabilities (dots) with the theoretical Gumbel probability distribution (the straight line) for the 1st of each 114 wind pairs for load indicator WINGRA14. The two curved lines are the 68 percent confidence bands. These curves give a measure of goodness of fit. Figure 4.6 illustrates a similar comparison for the DIBS I-Load. These Figs. indicate that there is an excellent agreement between the empirical and theoretical Gumbel probabilities. The algebraic sign for the LMM has been reversed solely for mathematical conveniences. Thus, the positive values (Figure 4.5 and Figure 4.6) on the ordinate scale, yield negative margins, that is, a 'No-Go' condition. From Figure 4.5, there are four wind profiles (dots above the zero line) that

produce load exceedances. The theoretical exceedance probability for this example, from Table 4.2 is 0.9603 (denoted as P{Y} for the 1st of the wind pairs; the empirical probability is 0.9565 (114-4)/(114+1). The theoretical probabilities that the LMM will not exceed the LA for the 1st and 2nd of the pairs in Table 4.2 are computed from the univariate Gumbel probability distribution using the reduced variates, $Y = (0 - \mu_y)/\alpha_y$ and $X = (0 - \mu_x)/\alpha_x$, respectively. These probabilities give the 'Go' probabilities for the load variables after accounting for the 1.4 safety factor, system's uncertainties and gust (flexible body) contributions to loads. But no allowance has been made for wind load persistence. From Table 4.2, it is seen that, by biasing to the wind profile measured 3.5 hours prior to launch time (T = 0), the DIBS or FIBS technique will increase the probability of 'Go' (no load exceedance). The computations and graphical comparisons used for the example described in Table 4.2 and Figures 4.5 and 4.6 were also made for all of the 63 ascent load variables. The 41 most wind sensitive variables have probability distribution functions that adequately fit the Gumbel distribution. Load indicators WINGRA14 and WINGLA14 have the highest probability of a 'No-Go' (load exceedance). If all the load variables were statistically independent, the launch probability, without allowance for wind load persistence, would be the product of the probabilities, P{X} or P{Y}, for all the load variables. It is known from the load algorithms and from sample correlation coefficients that the load variables are not independent. In fact some load variables are highly correlated with each other. Since no simple theoretical model was found to combine these probabilities, the empirical method of counting the wind profiles that yield load exceedances (non-exceedances) is used.

Table 4.2 Bivariate Gumbel parameters for Load Minimum Margin (LMM) and the probabilities for no load exceedances for LMM for 1st of pairs (y) and 2nd of pairs (x) from 114 winter KSC 3.5-hour wind pairs

I-LOAD	μ_y	μ_x	α_y	α_x	m	P{Y}	P{X}
BASELINE							
WING RA 14(-)	-5597	-5663	1746	1764	1.918	.9603	.9604
WING LA 14(-)	-5579	-5616	1712	1806	1.985	.9623	.9563
VTL 11(+)	-0.51	-0.50	0.09	0.09	2.019	.9965	.9954
VTL 11(-)	-0.34	-0.34	0.06	0.06	2.448	.9965	.9963
DIBS							
WING RA 14(-)	-5666	-5741	1339	1292	1.631	.9856	.9983
WING LA 14(-)	-5303	-5293	1278	1354	1.561	.9844	.9802
VTL 11(+)	-0.49	-0.48	0.05	0.05	1.230	.9999	.9999
VTL 11(-)	-0.36	-0.37	0.03	0.04	1.403	.9999	.9999
FIBS							
WING RA 14(-)	-6318	-6315	1496	1339	1.735	.9855	.9911
WING LA 14(-)	-5488	-5335	1391	1396	1.687	.9808	.9784
VTL 11(+)	-0.48	-0.46	0.06	0.05	1.350	.9997	.9998
VTL 11(-)	-0.38	-0.38	0.03	0.04	1.304	.9999	.9999

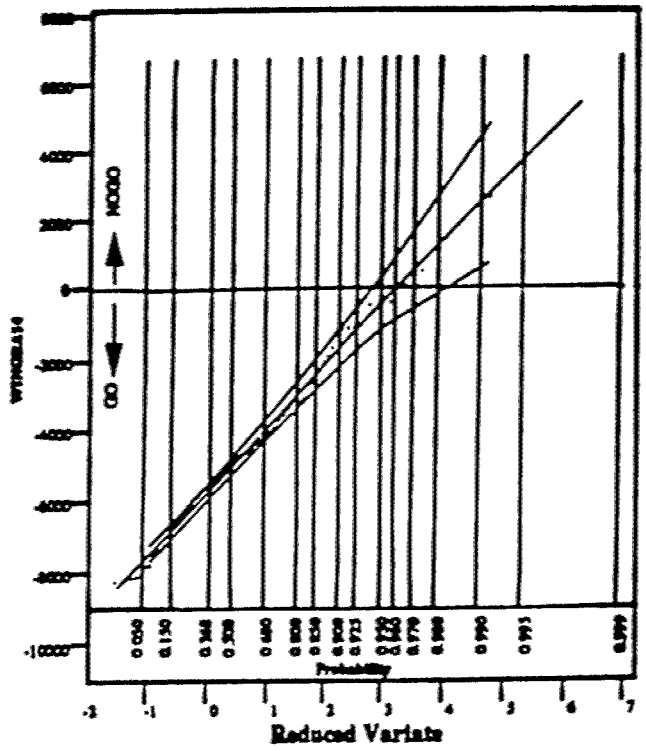

Figure 4.5 Gumbel extreme value probability distribution for LMM Baseline I-Load for WINGRA14 from 1st of 114 winter 3.5-hour wind pairs, KSC

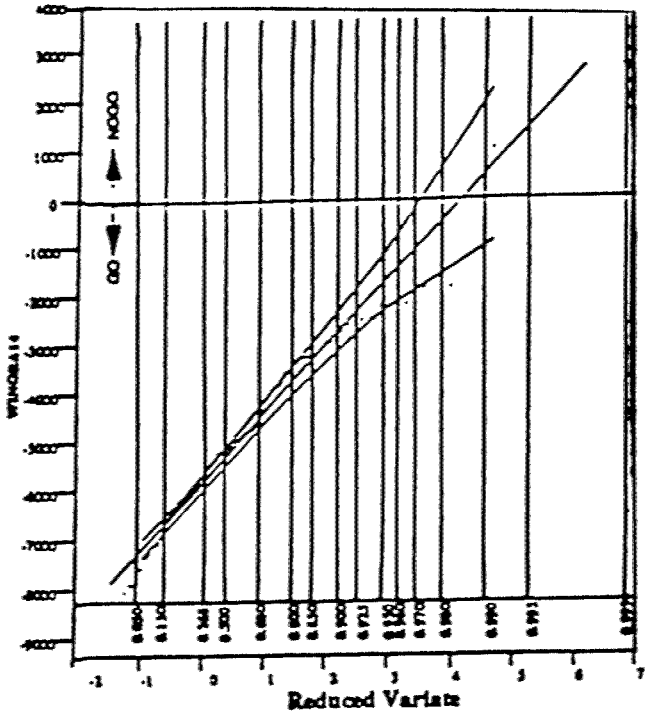

Figure 4.6 Gumbel extreme value distribution for LMM DIBS for WINGRA14 from 1st of 114 winter 3.5-hour wind pairs, KSC

The differences between the reduced variates for the LMM from the wind pairs were tested for goodness of fit to the logistic probability function. The fit is adequate for all the 41 load variables for the three I-Loads; this validates the use of the Gumbel m-case bivariate extreme value probability distribution functions.

4.6.2 Wind Loads Persistence Increment for LMM

The wind load persistence increment is derived from the conditional extreme value Gumbel probability distribution function for the m-case (Eq. 4.15). For the illustrated LMM statistics given in Table 4.3, the 1st column identifies the load variables for the three I-Loads, the 2nd column is the reduced variate X^* for LMM from the 1st of the wind pairs. $X^* = (0 - \mu_X)/\alpha_X$. The 3rd column, denoted by $| Y_{.99}$, is computed by obtaining the inverse solution to Eq. 4.15 for the conditional probability $P_c = 0.99$.

This is the value required to calculate the 99th conditional percentile values given in column 4, denoted as LALMM, which is the largest allowable load minimum margin to protect for 99 percent of the load change, given that the ascent load is determined from a wind profile measurement at T - 3.5 hours. It is computed by:

$$\text{LALMM} = \mu_Y + \alpha_Y (| Y_{.99}) \qquad (4.17)$$

Henceforth, this statistic is called the 99 percent wind load persistence increment. Column 5 in Table 4.3 gives the probability that the ascent loads will not exceed the LALMM which is computed using the univariate Gumbel distribution, i.e.:

$$\Pr\{\text{LALMM}\} = \exp\,[-e^{-| Y_{.99}}]\,. \qquad (4.18)$$

Column 5 gives the probability that there is no load exceedance after accounting for the 1.4 safety factor, the system's uncertainties and wind gust contributions to ascent loads, and the 99 percent 3.5 hour wind persistence increment. This probability increases for DIBS or FIBS compared to the Baseline I-Load; i.e., an increase in launch probability is indicated for DIBS or FIBS. For WINGRA14, the Go probability is 70.66 percent for Baseline, 88.50 percent for DIBS and 92.17 percent for FIBS.

Column 6 in Table 4.3 is the 99th percentile wind load change for LMM over the 3.5-hour time interval derived from the logistic distribution (Eq. 4.14):

$$\Delta L_{.99} = (\alpha_y/m)\,[\,-\ln\,(1/p - 1)] \qquad (4.19)$$

Because the logistic probability distribution is symmetric on either side of zero, the 1 and 99 percentiles are equivalent in magnitude but have opposite signs. The 99th percentile wind load changes over 3.5 hours (column 6) are, in general, larger than the absolute values for the conditional 99th percentile value given in column 4. This is as it should be, because no prior load is used as given information from the 1st of the wind pairs. Column

7 gives the probability that the LMM will not be exceeded using the 99th percentile wind load change. This probability is computed from the univariate Gumbel distribution by:

$$P\{\Delta L_{.99}\} = \exp - [e^{-(\Delta L_{.99} - \mu_y) / \alpha_y}] \qquad (4.20)$$

Comparing columns 5 and 7, it is seen that the wind load change probabilities are less than those using the conditional 99th percentile wind load increment. For example, in column 7, the WINGRA14 load variable for Baseline gives a 64.10 percent chance for Go whereas the conditional yields a 70.66 percent chance for Go (column 5). For this example (WINGRA14), the 98th interpercentile range is ±4182 (units unspecified): using ΔL = +4182 in Eq. 4.20 gives the most favorable probability for Go which is 99.63 percent. It is known that the wind load changes during the day-of-launch (DOL) countdown can become more favorable or less favorable for launch. From the logistics probability function, there is a 50/50 chance that the LMM wind load changes will either increase or decrease with respect to time. However, it is the 99 percent wind load persistence increment, derived from the conditional extreme value probability (LALMM Table 4.3), that is used for protection of the load allowable.

Table 4.3 The conditional 99th percentile values (LALMM) and the 99th percentile load change ($\Delta L_{.99}$) for LMM from 3.5-hour wind pairs

I-LOAD	X*	$V_{.99}$	LALMM[a]	$P_{(LALMM)}$	$\Delta L_{.99}$	$P(\Delta L_{.99})$
Col 1	Col 2	Col 3	Col 4	Col 5	Col 6	Col 7
BASELINE						
WING RA 14(-)	3 210	1 062	-3743	7066	4182	6410
WING LA 14(-)	3 109	0 986	-3891	6886	3964	6775
VTL 11(+)	5 372	3 422	-0 21	9679	0 205	9669
VTL 11(-)	5 607	3 752	-0 10	9768	0 1136	9777
DIBS						
WING RA 14(-)	4 443	2 103	-2850	8850	3773	7841
WING LA 14(-)	3 909	1 387	-3530	7790	3762	7412
VTL 11(+)	9 135	6 776	-0 14	9989	0 187	9977
VTL 11(-)	9 385	7 006	-0 13	9991	0 098	9998
FIBS						
WING RA 14(-)	4 718	2 507	-2567	9217	3963	8128
WING LA 14(-)	3 822	1 460	-3457	7928	3788	7448
VTL 11(+)	8 400	6 002	-0 12	9975	0 200	9906
VTL 11(-)	10 583	8 188	-0 13	9997	0 106	9999

a) Column 4 is the 99 percent wind loads persistence increment

A summary for the number of wind profiles that had a load exceedance for any one of the 41 load variables (No-Go) is given in Table 4.4 with or without the wind load persistence increment applied to both the 1st and the 2nd of the wind pairs. There is a great decrease in the percent of Go wind profiles when the wind load persistence increment is used. This analysis (Table 4.4) clearly shows the significance of the wind load persistence increment and the superiority of DIBS and FIBS compared to Baseline I-Load. For example, the percent of Go wind profiles for the 1st of the wind pairs without wind load persistence is 90 percent for Baseline, 98 percent for DIBS and 96 percent for FIBS. The percent of Go wind profiles for the first of the wind pairs with the wind load persistence is 38 percent for

Baseline, 63 percent for DIBS and 64 percent for FIBS. FIBS is equally as effective as DIBS in increasing the percent of Go wind profiles over that of the Baseline I-Load.

Table 4.4 Number of No-Go wind profiles and empirical Go probabilities for LMM for 41 STS load indicator variables from 114 winter 3.5-hour KSC wind pairs

I-LOAD	Without Wind Load Persistence		With 99% Conditional Wind Load Persistence[b]	
	# NO-GO Winds	% of GO[a] Winds	# NO-GO Winds	% of GO Winds
BASELINE				
1st of Pair	10	90	70	38
2nd of Pair	12	89	73	36
DIBS				
1st of Pair	1	98	42	63
2nd of Pair	2	97	47	58
FIBS				
1st of Pair	4	96	40	64
2nd of Pair	2	97	43	61

a. Percent GO Winds = (114 - # NO-GO Winds/115)100
b. Wind Load Persistence increment applied to both the 1st and 2nd of pairs.

4.6.3 Go and No-Go Combinations

This subsection presents a detailed statistical analysis for Go and No-Go combinations for individual load variables for LMM using the three I-Loads (Baseline, DIBS, and FIBS). The extreme value probability functions used in this analysis are:

$$\Phi\{Y\} = \exp\,[-e^{-Y}], \tag{4.21}$$

where, $Y = (L_1 - \mu_1)/\alpha_1$ is the reduced variate for LMM from the first of the wind pairs. This gives the $\Pr\{L_1 \le L_1^*\}$.

$$\Phi\{X\} = \exp\,[-e^{-X}], \tag{4.22}$$

where, $X = (L_2 - \mu_2)\alpha_2$ is the reduced variate for LMM from the second of the wind pairs. This gives the $\Pr\{L_2 \le L_2^*\}$.

$$\Phi\{X,Y; m\} = \exp[e^{-mX} + e^{-mY}]^{1/m} \tag{4.23}$$

This is the joint (bivariate) Gumbel m-case extreme value probability distribution function. This gives $\Pr\{L_2 \le L_2^*, L_1 \le L_1^*\}$. The five Gumbel parameters are from Table 4.2, and the wind load persistence increments are from Table 4.3. Further, we specify the following cases for Y and X:

(1) We assign $L_1 = 0$ and $L_2 = 0$ to yield the Go probability for LMM without wind load persistence for first and second of the wind pairs, respectively.

(2) We assign L_1 = LALMM and L_2 = LALMM, where LALMM is the wind load persistence increment (Table 4.3) to yield the Go probabilities for LMM with the wind load persistence increment for the first and second of the wind pairs, respectively.

(3) Also, we assign $L_2 = 0$ (without persistence for the second of wind pairs) and L_1 = LALMM (with wind load persistence for the first of wind pairs).

The theoretical joint extreme value probability functions for LMM from the first (Y) and second (X) of wind pairs are expressed as:

$$\text{(i)}\ \Pr\{Go_2, Go_1\} = \Phi\{X, Y; m\} \tag{4.24}$$

$$\text{(ii)}\ \Pr\{\text{No-}Go_2, Go_1\} = \Phi\{Y\} - \Phi\{X, Y; m\} \tag{4.25}$$

$$\text{(iii)}\ \Pr\{Go_2, \text{No-}Go_1\} = \Phi\{X\} - \Phi\{X, Y; m\} \tag{4.26}$$

$$\text{(iv)}\ \Pr\{\text{No-}Go_2, \text{No-}Go_1\} = 1 - \Phi\{X\} - \Phi\{Y\} + \Phi\{X, Y; m\} \tag{4.27}$$

The sum of the above probabilities is unity. From the above joint probability functions, the theoretical conditional probability functions are:

$$\text{(i)}\ \Pr\{Go_2|Go_1\} = \Phi\{X, Y; m\}/\Phi\{Y\} \tag{4.28}$$

$$\text{(ii)}\ \Pr\{\text{No-}Go_2|Go_1\} = \Phi\{Y\} - \Phi\{X, Y; m\}/\Phi\{Y\} \tag{4.29-1}$$

$$= 1 - \Pr\{Go_2|Go_1\} \tag{4.29-2}$$

$$\text{(iii)}\ \Pr\{Go_2|\text{No-}Go_1\} = (\Phi\{X\} - \Phi\{X, Y; m\})/(1 - \Phi\{Y\}) \tag{4.30}$$

$$\text{(iv)}\ \Pr\{\text{No-}Go_2|\text{No-}Go_1\} = (1 - \Phi\{X\} - \Phi\{Y\} + \Phi\{X, Y; m\})/(1 - \Phi\{Y\}) \tag{4.31-1}$$

$$= 1 - \Pr\{Go_2|\text{No-}Go_1\} \tag{4.31-2}$$

The sum of Eqs 4.28 and 4.29 = 1. and the sum of Eqs 4.30 and 4.31 = 1.

The computational forms for the above theoretical functions used to compute the empirical probabilities are:

$$\text{(i)}\ \Pr\{Go_1\} = n_1/(n+1) \tag{4.32}$$

where n_1 is the number of observed counts for Go_1 and n is the sample size.

$$\text{(ii)}\ \Pr\{\text{No-}Go_1\} = 1 - \Pr\{Go_1\} \tag{4.33}$$

(iii) $Pr\{Go_2\} = n_2/(n+1)$ (4.34)

where, n_2 is the number of observed counts for Go_2.

(iv) $Pr\{No\text{-}Go_2\} = 1 - Pr\{Go_2\}$ (4.35)

For the joint probabilities the computational forms are:

(i) $Pr\{Go_2,Go_1\}$ = the joint # of counts $\{Go_2, Go_1\}/(n+1)$ (4.36)

(ii) $Pr\{No\text{-}Go_2,Go_1\}$ = # of Go_1 counts/(n + 1) - $Pr\{Go_2,Go_1\}$ (4.37)

(iii) $Pr\{Go_2,No\text{-}Go_1\}$ = # of Go_2 counts/(n + 1) - $Pr\{Go_2,Go_1\}$ (4.38)

(iv) $Pr\{No\text{-}Go_2,No\text{-}Go_1\} = 1 - Pr\{Go_2\} - Pr\{Go_1\} + Pr\{Go_1,Go_2\}$ (4.39)

For the above joint Go and No-Go empirical functions, the only necessary data are the observed number of counts (n) for Go_1, Go_2 and the joint (simultaneous) observed number of counts $\{Go_1$ and $Go_2\}$; for this analysis the total sample size, n, is 114.

The computation forms are:

(i) $Pr\{Go_2|Go_1\}$ = the joint # of counts $\{Go_2,Go_1\}/[\#$ of Go_1 counts + 1] (4.40)

(ii) $Pr\{No\text{-}Go_2|Go_1\} = 1 - Pr\{Go_2|Go_1\}$ (4.41)

(iii) $Pr\{Go_2|No\text{-}Go_1\}$ = the joint # of counts $\{Go_2,No\text{-}Go_1\}/[\#No\text{-}Go_1$counts+1] (4.42)

(iv) $Pr\{No\text{-}Go_2|No\text{-}Go_1\} = 1 - Pr\{Go_2|No\text{-}Go_1\}$ (4.43)

For the above empirical conditional probability functions, the only necessary observed data are those for the joint probability functions plus the joint (simultaneous) observed number of counts for $\{Go_2$, No-$Go_1\}$. The empirical and theoretical probabilities presented in Tables 4.5 through 4.10 are computed using the foregoing application of the wind load persistence increment.

The number of observed wind profile counts is sufficiently large for Baseline WINGRA14 with the wind load persistence increment applied to both pairs (Table 4.5) to make feasible the comparisons between the empirical probabilities and the theoretical probabilities for the Go, No-Go, joint and conditional probabilities. Considering the sample size, there is good agreement between the observed and theoretical probabilities for this load variable. The theoretical probabilities for the WINGRA14 load variable for DIBS and FIBS are compared with the Baseline I-Load in Table 4.6. For this load variable, the Go

probabilities, the joint Go probabilities for the first and second of the wind pairs and the conditional probabilities for Go for the second wind profile, given that there is a Go for the first of wind pairs, all increase over the Baseline I-Load for DIBS and FIBS. The most undesirable situation (Table 4.6) is the conditional probability: Given that the WINGRA14 load variable is favorable for launch (Go 1st) at 3.5 hours prior to launch (T - 3.5 hours), then there is a 13.18 percent probability for a No-Go at T-0 using the Baseline I-Load; for DIBS, this probability is 5.18 percent and for FIBS it is 2.51 percent. Evaluations for the other conditional probabilities can be made for various scenarios. The Go, No-Go, the joint Go, No-Go, and conditional probabilities as in Table 4.6, for each of the 41 load variables for the three I-Loads, have been computed using the 3.5-hour 99 percent wind load persistence increment applied to the wind pairs. These statistics have important applications in the engineering ascent load assessment to identify the most wind sensitive load variables.

Table 4.5 Observed and theoretical probabilities (percent) for WINGRA14 for LMM with 99% wind load persistence increment applied to both wind pairs Baseline I-Load from 114 winter 3.5-hour KSC wind profile pairs

PROBABILITIES	Observed		Theoretical
	# Counts	P %	P %
GO 1st	83	72.2	70.77
NO-GO 1st	31	27.8	29.23
GO 2nd	78	67.8	71.41
NO-GO 2nd	36	32.2	28.59
Joint			
$Pr\{GO_2, GO_1\}$	70	60.9	61.44
$Pr\{NO\text{-}GO_2, GO_1\}$	13	11.3	9.33
$Pr\{GO_2, NO\text{-}GO_1\}$	9	7.0	9.97
$Pr\{NO\text{-}GO_2, NO\text{-}GO_1\}$	22	20.9	19.26
Conditional			
$Pr\{GO_2, GO_1\}$	70	83.3	86.82
$Pr\{NO\text{-}GO_2, GO_1\}$	13	16.7	13.18
$Pr\{GO_2, NO\text{-}GO_1\}$	9	28.1	34.11
$Pr\{NO\text{-}GO_2, NO\text{-}GO_1\}$	22	71.9	65.89

Table 4.6 Theoretical Probabilities (percent) for WINGRA14 for LMM with 99 % wind load persistence increment applied to both wind pairs from 114 KSC 3.5-hour winter wind profile pairs

	PROBABILITY (percent)		
EVENT	BASELINE	DIBS	FIBS
GO 1st	70.77	88.50	92.17
NO-GO 1st	29.23	11.50	7.83
GO 2nd	71.41	89.87	94.10
NO-GO 2nd	28.59	10.13	5.9
Joint			
$Pr\{GO_2, GO_1\}$	61.44	83.92	89.86
$Pr\{NO\text{-}GO_2, GO_1\}$	9.33	4.58	2.31
$Pr\{GO_2, NO\text{-}GO_1\}$	9.97	5.95	4.24
$Pr\{NO\text{-}GO_2, NO\text{-}GO_1\}$	19.26	5.54	3.59
Conditional			
$Pr\{GO_2 \mid GO_1\}$	86.82	94.82	97.49
$Pr\{NO\text{-}GO_2 \mid GO_1\}^a$	13.18	5.18	2.51
$Pr\{GO_2 \mid NO\text{-}GO_1\}$	34.11	51.79	54.19
$Pr\{NO\text{-}GO_2 \mid NO\text{-}GO_1\}$	65.89	48.21	45.81

(a) This is the most undesirable case.

Table 4.7 summarizes the Go (No-Go), joint and conditional probabilities for any one of the 41 load variables not exceeding (exceeding) the load allowable using the 99 percent wind load persistence increment applied to the wind pairs. These statistics have important applications in developing DOL scenarios for a launch decision (Go or No-Go) made at T - 3.5 hours. The most undesirable situation is the conditional probability $Pr\{No\text{-}Go_2 \mid Go_1\}$. For this case the Baseline I-Load gives 35.6 percent, DIBS is 26.0 percent and FIBS is 22.7 percent.

Table 4.7 The number of observed Go and No-Go LMM wind counts and percent probabilities with the 99 % wind load persistence increment applied to both 1st and 2nd wind pairs for 41 load variables from 114 winter 3.5-hour wind pairs KSC

	BASELINE		DIBS		FIBS	
EVENT	Counts	P %	Counts	P %	Counts	P %
GO 1st	44	38.3	72	62.6	74	64.3
NO-GO 1st	70	61.7	42	37.4	40	35.7
GO 2nd	41	35.7	67	58.3	71	61.7
NO-GO 2nd	73	64.3	47	41.7	43	38.3
Joint						
$Pr\{GO_2, GO_1\}$	29	25.2	54	47.0	58	50.4
$Pr\{NO\text{-}GO_2, GO_1\}$	15	13.0	18	15.7	16	13.9
$Pr\{GO_2, NO\text{-}GO_1\}$	12	10.4	13	11.3	13	11.3
$Pr\{NO\text{-}GO_2, NO\text{-}GO_1\}$	58	51.3	29	26.1	27	24.3
Conditional						
$Pr\{GO_2 \mid GO_1\}$	29	64.4	54	74.0	58	77.3
$Pr\{NO\text{-}GO_2 \mid GO_1\}^a$	15	35.6	18	26.0	16	22.7
$Pr\{GO_2 \mid NO\text{-}GO_1\}$	12	16.9	13	30.2	13	31.7
$Pr\{NO\text{-}GO_2 \mid NO\text{-}GO_1\}$	58	83.1	29	69.8	27	68.3

(a) This is the most undesirable situation.

In general, the STS DOL procedure is to perform ascent rigid body loads simulations using measured Jimsphere wind profiles taken at L-6.75, L-4.25, L-3.0, L-2.0 hours and at L-70 minutes. In case there is an unscheduled hold at T-20 minutes, the above procedure is repeated at hourly intervals until the vehicle is launched. For the STS operations decision, the 3.5-hour wind load persistence increment is applied at each of the L-times including L - 70 minutes. At L-3.0 hours, the 3.5-hour wind load persistence increment gives loads protection for an on-time launch at T = 0. (There are scheduled holds.) At L - 70 minutes, the 3.5-hour wind persistence increment gives loads protection up to the close of the launch window which is , typically, T = 0 plus 2 to 3 hours. These DOL procedures are based on practical operational time-line considerations. It requires about 1 hour from the Jimsphere release to measure the wind profile: Then about 2 1/2 hours is required to perform the rigid body loads simulations, engineering evaluations, validations and management conferences to reach a Go or No-Go launch decision. If the DOL operational time-line is reduced, then the wind loads persistence increment can also be reduced. In principle, if the DOL operational time-line can be reduced to some minutes prior T = 0 (near real time), then the rigid body wind load persistence increment is near zero. Hence, there would be no requirement to make allowances for the wind loads persistence increment. Therefore, the launch probabilities would be from our analysis presented in Table 4.4 without persistence.

Consider that the 3.5-hour wind load persistence increment is applied at T - 3.5 hours and that, in principle, this increment decreases to zero at T = 0. Under this assumption: what is the launch probability? To address this question, we perform the statistical analysis by applying the wind loads persistence increment only to the first of the pairs. These probabilities are computed for each of the 41 load variables for the three I-Loads as shown in Table 4.8 for WINGRA14. For example from Table 4.8 the Go probabilities for WINGRA14 with the 3.5-hour wind load persistence increment applied to the first of the pairs (Go 1st) are the same as in Table 4.6; but the Go probabilities for the second of the pairs without the wind load persistence (Table 4.8, Go 2nd) are much greater than with the wind load persistence increment (Table 4.6). Comparisons of the conditional $Pr\{Go_2|\ Go_1\}$without or with wind load persistence increment from Table 4.8 and Table 4.6 respectively are: for Baseline from Table 4.8, this probability is 99.73 percent (compared to 86.82 percent from Table 4.6); for DIBS it is 99.84 percent (94.82 percent) and for FIBS 99.90 percent (97.49 percent).

Table 4.8 Probabilities (percent) for WINGRA 14 for LMM with 99% wind load persistence increment applied to 1st of wind pairs and without the persistence increment for 2nd of wind pairs from 114 KSC 3.5-hour winter wind profile pairs

	PROBABILITY (percent)		
EVENT	BASELINE	DIBS	FIBS
GO 1st	70.77	88.50	92.17
NO-GO 1st	29.23	11.50	7.83
GO 2nd	96.04	98.83	99.11
NO-GO 2nd	3.96	1.17	0.89
Joint			
$Pr\{GO_2, GO_1\}$	70.58	88.36	92.08
$Pr\{NO\text{-}GO_2, GO_1\}$	0.19	0.15	0.09
$Pr\{GO_2, NO\text{-}GO_1\}$	25.47	10.47	7.03
$Pr\{NO\text{-}GO_2, NO\text{-}GO_1\}$	3.77	1.02	0.80
Conditional			
$Pr\{GO_2 \mid GO_1\}$	99.73	99.84	99.90
$Pr\{NO\text{-}GO_2 \mid GO_1\}$[a]	0.27	0.16	0.10
$Pr\{GO_2 \mid NO\text{-}GO_1\}$	87.12	91.09	89.83
$Pr\{NO\text{-}GO_2 \mid NO\text{-}GO_1\}$	12.88	8.91	10.17

(a) This is the most undesirable case.

Tables 4.9 and 4.10 contain the empirical probabilities for LMM with the wind load persistence increment applied to the first of the pair and without the persistence increment for the second of the pair. If any one of the 41 load variables has a load exceedance for a wind profile, then this is counted as a No-Go wind profile. We compare the Go_2 probabilities from Table 4.9 with those given in Table 4.7 for Go_1: For Baseline(Table 4.9), this probability is 88.7 percent (from Table 4.7 it is 38.3 percent);similarly, for DIBS it is 97.4 percent (62.6 percent); for FIBS it is 97.4 percent (64.3 percent). Table 4.10 presents the Go No-Go conditional probabilities computed from Table 4.9 and the 95 percent statistical confidence level (CL).

The lower and upper 95 percent CL is computed by:

$$CL = \frac{n}{n+t^2}\left[p + \frac{t^2}{2n} \pm t\left\{P\frac{(1-p)}{n} + \left(\frac{t}{2n}\right)^2\right\}^{\frac{1}{2}}\right] \qquad (4.44)$$

where t = 1.96 , p = number of counts/(n + 1) and (1 - p) = q.

Table 4.9 The number observed Go and No-Go LMM wind counts and percent probability with 99% wind load persistence increment for 1st of wind pairs and without wind load persistence increment for the 2nd of wind pairs for 41 load variables from 114 winter 3.5-hour wind pairs, KSC

EVENT	BASELINE		DIBS		FIBS	
	Counts	P %	Counts	P %	Counts	P %
GO 1st	44	38.3	72	62.6	74	64.3
NO-GO 1st	70	61.7	42	37.4	40	35.7
GO 2nd	102	88.7[a]	112	97.4[a]	112	97.4[a]
NO-GO 2nd	12	11.3	2	2.6	2	2.6
Joint						
$Pr\{GO_2, GO_1\}$	44	38.3	72	62.6	74	64.4
$Pr\{NO\text{-}GO_2, GO_1\}$	0	0.0	0	0.0	0	0.0
$Pr\{GO_2, NO\text{-}GO_1\}$	58	50.4	40	34.7	38	33.0
$Pr\{NO\text{-}GO_2, NO\text{-}GO_1\}$	12	10.3	12	2.6	2	2.6

(a) Suggested launch probabilities

Table 4.10 Probabilities (percent) and 95% confidence level of LMM for 41 load variables with 99% wind load persistence increment for 1st of pairs and without wind load persistence increment for 2nd of pairs, 114 winter 3.5-hour pairs, KSC

EVENT	COUNTS n	n	LOWER 95% CL	PROB. %		UPPER 95% CL
GO 1st	44	44	88.3	p	97.8	99.6
NO-GO 1st	0	44	0.4	q	2.2	11.7
GO 2nd	58	70	72.7	p	81.7	89.0
NO-GO 2nd	12	70	11.0	q	18.3	28.9
Joint						
$Pr\{GO_2, GO_1\}$	72	72	92.6	p	98.6	99.8
$Pr\{NO\text{-}GO_2, GO_1\}$	0	72	0.2	q	1.4	7.4
$Pr\{GO_2, NO\text{-}GO_1\}$	40	42	81.2	p	93.0	97.6
$Pr\{NO\text{-}GO_2, NO\text{-}GO_1\}$	2	42	2.4	q	7.0	18.8
Conditional						
$Pr\{GO_2 \mid GO_1\}$	74	74	92.8	p	98.7	99.8
$Pr\{NO\text{-}GO_2 \mid GO_1\}$[a]	0	74	0.2	q	1.3	7.2
$Pr\{GO_2 \mid NO\text{-}GO_1\}$	38	40	80.4	p	92.7	97.5
$Pr\{NO\text{-}GO_2 \mid NO\text{-}GO_1\}$	2	40	2.5	q	7.3	19.6

(a) This is the most undesirable case

A comparison is given below of the conditional probabilities for $Pr\{No\text{-}Go_2|Go_1\}$ from Table 4.10 Baseline with Table 4.7. For Baseline Table 4.10, this probability is 2.2 percent (Table 4.7, 35.6 percent); DIBS Table 4.10 is 1.4 percent (Table 4.7, 26.0 percent); and

Table 4.10 is 1.3 percent (Table 4.7, 22.7 percent). At this confidence level, there are no significant differences (Table 4.10) between DIBS and FIBS.

For this loads data set, Tables 4.9 and 4.10 are considered to be more realistic in quoting launch probabilities for mission planning than those contained in Table 4.7.

4.6.4 Peak Loads Analysis

A brief analysis has been performed using the PL data base from the 114 winter KSC 3.5-hour wind pairs. Table 4.11 presents the bivariate Gumbel parameters for this data sample.

For the load variables shown in Table 4.11, the m-parameters are not greatly different from those given in Table 4.2 for the LMM. Hence, the correlations between those load variables for the first and second of the wind pairs for PL are about the same as for the LMM. Also, shown in Table 4.11 is the 99th percentile load change ($\Delta L_{.99}$) computed from the logistic probability function. The $\Delta L_{.99}$ for the PL (Table 4.11) are not greatly different from those for LMM given in Table 4.3.

Table 4.11 Bivariate Gumbel parameters for Peak Load for 1st of wind pairs (y) and 2nd of wind pairs (x) and the 99th percentile load change ($\Delta L_{.99}$) from 3.5-hour wind pairs

I-LOAD	μ_y	μ_x	α_y	α_x	m	$\Delta L_{.99}$
(a) BASELINE						
WING RA 14(-)	18529	18443	1755	1751	2.017	3997
WING LA 14(-)	18129	18100	1709	1804	2.019	3885
VTL 11(+)	0.15	0.16	0.10	0.10	2.189	0.21
VTL 11(-)	0.20	0.20	0.08	0.08	2.322	0.16
(b) DIBS						
WING RA 14(-)	18465	18376	1310	1265	1.649	3750
WING LA 14(-)	18393	18415	1285	1354	1.586	3723
VTL 11(+)	0.17	0.19	0.06	0.06	1.285	0.21
VTL 11(-)	0.19	0.19	0.05	0.06	1.463	0.17
(c) FIBS						
WING RA 14(-)	17821	17806	1461	1320	1.745	3849
WING LA 14(-)	18206	18370	1396	1389	1.714	3742
VTL 11(+)	0.18	0.20	0.07	0.06	1.432	0.21
VTL 11(-)	0.16	0.17	0.05	0.06	1.307	0.18

Figs. 4.7 and 4.8 illustrate the Gumbel probability distribution from the PL for the WING RA14(-) load variable for the first of the wind pairs for Baseline and DIBS. Because this load variable has a negative sign convention, the algebraic sign has been reversed for mathematical convenience. The sample data (dots) in Figures 4.7 and 4.8 show an excellent fit to the Gumbel distribution. Figures 4.9 and 4.10 illustrate good agreement between the observed peak wind load 3.5-hour change and the theoretical peak wind load

change from the logistic probability function. The other load variables are also in good agreement. This justifies using the bivariate extreme value probability function, Gumbel case m, for peak load change. Analytically, the peak load margin with respect to the redline limit load (PLM) and the load minimum margin (LMM) are identical. Hence the PLM, so defined, could be used in the same statistical manner as the LMM.

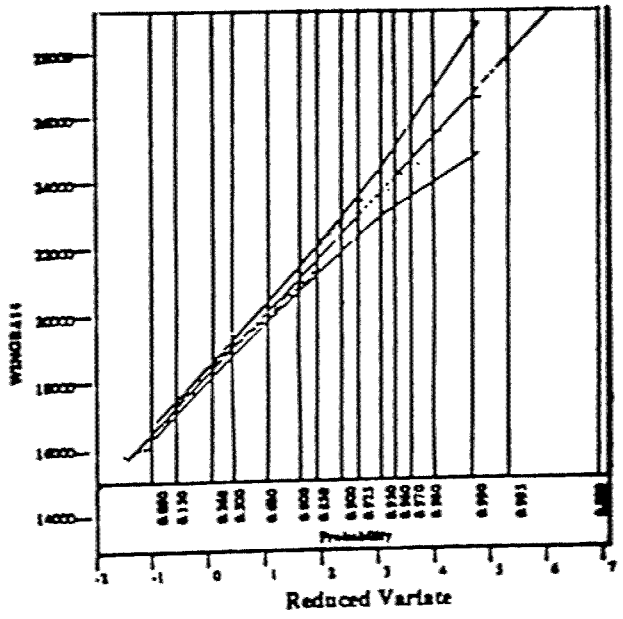

Figure 4.7 Gumbel extreme value probability distribution for Peak Loads for WING RA14 from 1st of 114 winter 3.5-hour wind pairs, KSC, using Baseline I-Load

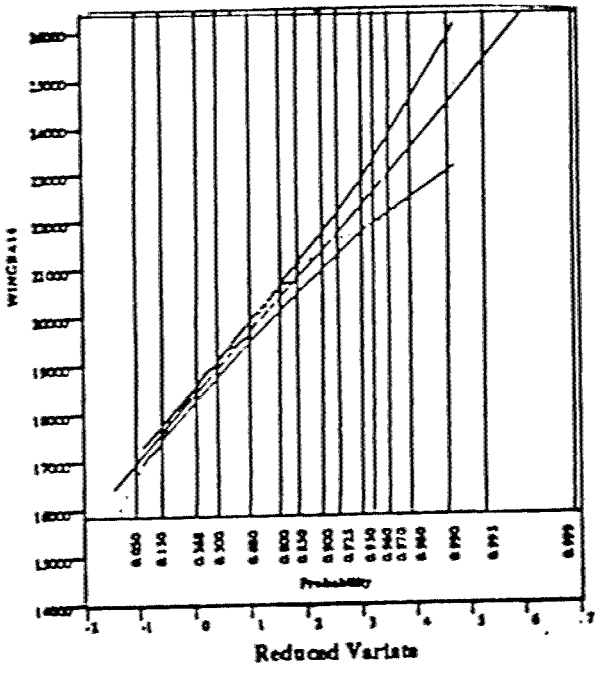

Figure 4.8 Gumbel extreme value probability distribution for peak loads for WINGRA14 from 1st of 114 winter 3.5-hour-wind pairs, KSC, using DIBS I-Load

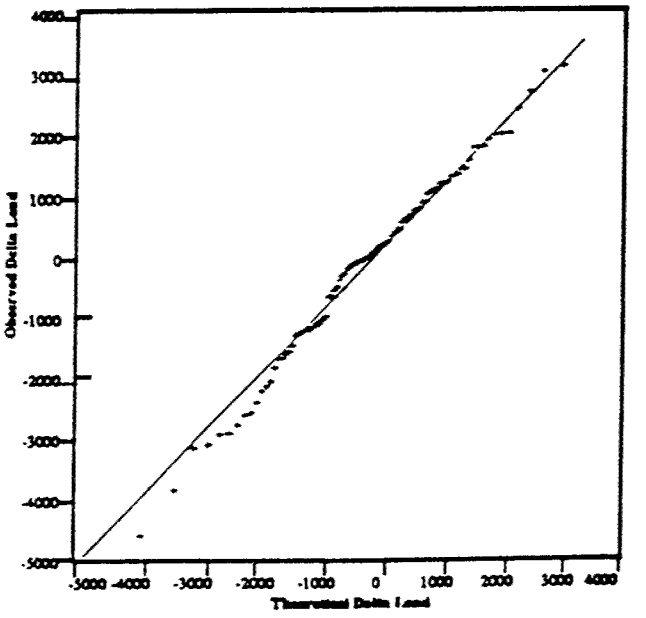

Figure 4.9 Observed and Theoretical (Logistic) Peak Load Differences Between 1st and 2nd of 114 Winter KSC 3.5-hour Wind Pairs for WINGRA14 Baseline I-Load

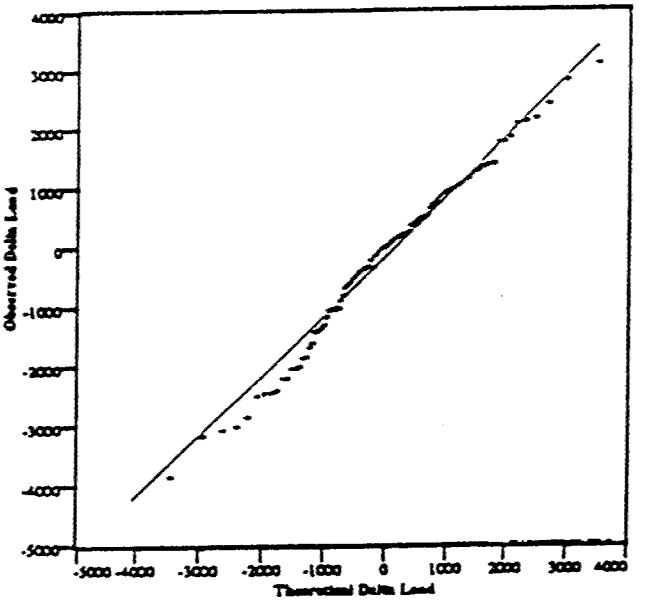

Figure 4.10 Observed and Theoretical (Logistic) Peak Load Differences Between 1st and 2nd of 114 Winter KSC 3.5-hour Wind Pairs for WINGRA14 DIBS I-Load

4.7 Conclusions

For the Space Transportation System (STS), the advantages in reducing the ascent wind loads by biasing to the Day-Of-Launch (DOL) measured wind profile using either the DIBS or FIBS steering commands techniques have been clearly demonstrated. The analytical statistical techniques presented in this section, using extreme value statistics, have many advantages over empirical statistical techniques for aerospace programmatic management decisions for design, trade studies, design assessments, and redesign and in the DOL Go/No-Go decision process. Because the analytical statistical techniques are general, they can be used for the above multifaceted purposes for future aerospace vehicles.

4.8 References

4.1 Smith, O.E., Adelfang, S.I. and Brown, R.P., "Ascent Structural Wind Loads for the National Space Transportation System," proceedings of the AIAA 26th Aerospace Sciences Meeting, AIAA Paper 88-0293, Jan. 1988.

4.2 Gumbel, E.J., *Statistics of Extremes*, Columbia University Press, New York, NY, 1958 (57-10160).

4.3 Gumbel, E.J. and Mustafi, C.K., "Some Analytical Properties of the Bivariate Extreme Distributions," American Statistical Association Journal, pp. 569 - 588, June 1967.

4.4 Smith, O. E. and Adelfang, S.I., "STS Ascent Structural Loads Statistics", Proceedings of the AIAA 30th Aerospace Sciences Meeting, AIAA Paper 92-0720, January, 1992.

5.0 WIND LOADS UNCERTAINTY ATTRIBUTABLE TO WIND PROFILE SMOOTHING AND TEMPORAL VARIABILITY

5.1 Introduction

The small wavelengths (WL < 1500 meters) in Jimsphere wind profiles at T-3.5 hours used in Space Shuttle pre-launch six degree-of-freedom trajectory and rigid body loads simulations have little or no relationship to the small scale wind perturbations experienced by the vehicle 3.5 hours later. This is demonstrated by comparison of the largest perturbations (+ and -) in the 10 to 12 km layer of the 1st and 2nd of the high pass filtered (WL ≤ 1500 m) Jimsphere winter 3.5-hour pairs (Figs. 5.1 and 5.2). In addition, as the wavelength decreases the perturbations in a Jimsphere wind profile become less correlated with the wind perturbations along the Space Shuttle ascent trajectory, even if that trajectory is centered at the mid-point of the 1-hr time interval associated with a Jimsphere measurement. Thus, there is uncertainty in these small wavelengths that can influence the assessment of wind loads for the commit-to-launch decision that is based on the T-3.5 hour Jimsphere wind profile. In addition there is also uncertainty in the post-flight evaluation of trajectory and loads based on the T-0 profile. Heretofore, only the loads uncertainty attributable to wind profile temporal variability is accounted for in assessments of vehicle launch capability (Refs.5.1 through 5.3). This uncertainty is accounted for with a load increment known as the wind load persistence increment (WLPI), which is calculated for each wind sensitive load indicator from a conditional extreme value (Gumbel) probability distribution. The statistical methodology used for protecting the commit-to-launch decision for wind loads temporal variability is also applicable for derivation of a larger load increment that protects for the combined uncertainties attributable to wind profile temporal variability and transient small wavelength wind profile perturbations that are essentially unknown along the vehicle flight path on DOL. The additional protection ensures that the integrity of the commit-to-launch decision is not compromised by using a smoothed (low-pass filtered wind profile) for trajectory and loads assessments. This profile could be derived from a Jimsphere profile (Ref. 5.4) or it could be from a relatively low resolution measurement system such as the Meteorological Sounding System (MSS) or the NASA 50-MHz Doppler Radar Wind Profiler (DRWP, Ref. 5.5). Because of the small time interval required to obtain a DRWP wind profile (5-minute intervals in support of NASA Space Shuttle launch operations) compared to one hour for a Jimsphere, the advantage of the DRWP is the potential for a 45 minute reduction of the time interval from the last loads simulation to the time of launch. From this study a detailed wind profile measurement would not be needed for pre- and post-flight assessments of vehicle trajectory and loads, if load increments that account for uncertainty in small wavelength perturbations are implemented.

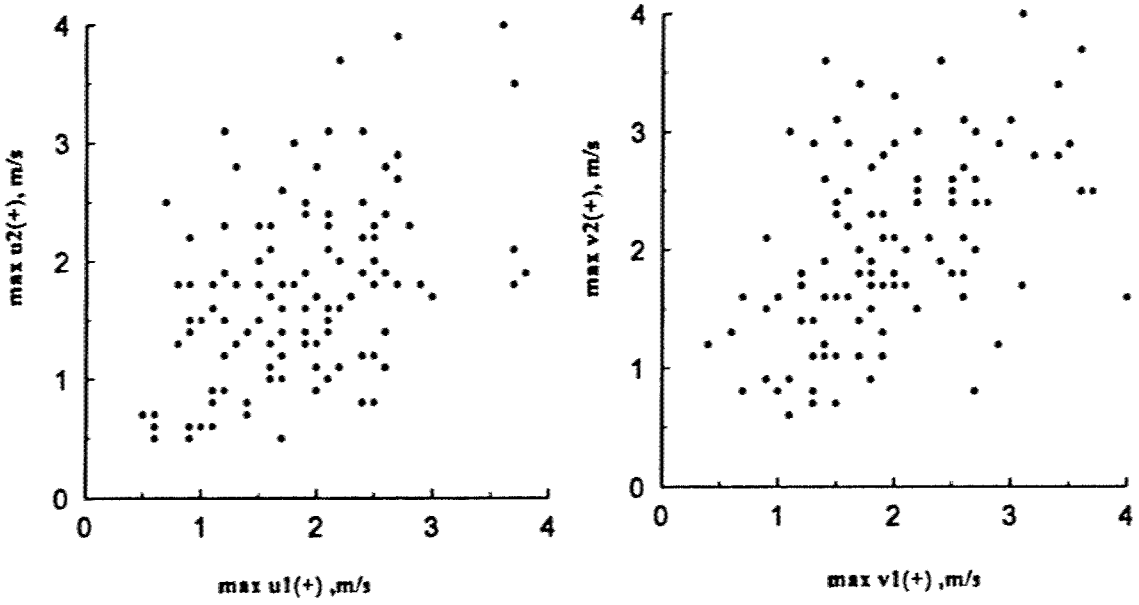

Figure 5.1 Extreme positive u and v wind component perturbations with wavelengths less than 1500 m in the 10 to 12 km altitude band, 1st versus 2nd of the KSC 3.5-hr Jimsphere wind profile pairs

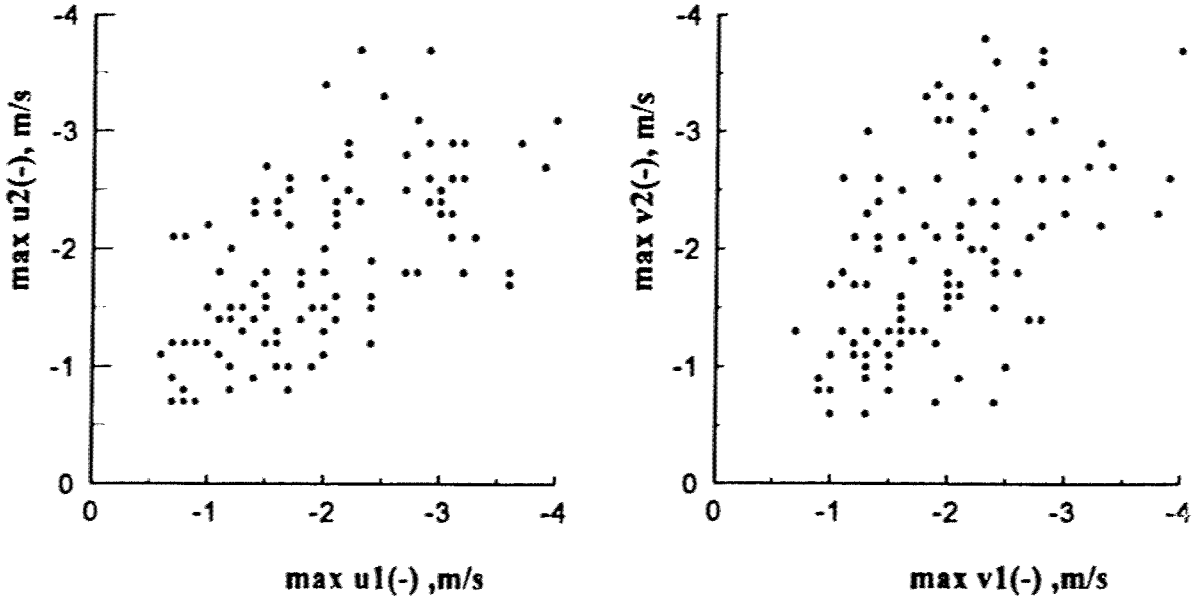

Figure 5.2 Extreme negative u and v wind component perturbations with wavelengths less than 1500 m in the 10 to 12 km altitude band, 1st versus 2nd of the KSC 3.5-hr Jimsphere wind profile pairs

5.2 Statistical Methodology

The decision to launch is based on an assessment of the load minimum margin (LMM) for each load indicator. For absolute values of load indicators the LMM is the minimum over the Mach range of 0.6 to 2.2 of the red line load (RL) minus the sum of the simulated load and the total uncertainty; a negative LMM is a No-Go. The RL is the load limit reduced by a 1.4 safety factor. The total uncertainty of the simulated load is the 'root-summed-squares' (RSS) of the systems uncertainties and the elastic body response to gust. A schematic for the definition of LMM is illustrated in Fig. 5.3 .

The statistical methodology described by Smith and Adelfang (Ref. 5.2) for calculation of the WLPI for load minimum margin (LMM) is also used herein with one important difference. For the original application, the derived WLPI, which represents loads uncertainty caused solely by the temporal variability of the wind, is based on loads

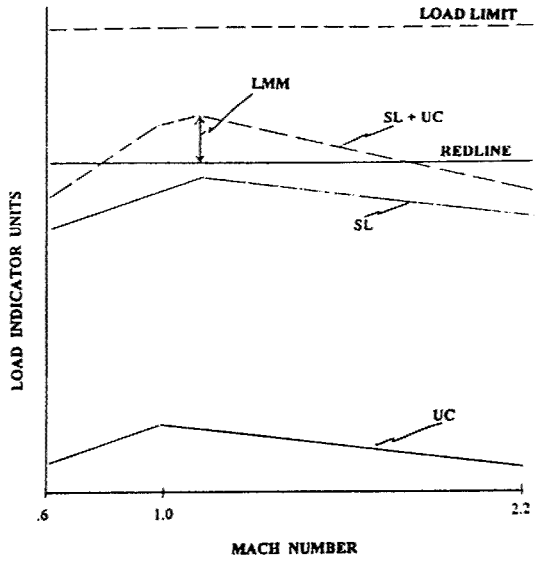

LMM = Load Minimum Margin
= minimum of (Redline - (SL+UC))
where,
Redline = load limit / 1.4
SL = simulated load
UC = load uncertainty attributed to systems dispersions and elastic body loads

Figure 5.3 Schematic for Load Minimum Margin (LMM) and Associated Variables

simulations for 114 KSC winter unfiltered 3.5 hour Jimsphere wind pairs. For the new application the additional uncertainty caused by low-pass filtering the first of the wind pairs is included in a revised wind load persistence increment (RWLPI). The RWLPI is calculated for 39 wind sensitive load indicators for each of three low-pass filtered versions of the first of the wind pairs (nominal filter cutoff wavelengths of 1500, 3000, and 6000m) in conjunction with the unfiltered second of the pairs.

The effectiveness of each RWLPI is evaluated by comparison of the number of No-Go profiles and No-Go indicators for WLPI and RWLPI. If this comparison is favorable it would be concluded that the additional protection afforded by the RWLPI produces no significant change in the evaluation of loads No-Go's or No-Go profiles, even though the simulation for the 1st of the pair is based on a filtered wind profile.

Another measure of the effectiveness of the RWLPI is the comparison of the empirical number of occurrences for the joint Go/No-Go combinations for the WLPI and the RWLPI applied to the unfiltered and filtered 1st of pairs respectively, with no increment applied to the 2nd of the pairs. The joint number of occurrences are for the following combinations:

1. Go1, No-Go2
2. Go1, Go2
3. No-Go1, No-Go2
4. No-Go1, Go2

The first combination is the most important because it represents a measure of the success in protecting the decision to launch; an occurrence of this combination means that the decision to launch would be invalidated by a post-launch loads analysis. Ideally there should be no occurrences of the first combination. However, one or two occurrences of the first combination could occur in this sample of 114 pairs because the WLPI and RWLPI are for a 99 percent conditional probability. The second combination represents the remainder of the Go for the 1st of the pair cases which have a high probability of also being Go for the 2nd of the pair because there is no protection increment applied to the 2nd of the pair; this is also an explanation for the large number of occurrences of the fourth combination compared to the third, which implies that a No-Go for the 1st of the pair has a high probability of becoming a Go for the 2nd of the pair.

5.3 Analysis

5.3.1 Wind Load Increments (WLPI and RWLPI)

The WLPI and RWLPI for a 99 percent conditional probability are calculated from LMM derived from loads simulations with 114 filtered and unfiltered KSC 3.5-hour winter Jimsphere wind pairs. The WLPI is calculated from the unfiltered 1st and 2nd of the wind pair; the three versions of the RWLPI are calculated from the three versions of the low-pass filtered 1st of pairs and the unfiltered 2nd of the pairs. The WLPI and the RWLPI for 39 load indicators are listed in Table 5.1. In nearly all cases the difference between RWLPI and WLPI is the additional increment required to protect for filtering the 1st of the wind pairs; the additional increment increases as the amount of low-pass filtering increases. The percentage ratios, RWLPI/WLPI, listed in Table 5.2 indicate that the largest increase in RWLPI relative to WLPI occurs between LP1500 and LP3000.

Table 5.1 99th Percentile Wind Load Persistence Increments WLPI and RWLPI

SEQ. #	LOAD INDICATOR	1ST OF PAIR / 2ND OF PAIR SIDE	UNFILTERED UNFILTERED WLPI	LP1500 UNFILTERED RWLPI	LP3000 UNFILTERED RWLPI	LP6000 UNFILTERED RWLPI
1	WINGRA14	(-)	-3305.35	-4067.23	-5411.31	-5884.62
2	WINGRA14	(-)	-4204.79	-4867.79	-6068.96	-6315.43
3	WINGRA15	(+)	45.89	68.29	132.51	176.81
4	WINGRA15	(+)	87.88	102.37	158.93	189.00
5	WINGRA17	(+)	45.77	61.64	98.09	126.29
6	WINGRA17	(+)	70.66	81.92	130.38	158.17
7	WINGRA18	(-)	-1235.90	-1625.09	-2612.48	-3073.59
8	WINGRA18	(-)	-1641.16	-1863.46	-2534.19	-2813.44
9	WINGRA19	(+)	38.94	53.29	97.77	114.57
10	WINGRA19	(+)	55.72	64.18	92.53	104.69
11	WINGRA16	(-)	-2256.24	-2902.32	-3707.58	-4070.84
12	WINGRA16	(-)	-2656.78	-3046.27	-4034.29	-4425.31
13	WINGRL21	(+)	28.04	44.39	72.25	88.99
14	WINGRA21	(+)	42.21	41.55	79.55	108.67
15	WINGR-A8	(-)	-49.25	-59.09	-105.71	-126.70
16	WINGL-A8	(-)	-118.44	-126.11	-158.15	-163.65
17	WINGRA20	(-)	-30.05	-43.14	-81.99	-93.57
18	WINGLA20	(-)	-61.07	-67.78	-101.15	-106.70
19	WINGRA22	(-)	-70.78	-96.30	-123.07	-128.78
20	WINGLA22	(-)	-77.83	-92.43	-123.35	-142.25
21	RWINGMX	(+)	3155150.00	4076294.00	6249931.00	7066222.00
22	LWINGMX	(-)	-4169323.00	-4734665.00	-6587483.00	-6942560.00
23	WLE-7	(+)	0.04	0.05	0.06	0.07
24	VTR-2	(+)	0.20	0.22	0.31	0.40
25	VTR-2	(-)	-0.21	-0.26	-0.34	-0.40
26	VTL-2	(+)	0.14	0.16	0.24	0.31
27	VTL-2	(-)	-0.21	-0.25	-0.39	-0.51
28	VTR-11	(+)	0.11	0.13	0.20	0.23
29	VTR-11	(-)	-0.20	-0.23	-0.35	-0.41
30	VTL-11	(+)	0.20	0.23	0.35	0.41
31	VTL-11	(-)	-0.11	-0.13	-0.20	-0.23
32	VTR-13	(+)	0.19	0.21	0.31	0.38
33	VTL-13	(+)	0.13	0.15	0.22	0.28
34	VTR-14	(-)	-0.20	-0.22	-0.35	-0.45
35	VTL-14	(-)	-0.13	-0.15	-0.23	-0.31
36	VTR-15	(+)	0.17	0.22	0.30	0.35
37	VTL-15	(+)	0.17	0.22	0.30	0.35
38	VTR-16	(+)	0.08	0.15	0.22	0.25
39	VTL-16	(+)	0.09	0.16	0.23	0.25

Table 5.2 Ratio of RWLPI to WLPI

SEQ. #	INDICATOR	1st of wind pair	LP filter for RWLPI 1500	3000	6000
1	WINGRA14	(-)	1.23	1.64	1.78
2	WINGRA14	(-)	1.16	1.44	1.50
3	WINGRA15	(+)	1.49	2.89	3.85
4	WINGRA15	(+)	1.16	1.81	2.15
5	WINGRA17	(+)	1.35	2.14	2.76
6	WINGRA17	(+)	1.16	1.85	2.24
7	WINGRA18	(-)	1.31	2.11	2.49
8	WINGRA18	(-)	1.14	1.54	1.71
9	WINGRA19	(+)	1.37	2.51	2.94
10	WINGRA19	(+)	1.15	1.66	1.88
11	WINGRA16	(-)	1.29	1.64	1.80
12	WINGRA16	(-)	1.15	1.52	1.67
13	WINGRL21	(+)	1.58	2.58	3.17
14	WINGRA21	(+)	0.98	1.88	2.57
15	WINGR-A8	(-)	1.20	2.15	2.57
16	WINGL-A8	(-)	1.06	1.34	1.38
17	WINGRA20	(-)	1.44	2.73	3.11
18	WINGLA20	(-)	1.11	1.66	1.75
19	WINGRA22	(-)	1.36	1.74	1.82
20	WINGLA22	(-)	1.19	1.58	1.83
21	RWINGMX	(+)	1.29	1.98	2.24
22	LWINGMX	(-)	1.14	1.58	1.67
23	WLE-7	(+)	1.16	1.42	1.71
24	VTR-2	(+)	1.08	1.57	2.00
25	VTR-2	(-)	1.23	1.60	1.87
26	VTL-2	(+)	1.15	1.69	2.18
27	VTL-2	(-)	1.22	1.89	2.47
28	VTR-11	(+)	1.18	1.77	2.04
29	VTR-11	(-)	1.15	1.74	2.07
30	VTL-11	(+)	1.15	1.74	2.08
31	VTL-11	(-)	1.20	1.76	2.02
32	VTR-13	(+)	1.13	1.67	2.00
33	VTL-13	(+)	1.17	1.70	2.15
34	VTR-14	(-)	1.13	1.78	2.28
35	VTL-14	(-)	1.15	1.80	2.46
36	VTR-15	(+)	1.35	1.81	2.07
37	VTL-15	(+)	1.33	1.80	2.07
38	VTR-16	(+)	1.84	2.64	2.94
39	VTL-16	(+)	1.92	2.70	2.91

5.3.2 Load Indicator WINGRA14(-) No-Go's

Load indicator WINGRA14(-) is selected for analysis because it is the most wind sensitive of the 39 indicators. As illustrated in Figure 5.4 the unfiltered 1st of the 114 wind pairs (ordinate) produces 3 No-Go's without WLPI (LMM < 0) and 18 with WLPI (LMM < WLPI). The number of No-Go's for WINGRA14 with either WLPI or RWLPI (LMM < RWLPI) applied to LMM derived from unfiltered or filtered 1st of the wind pairs are summarized in Table 5.3 . When WLPI is applied to LMM derived from filtered 1st of the pairs, the number of No-Go's decreases to 17, 7, and 2 for low-pass filters 1500, 3000 and 6000, respectively (Fig.5.4, abscissa, or Table 5.3); this is an obvious incorrect application of WLPI because the failure to account for the uncertainty caused by filtering the 1st of the wind pairs produces an unrealistically small number of No-Go's. When RWLPI is applied to LMM from filtered 1st of the pairs, there is consistency for the first two filters in the number of No-Go's relative to the 18 obtained from the proper application of WLPI to LMM (from unfiltered 1st of wind pair) ; the number of No-Go's is 21, 21, and 26 for low-pass filters 1500, 3000, and 6000, respectively.

This example shows that the RWLPI provides the additional load increment for WINGRA14 to protect for the additional loads uncertainty caused by smoothing the 1st of the wind pairs. Similar results can be demonstrated for all the wind sensitive load indicators.

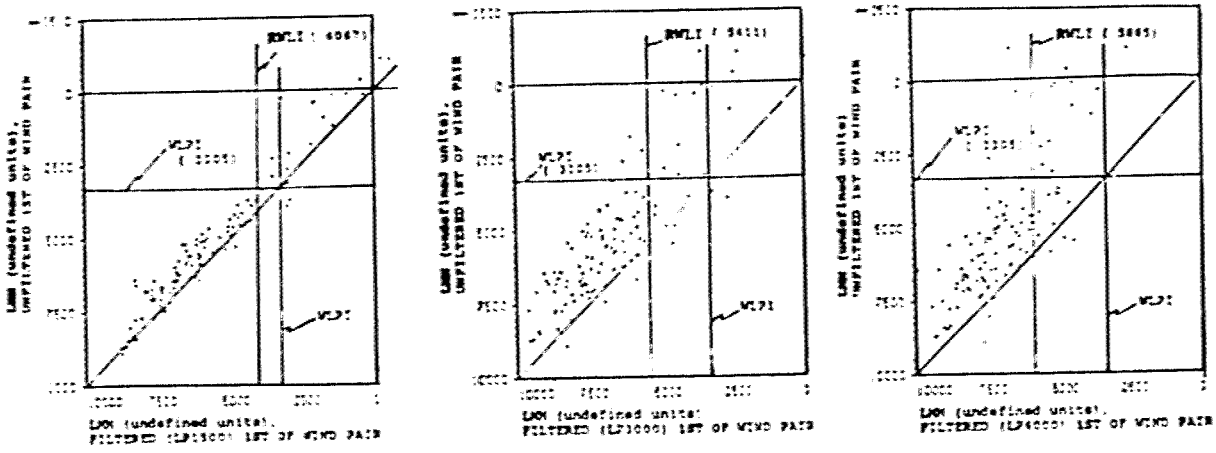

Figure 5.4 Load minimum Margin (LMM) for wing load indicator WINGRA14(-) for 1" of wind pairs low-pass filtered (LP1500, 3000 and 6000) and 1" of wind pairs unfiltered; derived load increments WLPI and RWLPI are indicated by straight lines

Table 5.3 Number of No-Go profiles for load indicator WINGRA14(-), 1st of 114 wind profile pairs, WLPI applied to LMM for unfiltered case and WLPI and RWLPI applied to LMM for the filtered cases

1st of pair filter	none	1500	3000	6000
type of increment	WLPI	WLPI	WLPI	WLPI
No-Go Profiles	18	17	7	2
type of increment		(*****	RWLPI	*****)
No-Go Profiles		21	21	26

5.3.3 No-Go Statistics, 1st of Pair

The statistics of load indicator No-Go's for the 1st of the 114 wind pairs, unfiltered and filtered, and without or with wind load increments are listed in Table 5.4 .

Table 5.4 The number and percent of 114 profiles that are No-Go and the number of No-Go load indicators for the 1st of the pair, without and with wind load increments WLPI and RWLPI

A) without wind load persistence increments

1st of pair filter	none	1500	3000	6000
No-Go Profiles	8	2	0	0
% No-Go Profiles	7.0	1.8	0.0	0.0
No-Go Load Indicators	9	5	0	0

B) with wind load persistence increments

type of increment	WLPI	(****	RWLPI	*****)
1st of pair filter	none	1500	3000	6000
No-Go Profiles	38	40	42	50
% No-Go Profiles	33.3	35.1	36.8	43.9
No-Go Load Indicators	21	18	18	19

A No-Go is counted if any one of the 39 load indicators is a No-Go. Without load increments the filtering reduces the number of No-Go profiles and No-Go indicators, which illustrates loads uncertainty caused only by wind profile filtering. If this uncertainty is not accounted for, most or all No-Go's become Go's, which essentially invalidates the loads assessments for the filtered 1st of the pairs. With load increments, the number of No-Go indicators is nearly constant for the RWLPI (18,18, and 19) compared to 21 for the WLPI; the number of No-Go profiles is also nearly constant for the first two versions of RWLPI (40 and 42 for filters 1500 and 3000 respectively) compared to 38 for the WLPI. The RWLPI for the 6000m filter yields 50 No-Go profiles, which is unrealistic compared to the 38 for the WLPI.

These statistics validate the RWLPI for the 1500- and 3000-m filters because the number of No-Go profiles and indicators are nearly the same as those obtained with WLPI derived from unfiltered wind profiles. Hence, a wind profile measurement system that has a resolution equivalent to a 1500- or 3000-m low-pass filtered Jimsphere wind profile could adequately support the pre-launch loads assessment process, if the appropriate RWLPI increment is implemented.

5.3.4 Joint Go/No-Go Statistics, 1st and 2nd of Wind Pairs

The joint number of occurrences of Go/No-Go combinations from a sample of 114 pairs, with filtering applied to the 1st of the wind pairs and load increments applied to the 1st of the pairs load indicators, are listed in Table 5.5. The first combination (Go 1st / No-Go 2nd) is the most important because it is a measure of the protection achieved with WLPI or RWLPI for the worst case when an increase of loads could change a Go for the 1st of the pair to a No-Go for the 2nd of the pair. As shown in Table 5.5, the number of occurrences of this combination for WLPI or RWLPI is within 1 count of the ideal value of none. The additional load increment included in the RWLPI ensures that a Go decision would not be compromised by using a low-pass filtered 1st of the wind pairs for the pre-launch loads simulation. The number of occurrences for the 2nd combination (Go 1st/Go 2nd) is also nearly equivalent to the ideal number, which is the number of Go's for the 1st of the pair.

For the third combination (No-Go 1st/No-Go 2nd) listed in Table 5.5, it is indicated that the number of occurrences (7 to 8) is nearly equivalent to the number of unfiltered wind profiles (8, in Table 5.4) that are No-Go without a wind load increment; obviously these eight profiles remain No-Go when the load increment is applied to the 1st of the pair and they remain No-Go for nearly all of the second of the same pair without the load increment. The remainder of the 1st of the pairs No-Go's are included in the fourth combination (No-Go 1st/Go 2nd) listed in Table 5.5. These No-Go's are caused by the load increment which must always be added to the LMM to protect for the worst case; since the actual load change is theoretically less than this load increment in 99 percent of the cases, many of these No-Go's become Go's when no increment is used for the 2nd of the pairs.

Table 5.5 Number of occurrences of Go/No-Go combinations from a sample of 114 simulation pairs with wind load increments and filtering applied to the 1st of the pair

1st of pair filter		none	1500	3000	6000
type of increment		WLPI	(***** RWLPI *****)		
combination					
1st of pr.	2nd of pr.	number of occurrences			
Go	No-Go	1	0	1	0
Go	Go	75	74	71	64
No-Go	No-Go	7	8	7	8
No-Go	Go	31	32	35	42

Note: A No-Go is counted if any one of the 39 load indicators is a No-Go

5.4 Conclusions

It has been demonstrated that wind profiles that do not contain the small scale perturbations (wavelength < 1500m) measured by the Jimsphere could be adequate for the Shuttle pre-launch wind profile and rigid body ascent loads assessments for the commit to launch decision. The analysis to support this conclusion, however, required high resolution Jimsphere pairs to derive the appropriate load allowances for the combined effects of temporal and reduced wind profile resolution. The combined effects are included in a 99 percentile wind load increment derived from filtered (smoothed) 1st of the 3.5-hr Jimsphere wind pairs and unfiltered 2nd of the pairs.

When the appropriate wind load increment is used, the joint number of occurrences of wind profile Go-NoGo's for the low-pass 1500m filtered 1st of the Jimsphere pairs and unfiltered 2nd of the Jimsphere pairs are in agreement with the Go/No-Go's for the unfiltered winds for both of the pairs.

The methodology for derivation of loads allowances described in this section would be applicable to all launch vehicle operational scenarios that require assessments of vehicle launch capability based on wind profile measurements on the day of launch.

5.5 References

5.1 Smith, O.E., Adelfang, S.I. and Brown, R.P., "Ascent Structural Wind Loads for the National Space Transportation System", AIAA Paper 88-0293, AIAA 26th Aerospace Sciences Meeting, Reno, NV, January 1988.

5.2 Smith, O.E., and Adelfang, S.I., "STS Ascent Structural Loads Statistics", AIAA Paper 92-0720, AIAA 30th Aerospace Sciences Meeting, Reno, NV, January 1992.

5.3 Norbraten, L., "Day-of-Launch I-Load Updates for the Space Shuttle", AIAA Paper 92-1274, AIAA Space Programs and Technologies Conference, Huntsville, AL, March 24-27, 1992.

5.4 Adelfang, S.I., Smith, O.E., and Batts, G.W., "Sensitivity of Wind Loads Uncertainties to Wind Profile Smoothing", AIAA Paper 94-0478, AIAA 32nd Aerospace Sciences Meeting, Reno, NV, January 1994 .

5.5 Wilfong, T.L., Smith, S.A., and Creasey, R.L., "High Temporal Resolution Velocity Estimates from a Wind Profiler", J. Spacecraft and Rockets, Volume 30, Number 3, May-June 1993, pp. 348-354.

6.0 GUST MODELS FOR LAUNCH VEHICLE ASCENT

6.1 Introduction

Assessments of elastic body and buffeting response to in-flight atmospheric disturbances or gusts are important in the establishment of vehicle design structural requirements and operational capability. Launch vehicles can have significant response to gusts that are not measurable with typical launch site winds aloft measurements such as the Jimsphere wind profile measurement system or the 50-Mhz Doppler Radar Wind Profiler (DRWP) used at Kennedy Space Center (KSC) in support of the Shuttle and DOD launch programs. It is not practical to perform elastic body loads analyses on the day-of-launch (DOL) because gusts are transient with time duration measured in seconds. (However, rigid body loads simulations are performed on DOL using measured Jimsphere wind profiles.) Thus, the commit-to-launch decision must be protected for gust uncertainty contributions to elastic body loads uncertainties. Discrete gust models used for establishment of trajectory and loads increments that account for launch vehicle elastic body and buffet response uncertainty on the day of launch are described. The origin and shortcomings of the classical NASA 9 m/s discrete gust model is discussed. A new discrete gust model that includes variation of gust magnitude as a function of altitude and gust length is presented for use in the establishment of vehicle elastic body and buffet response uncertainty on DOL.

6.2 Discrete Gust Model

This model is an improved definition that includes the variation of the gust amplitude as a function of gust width. It is for use in establishing the maximum structural response to the discrete gust when the vehicle elastic body mode wavelengths are synchronized with the gust wavelength. This development was first reported in a White Paper to the Space Shuttle Program (Ref. 6.1) for application in a study to re-establish the Space Shuttle orbiter Columbia vertical tail assembly elastic body load response to gust. The development is presented here to ensure wider distribution for future applications within the Space Shuttle program and for future launch vehicles. A literature review is presented that establishes the origin of the classical NASA discrete gust model heretofore used for elastic body loads analysis. This improved model, established with methods originally developed for military specification (MILSPEC) of requirements for the flying qualities of piloted aircraft (Ref. 6.2), includes the variation of gust amplitude with gust width, a factor which was not included in the classical NASA model. This methodology is also described in the NASA Terrestrial Guideline Document (Ref. 6.3). The empirical and theoretical equations for the non-dimensional gust magnitude as a function of non-dimensional gust width derived in this paper represent an improvement over the MILSPEC functions heretofore only available in graphical form. The theoretical equations are the first documented derivation of the MILSPEC functions. The practical implementation of these equations is for derivation of the dimensional gust magnitude, which requires specification of the length scale and standard deviation of turbulence. This study uses the most recent compilation (Ref. 6.3) of these parameters (originally derived for a Space Shuttle turbulence model, Ref. 6.8), which are a function of altitude and severity of turbulence.

With knowledge that the tail load anomaly occurs during transition to supersonic velocity in the vicinity of 20,000 ft (6 km) the gust magnitudes derived in this study may in certain circumstances provide some load alleviation compared to the 9 m/s NASA Space Shuttle Design Criteria standard (Ref. 6.9). The tail sensitivity to gust width is the critical factor that will determine the degree of load alleviation that may be achieved. If the sensitivity tends to be at small gust widths, then load alleviation is ensured.

6.3 Origin of the Classical NASA 9 m/s Gust

The original quasi-square-wave gust having an amplitude of 9 m/s with a gust width from 50 to 300 m had a gust gradient of 0.36 sec^{-1} for the first 25 m (or 9 m/s per 25 m) and a 0.36 sec^{-1} decrease for the last 25 m for a variable gust width of 50 to 300 m. This gust model first appeared (Ref. 6.10) in 1963 and has been modified over the years (Ref. 6.3) with a cosine leading and trailing edge of 30-m interval as shown in Fig. 6.1. It is not clear what probability of occurrence should be attached to this gust model. The design gust model amplitude (Fig. 6.1) is reduced to 7.65 m/s (0.85 of its value) when used in conjunction with the synthetic wind and wind shear model for the Shuttle ascent design (Ref. 6.9).

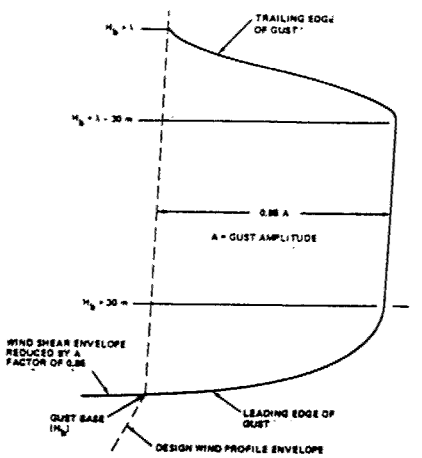

Figure 6. 1 Relationship between gust shape, design wind profile envelope, and speed buildup (shear) envelope

Early discrete wind gust models for missile design (Refs. 6.4, 6.5 and 6.6) are based on accelerometer measurements of turbulence by aircraft in horizontal flight. Aircraft measured turbulence is classified as light, moderate, and severe. The methodology used to convert aircraft turbulence taken over time of flight and horizontal distance to discrete gust for a vertical rising vehicle is not clearly addressed. Common sources for aircraft accelerometer measurement data in or near thunderstorms are the measurement series during 1941 and 1942 in the vicinity of Langley Field, VA and from the thunderstorm project near Orlando, FL in the summers of 1946 and 1947 (Refs. 6.4, 6.5).

The frequency distribution for derived gust magnitude from aircraft measurements traversing thunderstorms (Ref. 6.4) is reproduced here in Table 6.1(Table III of referenced document). The cumulative percentage frequency (CPF) for the 1947 thunderstorm gusts at 16,000-ft altitude derived from Table 6.1 is shown in Table 6.2. The percentile values for thunderstorm gust (Ref. 6.7) for altitudes from 1 to 14,000 ft reproduced herein as Table 6.3 were also derived from the data contained in Table 6.1.

Table 6.1 Frequency Distributions of Derived Gust

/	1941-42 investigation /						1946 investigation /					1947 investigation /				
	Frequency of gusts at altitude (Kft) of -															
U_{Δ}, ft/s	5 to 10	10 to 15	15 to 20	20 to 25	25 to 30	30 to 34	6	11	16	21	26	5	10	15	20	25
5 to 10	1855	635	860	570	640	410	3560	6000	5180	3920	2570	1430	3700	4000	2810	1370
10 to 15	522	283	376	249	279	171	1385	2230	2020	1590	940	510	1495	1720	1135	620
15 to 20	166	114	180	111	111	67	500	870	840	635	342	210	595	720	454	260
20 to 25	47	50	84	46	46	26	187	313	338	245	126	79	248	321	180	113
25 to 30	14	22	37	19	20	10	74	117	132	96	45	31	95	138	72	51
30 to 35	4	9	18	9	8	3	27	44	54	39	17	12	40	57	29	20
35 to 40	2	4	8	3	4	3	11	16	22	15	6	5	16	25	12	10
40 to 45	---	3	4	3	2	---	4	6	8	6	4	3	7	11	5	3
45 to 50	---	---	2	---	---	---	2	3	4	4	---	---	2	4	2	3
50 to 55	---	---	1	---	---	---	---	1	2	---	---	---	2	2	1	---
55 to 60	---	---	---	---	---	---	---	---	---	---	---	---	---	2	---	---
Totals	2640	1120	1570	1010	1110	690	5750	9600	8600	6550	4050	2280	6200	7000	4700	2450
Flight Miles	247	130	180	114	180	54	993	1565	1716	1422	1064	757	1340	1612	1208	939

Table 6.2 CPF for Wind Gust at 16,000-ft Alt. from 1946 Thunderstorm Project Near Orlando, FL

Gust Class Intervals, ft/sec	Frequency (counts)	CPF %
5-10	5180	60.22
10-15	2020	83.71
15-20	840	93.48
20-25	338	97.41
25-30	132	98.94
30-35	54	99.57
35-40	22	99.83
40-45	8	99.92
45-50	4	99.965
50-55	2	99.988
	Σ = 8600	

Table 6. 3 Cumulative Probability Distribution of Gust Velocities from 1 km to 14 km for Thunderstorm Turbulence (Ref. 6.7)

Probability (pct ≤)		50	68	84.1	97.7	99.0	99.86
Gust Velocity	m/s	2.40	3.10	4.60	7.80	9.10	12.50
	ft/s	17.87	10.17	109	25.58	29.85	41.00

Missing from this analysis are two very important gust characteristics: They are the gust width and shape. The US Air Force Titan and Delta vehicle programs use a "1- cosine" gust shape with 9 m/s amplitude and 304-m gust width. The important difference between the Air Force gust model and the NASA model is that the rise to 9 m/s takes place over 152m rather than 30 m for the NASA model.

6.4 Discrete Gust Magnitude as a Function of Gust Half-Width

The basis for the derivation of gust magnitude as a function of gust half-width is given in a military specification of requirements for the flying qualities of piloted aircraft (Ref. 6.2). This specification is significant because it is based on the same aircraft turbulence data used in studies (Refs. 6.4,6.5, and 6.7) that led to the establishment of the NASA classical 9 m/s gust. The gust model (V) has the "1-cosine" shape (Fig. 6. 2) defined by (Ref. 6.2):

$$V = 0, \quad d < 0 \ , \ d > 2d_m$$

$$V = \frac{V_m}{2}(1 - \cos(\pi d / d_m)) \ , \quad 0 \le d \le 2d_m$$

where, V_m is the gust magnitude and d_m is the gust half-width and d is distance.

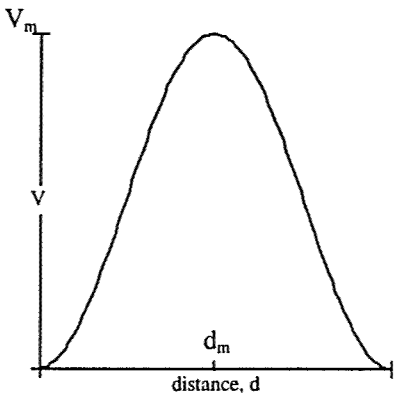

Figure 6.2 Discrete Gust Model ("1-cosine")

The MILSPEC relationship (Refs. 6.2 and 6.3) between non-dimensional gust magnitude V_m/σ and non-dimensional gust half-width d_m / L heretofore only available in graphical form is illustrated for the longitudinal and vertical gust component in Fig. 6.3; where, σ is the standard deviation of atmospheric turbulence and L is the scale length of atmospheric turbulence. The most recent compilation (Ref. 6.3) of these parameters (originally derived for a Space Shuttle turbulence model, Ref. 6.8) as a function of altitude and severity of turbulence is presented in Table 6.4.

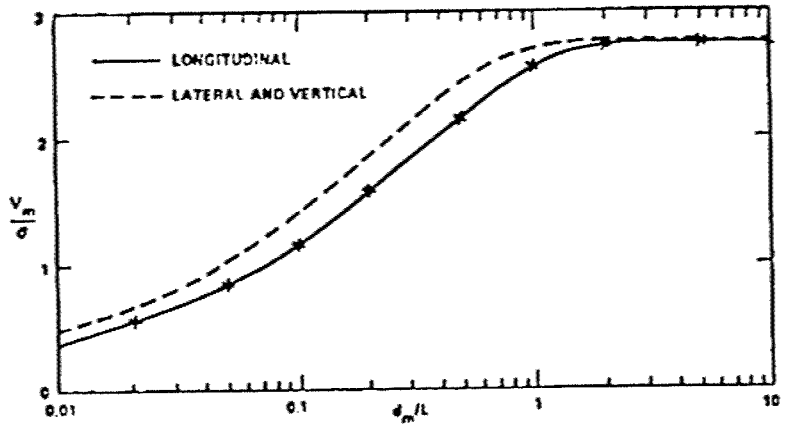

Figure 6.3 Non-dimensional Discrete Gust Magnitude V_m/σ as a Function of Non-dimensional Gust Half-Width, d_m/L

Table 6.4 Mean Horizontal and Vertical Turbulence Standard Deviations σ_h and σ_w, Length Scales L_h and L_w and Probabilities of Turbulence Severity Levels (light, moderate, and severe) as a Function of Altitude

	/ Light Turbulence			/Moderate Turbulence			/ Severe Turbulence /			Turbulence Length Scale	
Alt. MSL km	σ_h m/s	σ_w m/s	Probability of Light Turbulence	σ_h m/s	σ_w m/s	Probability of Moderate Turbulence	σ_h m/s	σ_w m/s	Probability of Severe Turbulence	L_h km	L_w km
1	0.17	0.14	0.776	1.65	1.36	0.199	5.70	4.67	0.025	0.832	0.624
2	0.17	0.14	0.8910	1.65	1.43	0.0979	5.80	4.75	0.0111	0.902	0.831
4	0.20	0.17	0.9199	2.04	1.68	0.0738	6.24	5.13	0.0063	1.04	0.972
6	0.21	0.17	0.9293	2.13	1.69	0.0650	7.16	5.69	0.0056	1.04	1.01
8	0.22	0.17	0.9247	2.15	1.69	0.0704	7.59	5.98	0.0049	1.04	0.98
10	0.22	0.17	0.9280	2.23	1.73	0.0677	7.72	6.00	0.0043	1.23	1.10
12	0.25	0.18	0.9464	2.47	1.79	0.0502	7.89	5.71	0.0034	1.80	1.54
14	0.26	0.19	0.9605	2.62	1.91	0.0368	6.93	5.05	0.0027	2.82	2.12
16	0.24	0.21	0.9639	2.44	2.10	0.0337	5.00	4.31	0.0024	3.40	2.60
18	0.22	0.21	0.9703	2.21	2.07	0.0277	4.07	3.81	0.0020	5.00	3.34
20	0.23	0.20	0.9804	2.26	1.99	0.0180	3.85	3.38	0.0016	8.64	4.41
25	0.27	0.21	0.9839	2.71	2.09	0.0146	4.34	3.34	0.0015	12.0	6.56
30	0.37	0.24	0.9797	3.73	2.39	0.0185	5.60	3.59	0.0018	28.6	8.88

For practical applications the relationship illustrated in Fig. 6.3 was first defined empirically in two segments for the range of d_m / L from .01 to 10 . The first segment ($0.01 \leq d_m / L < 5$) is a least squares fourth order polynomial.

$$V_m/\sigma = c_0 + c_1 x + c_2 x^2 + c_3 x^3 + c_4 x^4 \qquad (6.1)$$

where, $x = \log_{10}(d_m/L)$, L is in meters (10^3 L_h (km) in Table 6. 4), V_m and σ (σ_h in Table 6.4) are in m/s, $c_0 = 2.473886$, $c_1 = 0.9290348$, $c_2 = -0.54107229$, $c_3 = -0.18495605$, and $c_4 = 0.0300112814$. For the second segment ($5 \leq d_m/L \leq 10$), $V_m/\sigma = 2.80247$

For $d_m \geq 30$ meters and altitudes >14 km, L can be sufficiently large such that d_m/L can be less than 0.01 . For these cases a conservative approach is taken by assuming a constant value of 0.40776 for V_m/σ (which is the value of V_m/σ for $d_m/L = 0.01$, obtained from Eq. 6.1 for $x = \log_{10}(.01) = -2$). This is conservative because the relationship illustrated in Fig. 3 indicates that V_m/σ should continue to decrease for $d_m/L < (0.01)$.

For $d_m/L > 10$, a mathematical expression for V_m/σ is not needed for $d_m \leq 300$ meters because the value of d_m/L is smaller than 10 for L at all altitudes listed in Table 6.4 .. The largest value of d_m/L is at 1 km (for d_m=300 m and $L = L_h$=832 meters, $d_m/L = 0.3606$) .

Alternatively and preferably the MILSPEC relationship illustrated in Fig. 6. 3 is derived by integration in closed form of the Dryden power spectrum density (PSD) model for a variable lower bound for wave number Ω_i . The equations for the Dryden PSD's for the longitudinal and lateral components of atmospheric turbulence are:

$$\phi(\Omega) = \frac{2\sigma^2 L}{\pi}\left[\frac{1}{1+(L\Omega)^2}\right] \text{(longitudinal)} \qquad (6.2)$$

$$\phi(\Omega) = \frac{\sigma^2 L}{\pi}\frac{\left(1+3(L\Omega)^2\right)}{(1+(L\Omega)^2)^2} \text{(lateral)} \qquad (6.3)$$

where, $0 \leq \Omega \leq \infty$, σ^2 is the variance and L is the turbulence length scale. Integration of Eqs. 6.2 or 6.3 from zero to infinity yields σ^2. Integration from a lower bound other than zero yields a fractional value of σ^2 which is given by,

$$\int_{\Omega_i}^{\infty} \phi(\Omega)d\Omega = \sigma^2\left(1-\frac{2}{\pi}\tan^{-1}(L\Omega_i)\right) \text{ (longitudinal)} \qquad (6.4)$$

$$\int_{\Omega_i}^{\infty} \phi(\Omega)d\Omega = \sigma^2\left[1-\left[\frac{2}{\pi}\tan^{-1}(L\Omega_i) - \frac{L\Omega_i}{\pi\left(1+(L\Omega_i)^2\right)}\right]\right] \text{ (lateral)} \qquad (6.5)$$

The square roots of the integrals given by Eqs. 6.4 and 6.5 represent the fractional values of the total standard deviation contributed by the wavelength bands Ω_i to infinity. The derivation of the MIL-Standard non-dimensional discrete gust as a function of non-dimensional gust half-width (half-wavelength) requires the following assumptions:

1. The magnitude of the discrete gust is 2.8 times the fractional standard deviation.

2. The non-dimensional gust half-wavelength d_m/L is defined by

$$d_m/L = \frac{1}{\pi L \Omega_i}$$

$$\text{thus,} \quad L\Omega_i = \frac{1}{\pi(d_m / L)}$$

The non-dimensional gust magnitudes V_m/σ for the longitudinal and lateral components respectively are:

$$y_1 = 2.8\sqrt{1 - \frac{2}{\pi}\tan^{-1}(L\Omega_i)} \qquad (6.6)$$

$$y_2 = 2.8\sqrt{1 - \left[\frac{2}{\pi}\tan^{-1}(L\Omega_i) - \frac{L\Omega_i}{\pi(1+(L\Omega_i)^2)}\right]} \qquad (6.7)$$

The empirical and derived MILSPEC curves for the longitudinal gust component are illustrated in Fig. 6. 4. The dashed curve is the empirical least squares fit to MILSPEC longitudinal component (Eq.6.1). The solid curve is derived by closed form integration of the Dryden PSD expressed by Eq. 6.6.

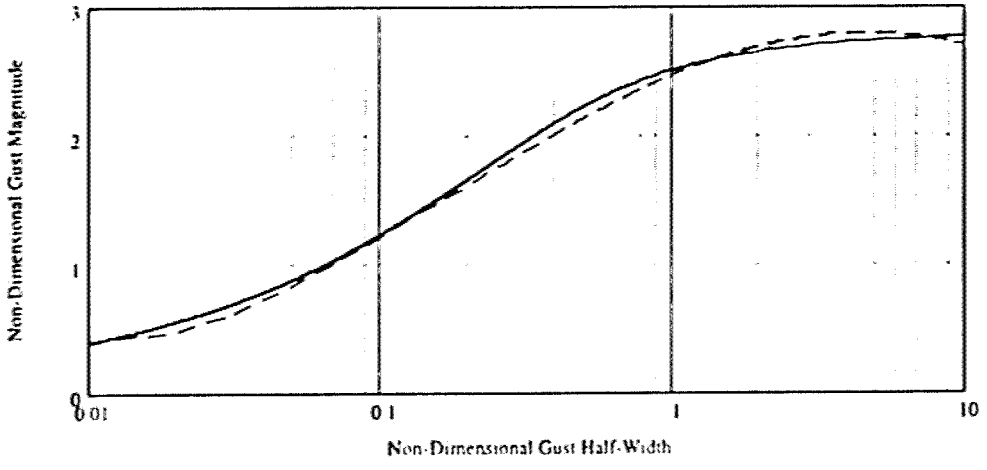

Figure 6.4 Least squares fit to MIL standard and closed form integration solution for non-dimensional longitudinal gust magnitude V_m/σ as a function of non-dimensional gust half-width, d_m/L

Values for V_m (m/s) at a selected altitude for a specified d_m (m) are calculated using the values of σ (m/s) and L (m) (σ_h and $10^3 L_h$ respectively) given in Table 6.4 or Table 2-79b of Ref. 6.3 and the appropriate expression for V_m / σ, which is selected based on the value of d_m / L as described above. The authors caution the reader that the caption at the top of the original Table 6.6 (2-79 b), which refers to "magnitudes (σ_h and σ_w)" , should read "standard deviations (σ_h and σ_w)". This has been verified by the principal author of the original report (C.G. Justus[8]).

A composite standard deviation, σ_c, for moderate and severe turbulence categories is calculated by weighting the standard deviations by the probability of each category (Table 6.4) according to:

$$\sigma_c = (P_s \sigma_s + P_m \sigma_m) / (P_s + P_m) \qquad (6.8)$$

where, P_s, P_m, σ_s and σ_m are the respective probabilities and standard deviations for severe and moderate turbulence.

The derived gust magnitudes for the longitudinal gust component as a function of turbulence severity (light, moderate, and severe), altitude and gust half-width, d_m, are listed in Table 6.5 and are illustrated for severe turbulence in Fig. 6.5 . The longitudinal component is defined as the horizontal gust in the direction of the mean wind. The longitudinal gust is superimposed with the steady state wind to excite the tail in the elastic body simulation model.

The risk probabilities for the occurrence of severe moderate and 'composite' turbulence are listed in Table 6.6. At 6 km the risk for severe turbulence is 0.56 percent; therefore, from Fig. 6.5 (or Table 6.5) and Table 6.6, for d_m equal 30 meters there is a 0.56 percent risk that a gust magnitude of 4.31 m/s will be exceeded. If the objective is to protect the orbiter vertical tail for a 1 percent risk for a 30-m half-width gust, it is conservative to protect for the 4.31 m/s gust (0.56 percent risk). If the amount of load alleviation needed is not obtained with the 4.31 m/s gust there are two approaches that can be considered. A small reduction of the 4.31 m/s value can be achieved if a value for the 1 percent risk level could be derived analytically, but an acceptable methodology is not available at present. A large reduction can be achieved at any altitude by deriving a gust magnitude that represents a composite value for moderate and severe turbulence. As listed in Table 6.7 the composite value at 6 km for d_m equal to 30 m is 1.52 m/s. This is achieved with a considerable penalty, which is an increase of the risk to 7.06 percent (third column in Table 6. 6) that this value will be exceeded.

Table 6. 5 Discrete Longitudinal Gust Magnitude as a Function of Altitude (km) and Gust Half-Width, d_m (m) for Light, Moderate, and Severe Turbulence

a) Light Turbulence

	Gust Magnitude(m/s) gust half width (m)									
Alt(km)	30	60	90	120	150	180	210	240	270	300
1.	0.12	0.18	0.21	0.24	0.27	0.29	0.30	0.31	0.33	0.34
2.	0.11	0.17	0.21	0.24	0.26	0.28	0.29	0.31	0.32	0.33
4.	0.12	0.18	0.23	0.26	0.29	0.31	0.33	0.34	0.36	0.37
6.	0.13	0.19	0.24	0.27	0.30	0.32	0.34	0.36	0.37	0.39
8.	0.13	0.20	0.25	0.29	0.32	0.34	0.36	0.38	0.39	0.41
10.	0.12	0.18	0.23	0.26	0.29	0.32	0.34	0.36	0.37	0.38
12.	0.11	0.16	0.21	0.25	0.28	0.30	0.33	0.35	0.36	0.38
14.	0.11	0.13	0.17	0.20	0.23	0.25	0.27	0.29	0.31	0.33

b) Moderate Turbulence

	Gust Magnitude,(m/s) gust half width (m)									
Alt(km)	30	60	90	120	150	180	210	240	270	300
1.	1.14	1.70	2.09	2.37	2.59	2.77	2.92	3.05	3.16	3.26
2.	1.08	1.63	2.01	2.29	2.51	2.69	2.84	2.97	3.08	3.18
4.	1.23	1.86	2.31	2.66	2.93	3.15	3.34	3.50	3.64	3.77
6.	1.28	1.95	2.42	2.77	3.06	3.29	3.48	3.65	3.80	3.93
8.	1.29	1.96	2.44	2.80	3.08	3.32	3.52	3.69	3.84	3.97
10.	1.21	1.85	2.32	2.68	2.98	3.22	3.42	3.60	3.76	3.90
12.	1.11	1.63	2.08	2.45	2.75	3.01	3.23	3.43	3.60	3.76
14.	1.06	1.32	1.68	2.00	2.28	2.53	2.75	2.95	3.12	3.29

c) Severe Turbulence

	Gust Magnitude (m/s) gust half width (m)									
Alt km	30	60	90	120	150	180	210	240	270	300
1	3.94	5.89	7.20	8.18	8.94	9.56	10.08	10.52	10.91	11.25
2	3.81	5.73	7.06	8.04	8.81	9.45	9.98	10.43	10.83	11.18
4	3.76	5.70	7.08	8.12	8.95	9.63	10.21	10.70	11.14	11.52
6	4.31	6.54	8.12	9.32	10.27	11.05	11.71	12.28	12.78	13.22
8	4.57	6.93	8.61	9.88	10.89	11.72	12.42	13.02	13.54	14.01
10	4.21	6.40	8.03	9.29	10.30	11.14	11.85	12.47	13.01	13.49
12	3.54	5.19	6.64	7.81	8.78	9.61	10.32	10.95	11.50	12.00
14	2.82	3.50	4.44	5.29	6.04	6.70	7.28	7.80	8.27	8.69

As shown in Table 6.5c the smallest gust half-width d_m associated with a 9 m/s gust is about 100 meters at 8 km.

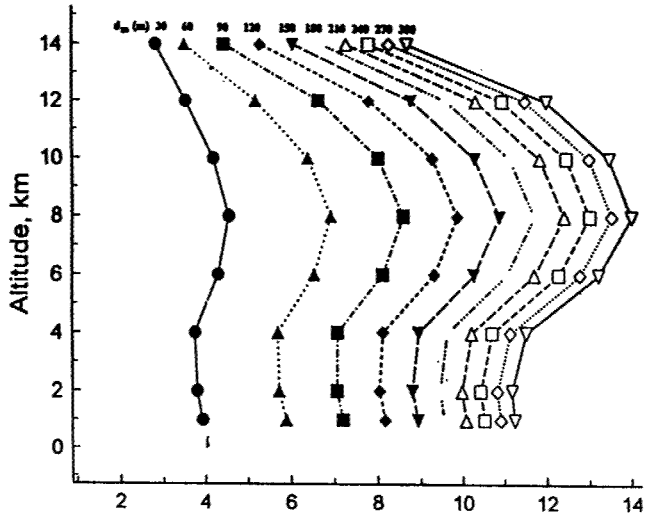

Figure 6. 5 Discrete Longitudinal Gust Magnitude as a Function of Altitude (km) and Gust Half-Width, d_m (m) for Severe Turbulence

Table 6.6 Risk Probability (percent) for Moderate, Severe, and Composite (Moderate plus Severe) Turbulence, 1 to 20 km

Alt.(km)	Moderate	Severe	Composite
1	19.90	2.50	22.40
2	9.79	1.11	10.90
4	7.38	0.63	8.01
6	6.50	0.56	7.06
8	7.04	0.49	7.53
10	6.77	0.43	7.20
12	5.02	0.34	5.36
14	3.68	0.27	3.95

Table 6.7 Discrete Longitudinal Gust Magnitude (m/s) as a Function of Altitude (km) and Gust Half-Width, d_m (m), Composite (Moderate and Severe Turbulence)

	Gust Magnitude,(m/s) gust half width (m)									
Alt(km)	30	60	90	120	150	180	210	240	270	300
1.	1.45	2.17	2.66	3.02	3.30	3.52	3.72	3.88	4.02	4.15
2.	1.36	2.05	2.52	2.87	3.15	3.38	3.57	3.73	3.87	4.00
4.	1.43	2.17	2.69	3.09	3.40	3.66	3.88	4.07	4.23	4.38
6.	1.52	2.31	2.87	3.29	3.63	3.90	4.14	4.34	4.51	4.67
8.	1.51	2.29	2.84	3.26	3.59	3.87	4.10	4.29	4.47	4.62
10.	1.39	2.12	2.66	3.08	3.41	3.69	3.93	4.13	4.31	4.47
12.	1.26	1.85	2.37	2.79	3.13	3.43	3.68	3.90	4.10	4.28
14.	1.18	1.47	1.87	2.23	2.54	2.82	3.06	3.28	3.48	3.65

This discussion has emphasized the importance of the results for the smallest gust half-widths. It is also important to point out that the improved model produces gust magnitudes larger than 9 m/s as gust half-widths become large; for example, at 6 km the magnitude for severe turbulence exceeds 9 m/s for d_m greater than 90 meters. Acceptance of this method for specification of gust magnitude would require that adequate protection for these magnitudes greater than 9 m/s be established.

6.5 Conclusion

A rational for derivation of a discrete gust magnitude that is a function of altitude and gust half-width has been developed. This rational is based on established methods that are included in military specification of requirements for the flying qualities of piloted aircraft. This specification is significant because it is based on the same aircraft turbulence data used in studies that established the NASA classical 9 m/s gust. Based on a review of these studies there is no evidence that supports application of the 9 m/s for discrete gusts with half-widths as small as 30 meters. The shortcoming of the NASA classical 9 m/s gust model is that it does not include a relationship between gust magnitude and gust half-width. As indicated in this study the inclusion of this relationship may provide the needed load relief for Space Shuttle tail elastic body response for small gust half-widths during severe turbulence. However, protection of other vehicle structures sensitive to larger gust half-widths would have to be established because the new model has gust magnitudes greater than 9 m/s for gust half-width as small as 100 meters (Table 6.5c).

The material in this section has also been published in Reference 6.11.

6.6 References

6.1 Adelfang, S. I., and Smith, O. E., "Wind Gust for Shuttle Ascent, Part II.", White Paper prepared for Electromagnetics and Aerospace Environments Branch (EL23) in support of Shuttle Systems Integration office, March 25, 1997.

6.2 MIL-F-8785B (ASG), "Military Specification Flying Qualities of Piloted Airplanes," August 7, 1969.

6.3 Johnson, D. L. (editor), "Terrestrial Environment (Climatic) Criteria Guidelines for Use in Aerospace Vehicle Development, 1993," NASA TM 4511, August 1993.

6.4 Tolefson, H. B., "Summary of Derived Gust Velocities Obtained from Measurements within Thunderstorms," NACA Report 1285 (supersedes NACA Technical Note 3538), Langley Aeronautical Laboratory, Langley Field, VA, July 27, 1955.

6.5 Tolefson, H. B , "Preliminary Analysis of NACA Measurements of Atmospheric Turbulence within a Thunderstorm - U.S. Weather Bureau Thunderstorm Project," NACA Technical Note 1233, Langley Aeronautical Laboratory, Langley Field, VA, January 29, 1947.

6.6 NACA Technical Note 4332, "An Approach to the Problem of Estimating Severe and Repeated Gust Loads for Missile Operations," by Press, H. and Steiner, R., Langley Aeronautical Laboratory, Langley Field, VA, September 1958.

6.7 Vaughan, W. W., "Analysis of Discrete Atmospheric Gust Velocity Data for Use in Missile Design and Performance Studies," ABMA Report No. DA-TR-68-59, November 20, 1959.

6.8 Justus, C. G., Campbell, W. C., Doubleday, M. K., and Johnson, D. L., "New Atmosphere Turbulence Model for Shuttle Applications," NASA TM 4168, January 1990.

6.9 "Space Shuttle Flight and Ground System Specification," Volume X, Appendix 10.10, Natural Environment Design Requirements, NASA NSTS 07700, Volume X, Revision J, June 14, 1990.

6.10 Daniels, G. E., "Natural Environment (Climatic) Criteria Guidelines for Use in MSFC Launch Vehicle Development, 1963 Revision," MTP-AERO-63-8, January 28, 1963.

6.11 Adelfang, S. I. And Smith, O. E.: "Gust Models for Launch Vehicle Ascent." AIAA paper 98-0747, 36th Aerospace Sciences Meeting, January 1998, Reno, NV.

7.0 WIND PROFILE MEASUREMENT SYSTEMS

Since 1960, the instrumentation, tracking, and data reduction techniques of the Eastern Test Range (ETR) standard Rawinsonde system have been updated. A special high resolution ETR Rawinsonde system (formerly called Windsonde) with greater accuracy than the standard Rawinsonde has also been developed. Hence, the quality and resolution of wind, temperature, pressure, and relative humidity profile measurement capability with Rawinsondes have been improved at ETR.

The Jimsphere wind profile measurement system was developed at MSFC in the 1960's for the Saturn program and is still used in the Space Shuttle program (Ref. 7.1, 7.2, 7.3, 7.4). The NASA 50MHz Doppler Radar Wind Profiler (DRWP) was developed jointly between MSFC and JSC in the 1986-89 period for the Space Shuttle program. Currently, the 45th Space Wing, Air Force Space Command, Patrick AFB, Florida is developing the Automated Meteorological Profiler System (AMPS) for the ETR. Because NASA is an ETR user, the Space Shuttle program has an interest in this system.

Brief descriptions of the Jimsphere, DRWP, and AMPS systems are given below.

Jimsphere

The Jimsphere system produces the highest resolution and greatest accuracy wind profile of all measurement systems. Hence, it is used as a standard for comparison of wind profile measurement systems. To illustrate the historical development of the Jimsphere, photographs taken during a test of constant volume spheres, one smooth (ROSE), and the other with conical protuberances (Jimsphere), is shown in Fig. 7.1 . This test was conducted at MSFC, August 2, 1963 during stable atmospheric conditions and light winds. The smooth sphere was released at 11:52 p.m. and shortly thereafter (11:54 p.m.) the sphere with cones was released. The smooth sphere (ROSE) shows induced perturbations (which would be interpreted as wind) that are larger than the perturbations induced by the roughened sphere (Jimsphere). The cones on the Jimsphere reduce the aerodynamic vortex shedding responsible for the observed perturbations of the balloon trajectory. The cones serve the same purpose as dimples on a golf ball.

The Jimsphere balloon is tracked by a FPS-16 radar or one having the equivalent precision. The standard data reduced for MSFC yields wind speed and direction at 25m altitude intervals. Jimsphere wind databases have been used in wind profile models and design assessments for the Space Shuttle. Samples of Jimsphere 3.5-hour pairs taken at KSC were used to establish wind loads persistence for the Space Shuttle. The Jimsphere system is a Space Shuttle operational requirement for pre-launch wind monitoring and post-flight evaluations. The specifications of the standard Jimsphere are given in Table 7.1.

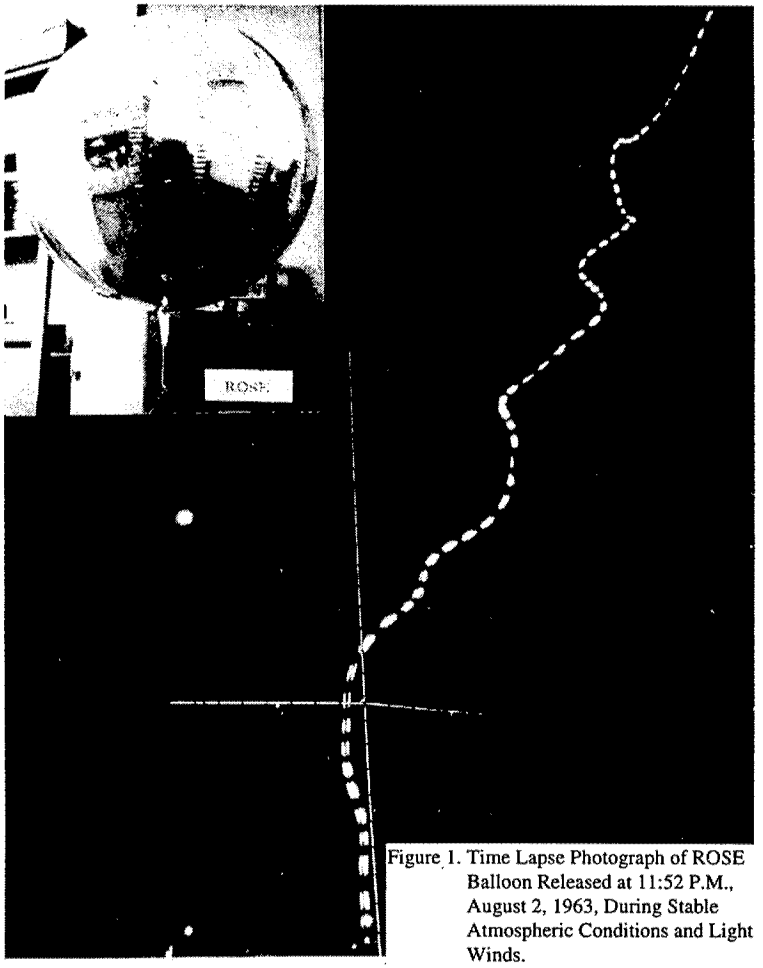

Figure 1. Time Lapse Photograph of ROSE Balloon Released at 11:52 P.M., August 2, 1963, During Stable Atmospheric Conditions and Light Winds.

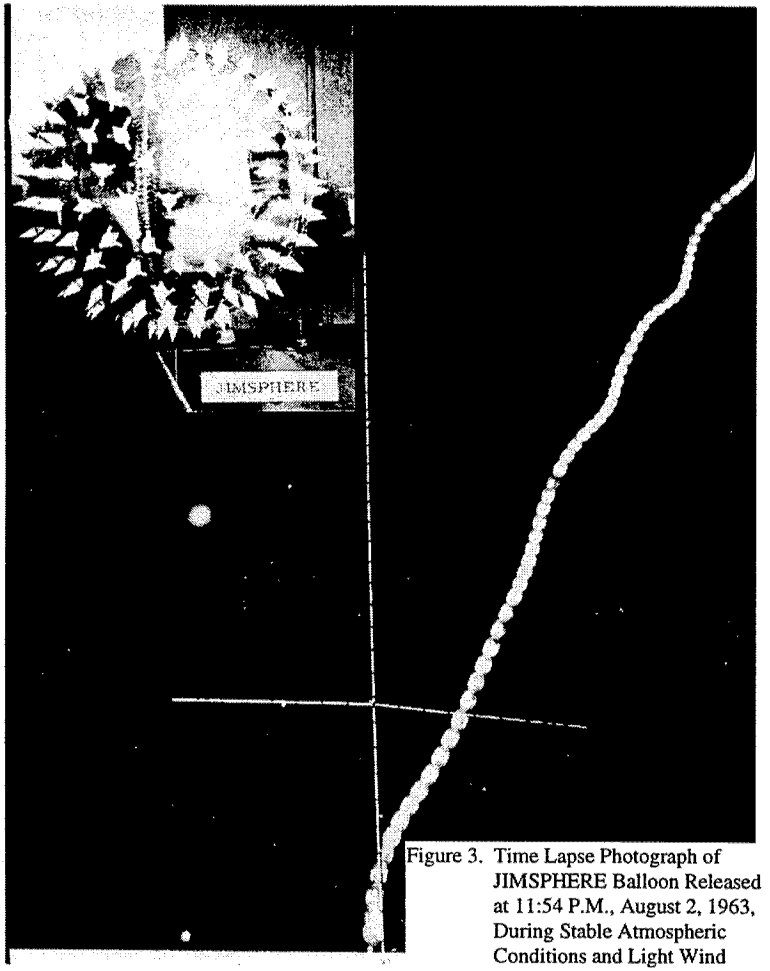

Figure 3. Time Lapse Photograph of JIMSPHERE Balloon Released at 11:54 P.M., August 2, 1963, During Stable Atmospheric Conditions and Light Wind

ROSE **Jimsphere**

Figure 7.1 A ROSE and Jimsphere Test at MSFC, August 2, 1963

Table 7.1 Jimsphere Specifications (ML-632/um)

Type	Aerodynamically stabilized, constant volume, super pressure balloon constructed of ½ mil aluminized mylar
Inflated Diameter	2.0 m
Typical Free Lift	4.7 kg
Typical Gross Lift	5.1 kg
Inflation Volume	4.2 m^3
Nominal Float Altitude	17-18 km
Roughness Elements	398 cones, 7.6 cm (base) X 7.6 cm (height)

The Jimsphere measures only 50 percent of the amplitude of wind profile perturbations at a wavelength of 90 m, and > 95 percent of the amplitude for wavelengths > 300 m (Ref. 7.5, 7.6, 7.7). Fig. 7.2 shows the magnitude (vector modulus) of the wind perturbations for a sample of high-pass filtered Jimsphere profiles. The high pass filters are for nominal cut-off wavelengths λ_c of 500, 1500, 3000, and 6000m. It is shown that the classical NASA 9m/s gust is not detected by the Jimsphere system for wavelengths less than 1500m. Hence, other means for wind gust modeling are required as discussed in Section 6.

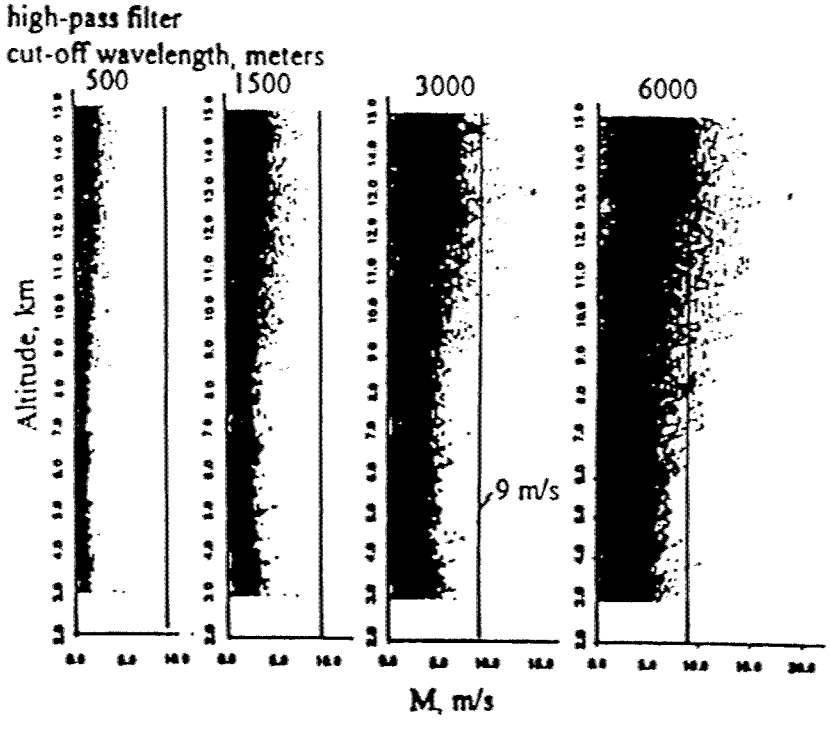

Figure 7.2 Wind perturbation vector modulus for high pass filtered Jimsphere sample of 150, February Jimsphere sample, KSC

NASA 50MHz Doppler Radar Profiler (DRWP)

The DRWP development was underway by MSFC before the Challenger accident in 1986. Then the development was accelerated to completion by a joint effort between MSFC and JSC. This system is located at KSC. The antenna is a phased array of coaxial-collinear elements which the radar uses to create three beams - one vertical and two orthogonal 15 degrees off the zenith on azimuths of 135 degrees (mode 1) and 45 degrees (mode 2) (Ref. 7.8). There are 112 gates; the lowest gate is at 2 km and the last at 18.6 km. This yields wind components that are average values for an altitude layer of 150 m. The wind components are converted to wind speed and direction. Currently there is approximately 5 years of DRWP data at MSFC at 5-minute intervals with some missing periods. The DRWP wind profiles are monitored for each Space Shuttle launch to detect any rapid change with respect to time and compared with the Jimsphere wind profiles which are made at L-6 hr 15 min., L-4 hr 30 min., L-3 hr 25 min., L-2 hr 15 min., L-70 min and L+15 min. The L-4 hr 30 min Jimsphere is used for trajectory and loads analysis for the commit- to-launch decision.

Automated Meteorological Profiling System (AMPS)

The AMPS is under development for the Eastern Test Range (ETR). AMPS balloon tracking will be with the Global Positioning System (GPS) which will replace the traditional ground based radar. This system is scheduled to be in operation in the year 2000 or 2001. In principle the GPS balloon tracking should produce more accurate winds because the radar tracking errors at the low elevation angles for long slant ranges are eliminated by the GPS. The AMPS has two measurement modes. One is a Jimsphere with the aluminized mylar removed to permit GPS signal transmission. This mode is called the High Resolution Flight Element (HRFE). The HRFE yields a detailed wind profile to 16.7- km altitude. The second mode called the Low Resolution Flight Element (LRFE) replaces the Rawinsonde system. The LRFE will measure the wind, pressure, temperature, and relative humidity profiles to 30-km altitude. Density is derived from pressure, temperature, and relative humidity.

The AMPS system has the potential to establish a wind profile database concurrently with atmospheric parameters, pressure, temperature, and density for KSC. This database will be most valuable provided that a special measuring program (SMP) in support of launch vehicle development is established early in the AMPS operational phase. This measuring program should be over a 5-year period with a sampling frequency of at least four per day. At present the atmosphere models and wind models for aerospace vehicle programs are treated separately. A wind and atmosphere pairs database to be established with the proposed AMPS/SMP would be used for future aerospace vehicle design assessments and day-of-launch ascent guidance and control design. It is suggested that NASA and ETR jointly establish the details for this proposed measuring program at the beginning of the AMPS operational phase.

7.1 References

7.1 Scoggings, J. R.: "An Evaluation of Detail Wind Data as Measured by the FPS-16/Radar/Sperical Balloon Technique." NASA TN D-1572, May 1963.

7.2 Rogers, R. R. and Cammitz, H. G.: "Project Baldy, An investigation of Aerodynamically-Induced Balloon Motions." Final Report NAS8-11140, Carnell Aeronautical Laboratory, Inc., 1965, pp. 80.

7.3 Scoggins, J. R.: "Sphere Behavior and Measurement of Wind Profiles." NASA TN D-3994, 1967.

7.4 DeMandel, R. E. and Krivo, S. J.: "Selecting Digital Filters for Application to Detailed Wind Profiles." NASA CR-61325, 1969.

7.5 DeMandel, R. E. and Krivo, S.J.: "Radar/Balloon Measurement of Vertical Air Motions Between the Surface and 15 km." J. Appl. Meteor., Vol. 10, April 1971, pp. 313-319.

7.6 Fichtl, G. H., DeMandel, R. E., and Krivo, S. J.:"Aerodynamic Properties of Rough Spherical Balloon Wind Sensors." NASA TN D-6373, June 1971.

7.7 Fichtl, G. H.: "Spericial Balloon Response to Three-Dimensional Time-Dependent Flows." NASA TN D-6829, July 1972.

7.8 Wilfong, T.S., Smith, S. and Creasey, R., "High Temporal Resolution Velocity Measurements from a Wind Profiler", J. Spacecraft and Rockets, pp.348-354, Vol. 30, No.3, May-June 1993.

CONCLUDING REMARKS

The evolutionary process in the development of ascent wind profile models for aerospace vehicle design is traced from the beginning of the NASA space program to the present. A review of past works, current practices, and lessons learned points the way for improvements in ascent wind models and operating techniques for future aerospace vehicle programs. The technological advances in wind profile measuring systems and engineering analysis have lead to ever increasing complex and more realistic wind profile models for space vehicle design and day-of-launch operations.

APPENDIX

CONSTRUCTION OF PROBABILITY ELLIPSES

The mathematical construction of probability ellipses is useful in establishing that wind data samples are bivariate normal . The construction is also used for graphical displays. A convenient procedure for mathematical construction and graphical display of ellipses is presented below. The conic form of the equation for a family of probability ellipses depending on the value of λ_e is:

$$AX^2 + BXY + CY^2 + DX + EY + F = 0 \qquad [A.1]$$

where,

$$A = \sigma_y^2 \ , \ B = -2\rho\sigma_x\sigma_y \ , \ C = \sigma_x^2 \ ,$$

$$D = 2\sigma_x\sigma_y\rho\overline{Y} - 2\sigma_y^2\overline{X} = -\left(B\overline{Y} + 2A\overline{X}\right)$$

$$E = 2\sigma_x\sigma_y\rho\overline{X} - 2\sigma_x^2\overline{Y} = -\left(B\overline{X} + 2C\overline{Y}\right)$$

$$F = A\overline{X}^2 + C\overline{Y}^2 + B\overline{XY} - AC(1-\rho^2)\lambda_e{}^2$$

where,

$\overline{X}, \overline{Y}, \sigma_x, \sigma_y$ are the means and standard deviations of variables X and Y , ρ is the linear correlation coefficient for X and Y,

$\lambda_e = \sqrt{-2\ln(1-P)}$, and P is probability.

The bivariate normal probability density function has a constant value on these ellipses; therefore, the ellipses of Eq. A.1 are referred to as ellipses of equal probability. For most applications the interest is in determining the probability that a point (x,y) falls inside a given ellipse.

The ranges for X and Y, used for establishing graphics scales and computational procedures, are given by:

$$X_{L,S} = \overline{X} \pm \sigma_x\lambda_e \qquad [A.2]$$

$$Y_{L,S} = \overline{Y} \pm \sigma_y\lambda_e \qquad [A.3]$$

Solution of the quadratic equation A.1 yields values of Y for each value of X incremented within the range of X smallest to X largest . The centroid $(\overline{X},\overline{Y})$ for the family of probability ellipses (for various values of P) is plotted as a point.

For wind data samples, the general notations for the bivariate normal distribution are replaced by the corresponding sample values for the zonal and meridional wind components, which are the mean values, $\overline{U}$ and $\overline{V}$; the standard deviations, SU and SV; and the correlation coefficient, r(U,V).

In the wind analysis, P-percent of the wind vectors fall within the specified probability ellipse. From this point of view, a specified probability ellipse gives the joint probability that P-percent of the U-V components lie within the given ellipse.

When $\sigma_x^2 = \sigma_y^2 = \sigma^2$ and $\rho = 0$ in the bivariate normal distribution, the probability ellipses of A.1 reduce to circles whose centers are at the means $\overline{X},\overline{Y}$. The radii of the probability circles are $\sigma_{VI}\lambda_c$, where

$$\sigma_{VI} = \sqrt{2\sigma^2} \qquad [A.4]$$

and.

$$\lambda_c = \sqrt{-\ln(1-P)} \qquad [A.5]$$

The example of wind probability ellipses for P = .50, .95, and .99 illustrated in Fig. A-1 is for the following parameters: $\overline{U}$ = -3.01 m/s , $\overline{V}$ = -3.19 m/s, SU = 8.66 m/s , SV = 6.85 m/s and ρ = 0.322

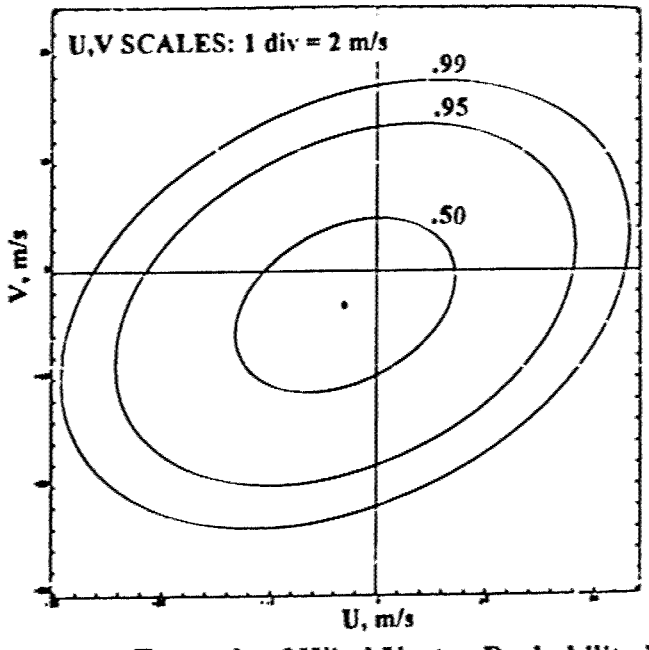

Figure A-1 An Example of Wind Vector Probability Ellipses

REPORT DOCUMENTATION PAGE

Form Approved
OMB No. 0704-0188

1. AGENCY USE ONLY *(Leave Blank)*	2. REPORT DATE	3. REPORT TYPE AND DATES COVERED
	October 1998	Contractor Report (Final)

4. TITLE AND SUBTITLE
A Compendium of Wind Statistics and Models for the NASA Space Shuttle and Other Aerospace Vehicle Programs

5. FUNDING NUMBERS
NAS8–60000

6. AUTHORS
O.E. Smith and S.I. Adelfang

7. PERFORMING ORGANIZATION NAMES(S) AND ADDRESS(ES)
Computer Sciences Corporation
Huntsville, Alabama

8. PERFORMING ORGANIZATION REPORT NUMBER
M–899

9. SPONSORING/MONITORING AGENCY NAME(S) AND ADDRESS(ES)
George C. Marshall Space Flight Center
Marshall Space Flight Center, Alabama 35812

10. SPONSORING/MONITORING AGENCY REPORT NUMBER
NASA/CR—1998–208859

11. SUPPLEMENTARY NOTES
Prepared for Systems Analysis and Integration Laboratory, Science and Engineering Directorate.
Technical Monitor: Steve Pearson

12a. DISTRIBUTION/AVAILABILITY STATEMENT
Unclassified–Unlimited
Subject Category 18
Standard Distribution

12b. DISTRIBUTION CODE

13. ABSTRACT *(Maximum 200 words)*

The wind profile with all of its variations with respect to altitude has been, is now, and will continue to be important for aerospace vehicle design and operations. Wind profile databases and models are used for the vehicle ascent flight design for structural wind loading, flight control systems, performance analysis, and launch operations. This report presents the evolution of wind statistics and wind models from the empirical scalar wind profile model established for the Saturn Program through the development of the vector wind profile model used for the Space Shuttle design to the variations of this wind modeling concept for the X–33 program. Because wind is a vector quantity, the vector wind models use the rigorous mathematical probability properties of the multivariate normal probability distribution. When the vehicle ascent steering commands (ascent guidance) are wind biased to the wind profile measured on the day-of-launch, ascent structural wind loads are reduced and launch probability is increased. This wind load alleviation technique is recommended in the initial phase of vehicle development. The vehicle must fly through the largest load allowable versus altitude to achieve its mission. The Gumbel extreme value probability distribution is used to obtain the probability of exceeding (or not exceeding) the load allowable. The time conditional probability function is derived from the Gumbel bivariate extreme value distribution. This time conditional function is used for calculation of wind loads persistence increments using 3.5–hour Jimsphere wind pairs. These increments are used to protect the commit-to-launch decision. Other topics presented include the Shuttle Shuttle load-response to smoothed wind profiles, a new gust model, and advancements in wind profile measuring systems. From the lessons learned and knowledge gained from past vehicle programs, the development of future launch vehicles can be accelerated. However, new vehicle programs by their very nature will require specialized support for new databases and analyses for wind, atmospheric parameters (pressure, temperature, and density versus altitude), and weather. It is for this reason that project managers are encouraged to collaborate with natural environment specialists early in the conceptual design phase. Such action will give the lead time necessary to meet the natural environment design and operational requirements; and thus, reduce development costs.

14. SUBJECT TERMS
natural space environment, winds aloft, wind statistics and models

15. NUMBER OF PAGES
116

16. PRICE CODE
A06

17. SECURITY CLASSIFICATION OF REPORT	18. SECURITY CLASSIFICATION OF THIS PAGE	19. SECURITY CLASSIFICATION OF ABSTRACT	20. LIMITATION OF ABSTRACT
Unclassified	Unclassified	Unclassified	Unlimited

National Aeronautics and
Space Administration
AT01S
George C. Marshall Space Flight Center
Marshall Space Flight Center, Alabama
35812